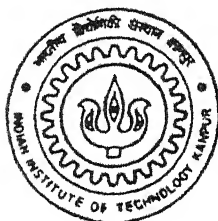


# PHOTOVOLTAIC AIRCONDITIONING, REFRIGERATION AND HEATING: AN ENVIRONMENTAL FRIENDLY OPTION

by

**Kirti Kumar Dhawan**



TH  
E/1999/P  
D 535f

DEPARTMENT OF ELECTRICAL ENGINEERING  
**INDIAN INSTITUTE OF TECHNOLOGY KANPUR**

September, 1999

# PHOTOVOLTAIC AIRCONDITIONING, REFRIGERATION AND HEATING: AN ENVIRONMENTAL FRIENDLY OPTION

A Thesis Submitted  
in Partial Fulfillment of the Requirements  
for the Degree of  
Doctor of Philosophy

by  
**Kirti Kumar Dhawan**

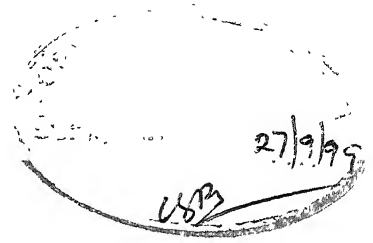


to the  
**DEPARTMENT OF ELECTRICAL ENGINEERING  
INDIAN INSTITUTE OF TECHNOLOGY KANPUR**  
September, 1999

300 / EE  
134205.....

134205





# Certificate

## Certificate

It is to certify that the work contained in the thesis entitled **Photo-Voltaic Airconditioning, Refrigeration and Heating: An Environmental Friendly Option** by Mr. Kirti Kumar Dhawan, has been carried out under my supervision and that this work has not been submitted elsewhere for a degree.

Dr. Manohar Prasad

Professor

Department of Mechanical Engineering

IIT Kanpur

September, 1999



# Acknowledgements

It is a rare opportunity to have Professor Manohar Prasad as my thesis supervisor. I am highly indebted to him for the inspiring guidance and useful discussions I had with him throughout the course of this work.

I am highly indebted to Professor G.K.Dubey for his guidance, suggestions and technical feedback in doing the literature survey and finally suggesting this problem and his advice for solving the same.

I am also grateful to Dr. B.G.Fernandes for his guidance and help in purchasing photovoltaic array and batteries. His time to time comments and suggestions has immensely helped in solving this problem.

My sincere thanks to Dr. U.S.Dixit, Asst. Prof., Mechanical Engineering Department, I.I.T. Guwahati for his sincere and consistent help throughout this work.

Thanks are due to Shri P. P. Bhola for his timely help and full cooperation in setting up and conducting the experiment.

I wish to thank Shri R.K.Bajpai for his excellent drawings/tracings and Shri A.K.Sriv for his error free typing.

Kirti Kumar Dhawan

# Publications

Following publications have been communicated out of this work:

## Accepted

Following publications have been accepted:

1. ‘Application of Fuzzy Set Theory to Photovoltaic Airconditioning’ in 1999 International Appliance Technical Conference, Florida, U.S.A. Under Consideration for publication in IEEE Transactions: Industry Applications.
2. ‘Photovoltaic Airconditioning: An Environmental Friendly Option’ in 20th International Congress of Refrigeration, IIR/IIF, Sydney, 1999.

## Under Review

Following publications are under review and consideration for publication:

1. ‘Photovoltaic Heating’ in Journal of Solar Energy Engineering, Milwaukee, Wisconsin, U.S.A.
2. ‘Photovoltaic Airconditioning and Heating: Optimum Load Matching of a Battery Connected Photovoltaic Array’ in 2000 International Appliance Technical Conference, Florida, U.S.A.

3. 'Photovoltaic Refrigeration' in Indian Journal of Engineering and Materials Sciences, National Institute of Science Communication, New Delhi, India.

# Synopsis

The sources of conventional energy are dwindling fast with a corresponding rise in cost. Therefore, considerable attention is being paid to other alternative sources of energy. Solar energy is one of the non-conventional energy resources which has the advantage of being freely available in plenty, particularly in India. It can be harnessed as thermal energy for water heating, cooking, absorption-refrigeration and solar thermal power generation. It can be converted directly into electricity by using photovoltaic array. A photovoltaic array, called PV array, consists of a number of solar cells arranged in series and parallel. The electrical energy generated in the array can be stored in a battery and can be used to run a compressor of a vapor-compression system or to heat the generator of a vapour absorption system.

The airconditioning, refrigeration and heating require energy in the form of heat (in the generator of a vapour absorption system) or in the form of work (to run the compressor of a vapor compression system). They require mostly the same type of appliances and process and differ in application. Whereas, in the context of hot countries like India, airconditioning is understood as a process of cooling a surrounding, the heating means the reverse of it in which a space is heated by the rejected heat of condenser. The refrigeration is defined as the artificial withdrawal of heat, producing in a substance or within a space a temperature lower than that which would exist under the natural influence of surroundings. Thus, refrigerating machine is an integral part

of airconditioning system.

The term photovoltaic airconditioning, heating and refrigeration means running these systems by the solar energy converted in the form of electricity. As the solar energy is not available round the clock and also the weather conditions are highly uncertain, the electrical energy is stored in the battery. Apart from the continuous depletion of natural resources and degradation of environment due to burning of fossil fuels, the solar energy is very much relevant for remote area applications. However, at present, the solar energy is very costly and therefore, the size of the array should be selected judiciously.

In the present work, a computer code is developed to find out the array size depending on the application. A model has been proposed for finding out the array photo-generated current. The model is validated by conducting experiments on a 100 W photovoltaic array at IIT Kanpur. The cooling load, heating load and refrigeration load are computed on timely basis based on ASHRE handbook. Feasibility of two types of systems- vapour compression and vapour absorption system is considered. It is seen that the vapour compression system is economical. In this, the electrical energy will be used to run a D. C. motor which will be used to drive the compressor.

As the weather conditions are highly uncertain, the fuzzy set theory is employed to find out the array size. In this, the weather parameters are expressed as linear triangular fuzzy numbers and possibility distribution for array size is obtained. Then, a method has been proposed to find out the array size based on the subjective requirement of the designer.

Once a proper size of the array is chosen, it has to be matched with the load connected to it. The load is a battery of 12 V or 24 V. By load matching is meant the proper selection of series and parallel rows of cells for a given total number of cells. A load matching factor is defined as the ratio of energy stored over the day to

the maximum possible energy stored over a day. The number of series and parallel rows of cells and internal resistance of the battery is found by solving the optimization problem to maximize the stored energy with the constraint of total number of cells and generated voltage being greater than the battery voltage. A parametric study has been carried out and it is seen that a load matching factor of more than 0.95 may easily be obtained. However, the system will be highly inefficient in case of a load mismatch.

The study has been also carried out to find out the proper inclination of the array in order to get maximum output from the insolation. For this purpose also, an optimization algorithm has been employed. *It has been also suggested to cover the space by photovoltaic array in a manner in which it will fulfill the twin objective of shading the roof to reduce the cooling load (refrigeration requirement) and generating electricity.* Finally, the environmental benefits of using photovoltaic systems are studied in detail. It is seen that use of solar energy will reduce carbon dioxide level and ash particulates in the environment.

Thus, the present work studies various aspects of the photovoltaic airconditioning, refrigeration and heating and discusses the importance of its use. The use of a new model for array-photo-generated current, application of the fuzzy set theory and a methodology to find out the optimum load matching and inclination of the array and environmental study are the main features of the present work.

# Contents

Certificate	i
Acknowledgements	ii
Publications	iii
Synopsis	v
Table of Contents	viii
List of Figures	xii
List of Tables	xvi
Nomenclature	xvii
<b>1 INTRODUCTION AND LITERATURE REVIEW</b>	<b>1</b>
1.1 Introduction . . . . .	1
1.2 Literature Review . . . . .	7
1.3 Scope and Objective of the Present Work . . . . .	10
1.4 Organization of Thesis . . . . .	11
<b>2 DETERMINATION OF PHOTOVOLTAIC ARRAY SIZE</b>	<b>12</b>
2.1 Introduction . . . . .	12
2.2 Characteristics of Photovoltaic Array . . . . .	13

2.3	Radiation Falling on the Surface . . . . .	18
2.4	Estimation of Cooling/Heating/Refrigeration Load . . . . .	23
2.5	Estimation of Size of PV Array . . . . .	28
2.6	Results and Discussion . . . . .	29
2.6.1	Results for airconditioning . . . . .	29
2.6.2	Results for Heating . . . . .	37
2.6.3	Results for Refrigeration . . . . .	45
2.7	Summary . . . . .	53
<b>3</b>	<b>APPLICATION OF FUZZY SETS TO THE ARRAY SIZE ESTIMATION</b>	<b>54</b>
3.1	Introduction . . . . .	54
3.2	Parametric Study . . . . .	55
3.3	Fuzzy Set Modeling of Various Parameters . . . . .	57
3.4	Results with Fuzzy Parameters . . . . .	66
3.5	Summary . . . . .	82
<b>4</b>	<b>OPTIMUM LOAD MATCHING OF A BATTERY CONNECTED PHOTOVOLTAIC ARRAY</b>	<b>84</b>
4.1	Introduction . . . . .	84
4.2	Load Characteristics . . . . .	85
4.3	Load Matching Factor . . . . .	86
4.4	Selection of Battery Voltage and Capacity . . . . .	87
4.5	Problem Formulation . . . . .	87
4.6	Solution Procedure . . . . .	88
4.7	Results and Discussion . . . . .	88
4.7.1	Optimized Combination of Cells and Internal Resistance . . . . .	89
4.7.2	Effect of Internal Resistance . . . . .	89
4.7.3	Sensitivity Analysis with Changing Battery Voltage . . . . .	94
4.7.4	Load Matching Factor for Different Months . . . . .	94
4.7.5	Summary . . . . .	94



<b>5</b>	<b>ARRANGEMENT OF PV ARRAY AND ENVIRONMENTAL BENEFITS</b>	<b>98</b>
5.1	Introduction . . . . .	98
5.2	Reduction in the Cooling Load due to Coverage of Roof . . . . .	99
5.3	Optimum Arrangement of Array . . . . .	101
5.4	Results and Discussion . . . . .	101
5.4.1	Energy Saving due to Roof Coverage . . . . .	102
5.4.2	Optimum Arrangement of the Array . . . . .	115
5.4.3	Reduction in the Atmospheric Pollution . . . . .	115
5.5	Summary . . . . .	121
<b>6</b>	<b>CONCLUSIONS AND SUGGESTIONS</b>	<b>122</b>
6.1	Conclusions . . . . .	122
6.1.1	Estimation of Photovoltaic Array Size for Airconditioning, Heating, and Refrigeration . . . . .	122
6.1.2	Application of Fuzzy Set Theory for Array Size Estimation . . . . .	123
6.1.3	Optimum Matching of the Array with Battery . . . . .	123
6.1.4	Saving of Pollution by using Photovoltaic Array . . . . .	124
6.2	Suggestions . . . . .	124
6.2.1	Development of Photovoltaic Airconditioner without Battery: . . . . .	124
6.2.2	Development of Photovoltaic Airconditioner with Battery: . . . . .	125
6.2.3	Development of Photovoltaic 100W Refrigerator: . . . . .	125
6.2.4	Development of Electrically Controlled Compressor: . . . . .	125
	<b>REFERENCES</b>	<b>127</b>
	<b>APPENDIX</b>	
<b>A</b>	<b>Values of the Constants A, B and C used for Predicting Hourly Solar Radiation on Clear Days</b>	<b>132</b>
<b>B</b>	<b>Transmissivity and Absorptivity of Ordinary Glass</b>	<b>133</b>

C Infiltration load	134
D Ventilation air requirement	136
E Heat Liberated due to Occupancy	139
F Heat of Respiration of Products in J/kg per 24 hours	140
G Specifications of the room selected for study	142
H Specifications of Photovoltaic Array	144
I Particulars of the Refrigerator	145
J Calculations of COP for Refrigerant R-12	146
K Characteristic Function	149
L Complex Search Method	155

# List of Figures

1.1	Schematic diagram of a refrigeration system. . . . .	3
1.2	The basic absorption unit. . . . .	5
1.3	Block diagram of a refrigeration system using PV array. . . . .	6
2.1	PV array output experimental and theoretical (clear sky day in March).	15
2.2	PV array output experimental and theoretical (little cloudy and dusty day in May). . . . .	16
2.3	Effect of Insolation on the I-V and P-V characteristics of crystalline silicon solar cells. . . . .	17
2.4	Equation of time correction. . . . .	20
2.5	Cooling load in May. . . . .	31
2.6	Electric power requirement for May. . . . .	32
2.7	Electric power available in May. . . . .	33
2.8	Cooling load in September. . . . .	34
2.9	Electric power requirement for September. . . . .	35
2.10	Electric power available in September. . . . .	36
2.11	Heat load in the month of January. . . . .	39
2.12	Power required and available in the month of January for vapour com- pression system. . . . .	40
2.13	Power required and available in the month of January for vapour ab- sorption system. . . . .	41
2.14	Heat load in the month of November. . . . .	42

2.15	Power required and available in the month of November for vapour compression system. . . . .	43
2.16	Power required and available in the month of November for vapour absorption system. . . . .	44
2.17	Refrigeration load in May. . . . .	47
2.18	Electric power required in May. . . . .	48
2.19	PV array output in May. . . . .	49
2.20	Refrigeration load in January. . . . .	50
2.21	Electric power required in January. . . . .	51
2.22	PV array output in January. . . . .	52
3.1	Effect of max. temperature on cooling load. . . . .	58
3.2	Effect of max. temperature on array output. . . . .	59
3.3	Effect of min. temperature on cooling load. . . . .	60
3.4	Effect of min. temperature on array output. . . . .	61
3.5	Effect of relative humidity on cooling load. . . . .	62
3.6	Effect of fractional cloud cover on cooling load. . . . .	63
3.7	Effect of fractional cloud cover on array output. . . . .	64
3.8	Effect of no. of occupants on cooling load. . . . .	65
3.9	Possibility distribution of cooling load (for the month of April). . . . .	67
3.10	Possibility distribution of cooling load (for the month of May). . . . .	68
3.11	Possibility distribution of cooling load (for the month of June). . . . .	69
3.12	Possibility distribution of cooling load (for the month of July). . . . .	70
3.13	Possibility distribution of cooling load (for the month of August). . . . .	71
3.14	Possibility distribution of cooling load (for the month of September). . . . .	72
3.15	Possibility distribution of cooling load (for the month of October). . . . .	73
3.16	Possibility distribution of array wattage (for the month of April). . . . .	74
3.17	Possibility distribution of array wattage (for the month of May). . . . .	75
3.18	Possibility distribution of array wattage (for the month of June). . . . .	76
3.19	Possibility distribution of array wattage (for the month of July). . . . .	77
3.20	Possibility distribution of array wattage (for the month of August). . . . .	78

3.21	Possibility distribution of array wattage (for the month of September).	79
3.22	Possibility distribution of array wattage (for the month of October).	80
4.1	Effect of array configuration (npxns) on the load matching factor (for 12V battery and 400 cell array).	90
4.2	Effect of internal resistance on load matching factor (for 12V battery and 400 cell array).	92
4.3	Effect of internal resistance on load matching factor (for 12V battery and 7040 cell array).	93
4.4	Variation of load matching factor with battery voltage ( $n_p = 12$ , $n_s = 33$ , $I_R = 0$ ).	95
4.5	Variation of load matching factor with battery voltage ( $n_p = 227$ , $n_s = 31$ , $I_R = 0$ ).	96
5.1	PV array covered roof.	100
5.2	Variation of cooling load with Time for May.	103
5.3	Variation of cooling load with Time for August.	104
5.4	Electric power needed for airconditioning v/s Time (for the month of May).	105
5.5	Electric power needed for airconditioning v/s Time (for the month of August).	106
5.6	Effective power output from PV array v/s Time (for the month of May).	107
5.7	Effective power output from PV array v/s Time (for the month of August).	108
5.8	Variation of cooling load with Time for exposed room (for the month of May).	109
5.9	Variation of cooling load with Time for exposed room (for the month of August).	110
5.10	Electric power needed for Airconditioning v/s Time for exposed room (for the month of May).	111

5.11	Electric power needed for Airconditioning v/s Time for exposed room (for the month of August). . . . .	112
5.12	Effective power output from PV array v/s Time for exposed room (for the month of May). . . . .	113
5.13	Effective power output from PV array v/s Time for exposed room (for the month of August). . . . .	114
5.14	Kg of $CO_2$ v/s Time (for the month of May). . . . .	116
5.15	Kg of $CO_2$ v/s Time (for the month of August). . . . .	117
5.16	Kg of $CO_2$ v/s Time for exposed room (for the month of May). . . . .	118
5.17	Kg of $CO_2$ v/s Time for exposed room (for the month of August). . . . .	119
5.18	Kg. of coal-ash saved v/s Time. . . . .	120
J.1	p-h chart of R-12 . . . . .	148
K.1	Membership functions of (a) $(\sigma_y)_o$ ; (b) b; (c) n; (d) coefficient of friction	153

# List of Tables

2.1	Total Energies (in kWh) per day required and available in different months for airconditioning. . . . .	37
2.2	Total Energies (in kWh) per day required and available in different months for heating . . . . .	45
2.3	Energies required and available per day for 100 W refrigerator. . . . .	53
4.1	Optimized Parameters for the Array . . . . .	91
4.2	Arrangement of smaller array(400 cells) for $1.2\Omega$ internal resistance battery	94

# Nomenclature

## *Capital letters*

A	Fuzzy set A
$AV_T$	Equivalent thermal voltage of the photovoltaic array
$A_{sun}$	Glass area directly exposed to sun
B	Fuzzy set B
COP	Coefficient of performance
$CO_2$	Carbon dioxide
$\mathcal{E}_B$	Energy stored in a battery over a day
$E_{B_{max}}$	Maximum possible energy generated from solar energy over a day
I	Load current of photovoltaic array
$I_{ph}$	Array photo-generated current
$I_r$	Reverse saturation current of the photovoltaic array
$I_1$	Photo-generated current per photovoltaic cell
$I_s$	Reverse saturation current per photovoltaic cell
$I_G$	Array photo-generated current at solar noon
$I_{mp}$	Maximum power point current
$I_t$	Total intensity of the solar radiation
$I_g$	Hourly global radiation
$I_b$	Hourly beam radiation
$I_d$	Hourly diffuse radiation
$I_{bn}$	Beam radiation in the direction of the array
$I_T$	Flux falling on a tilted surface
$K_i$	Thermal conductivity of the $i^{th}$ layer
LAT	Local apparent time
M	Load matching factor



$M_{opt}$	Optimum load matching factor
$N_s$	Number of cells in series in photovoltaic array
$N_p$	Number of parallel strings in the photovoltaic array
$N_{ach}$	Number of air changes per day
$N_a$	Maximum number of cells in the array
$P$	Photovoltaic array output power
PV	Photovoltaic
$P_{mp}$	Maximum power point power
PI	Performance index
$P_A$	Power available in the battery
$P_B$	Power stored in the battery
$Q$	Heat gain of a space through glass
$\dot{Q}_k$	Structure heat load on $k^{th}$ surface
$\dot{Q}_{sta}$	Total structure heat load at time $t_a$
$Q_{infil}$	Infiltration load
$R_c$	Series resistance per photovoltaic cell
$R_s$	Total series resistance of the photovoltaic array
$R_h$	Relativity humidity
$R_b$	Tilt factor for the beam radiation
$R_d$	Tilt factor for the diffuse radiation
$R_r$	Tilt factor for the reflected radiation
$R_e$	Internal resistance of the battery
T	Photovoltaic array temperature
$T_{in}$	Inside design temperature
$T_0$	Photovoltaic cell reference temperature
$T_o$	Outside Temperature
$T_{min}$	Minimum temperature in a day
$T_{max}$	Maximum temperature in a day
$T_s$	Sol-air temperature
$T_{w,o}$	Temperature of the outside surface
$T_{db}$	Dry bulb temperature
$\bar{T}_{sk}$	Mean outside sol-air temperature on the $k^{th}$ surface
$T_{sk(t_a-\tau)}$	Sol-air temperature at ( $t_a - \tau$ ) time
UA	Product of overall heat transfer coefficient and surface area
U	Overall heat transfer coefficient
V	Photovoltaic array voltage
$V_T$	Photovoltaic cell thermal voltage

$V_{mp}$	Maximum power point voltage
$V_w$	Velocity of the outside air
$V_{room}$	Volume of the room
$V_{air}$	Specific volume of the air at outside temperature
$V_L$	Load Voltage
$V_e$	Induced emf in the battery
$W$	Solar hour angle
$X_i$	Thickness of $i^{th}$ layer

### *Small letters*

$a$	Absorptivity
$a, b$	Photovoltaic cell coefficient. depending upon semiconductor material used.
$a_t$	Absorptivity of the structure
$av.g.p$	Average grade point
$f_i$	Inside film coefficient of heat transfer
$f_o$	Outside film coefficient of heat transfer
$h$	Expert estimate for high value
$h_i$	Inside convective coefficient of $i^{th}$ layer
$h_a$	Enthalpy of outside air
$h_o$	Outside air convective heat transfer coefficient.
$l$	Expert estimate for low value
$m$	Expert estimate for most likely
$q$	Rate of heat transfer
$r$	Reflectivity
$t$	Solar time
$t_a$	Actual time
$t_{sr}$	Sunrise time
$t_{ss}$	Sunset time

### *Greek letters*

$\beta$	Slope
$\gamma$	Surface azimuth angle
$\delta$	Declination angle
$\epsilon$	Emissivity of the surface
$\lambda_k$	Corresponding decrement factor for the $k^{th}$ surface
$\phi$	Latitude of the place
$\mu(x)$	Membership function
$\rho$	Reflectivity
$\tau$	Time-delay
$\theta_z$	Zenith angle ( Angle of incidence on a horizontal surface )

### *Subscript*

$D$	Denotes the terms for the direct radiation
$d$	Denotes the terms for the diffused radiation

# Chapter 1

## INTRODUCTION AND LITERATURE REVIEW

### 1.1 Introduction

Airconditioning is defined as the simultaneous control of temperature, humidity, cleanliness and air motion. Depending upon the requirement, air conditioning is divided into the summer air conditioning and the winter air conditioning. In some hot countries of the world, the term air conditioning is usually employed for summer air conditioning and for winter air conditioning the term heating is used.

The refrigeration may be defined as the artificial withdrawal of heat, producing in a substance or within a space a temperature lower than that which would exist under the natural influence of surroundings. A refrigerating machine is an integral part of the air conditioning system, because if the surrounding temperature is higher than the room temperature, heat is to be removed from the space to be air conditioned. However, for the places where surroundings are at a temperature lower than the required temperature, the heating has to be done. The machinery which performs the heating

process is called a heat pump. The main difference between the refrigeration system and heat pump can be physically conceived of from the fact that in the former there is pumping of heat out of the system as against pumping of heat from surroundings into the system in the latter. Thus, a refrigeration system can be used as a heat pump by suitable arrangements, which would cause refrigerant to flow in such a way that heat is transferred to the conditioned space and is drawn from the surroundings.

The vapour compression refrigeration system is the most widely used refrigeration system. It basically requires electrical energy to run a compressor. The compressor raises the pressure of the refrigerant vapour, thus raising its boiling point. The vapour is condensed in a condenser. The condensed liquid is throttled through a valve or a capillary tube into the evaporator. As a result, the pressure drops causing the boiling point of the refrigerant to drop. Therefore, the refrigerant evaporates (and takes heat) at much lower temperature thus cooling and dehumidification of the conditioned space. The low-pressure vapour is sucked by the compressor and cycle continues.

Figure (1.1) shows the schematic diagram of a refrigeration system along with process of energy supply to the system. In order to produce electricity to run the compressor, the fuel is burnt in the boiler. The steam coming from the boiler enters a steam turbine which produces mechanical energy to run the generator. The generator produces electricity which is transmitted to various places. There are losses at every stage.

In refrigeration, an important term called refrigeration effect is defined as the amount of cooling produced by a system. This cooling is obtained at an expense of some form of energy. Hence, it is customary to define a term known as Coefficient of Performance (COP):

$$\text{COP} = \frac{\text{Refrigeration effect}}{\text{energy input}} \quad (1.1)$$

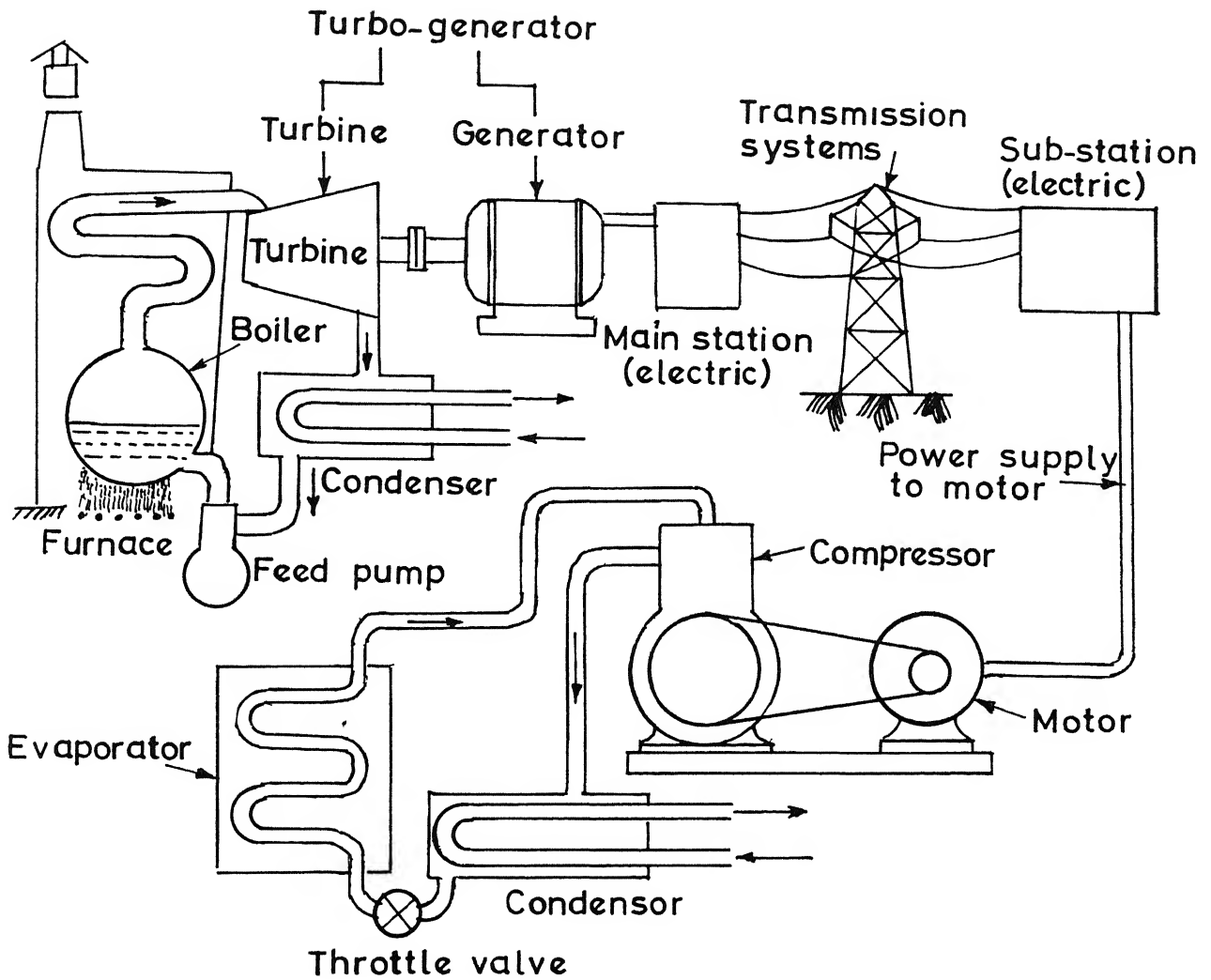


**Fig.1.1 Schematic diagram of a refrigeration system.**

For a heat pump the term. PI (Performance Index), is defined as,

$$PI = \frac{\text{Heating effect}}{\text{energy input}} = 1 + COP \quad (1.2)$$

If the same system is used as a refrigerator and a heat pump with operating conditions unchanged, then PI of the heat pump will be COP of refrigerator plus one.

In the case of vapour-compression system driven by electricity, COP is based on electrical energy input. However, when comparing two systems employing different forms of energies, total energy input (which includes losses) should be taken into account. For example, in the arrangement of Figure (1.1), COP calculated on the basis of energy supply through fuel may be just about one third of that calculated on the basis of energy supply through electric input to compressor.

The vapour-absorption refrigeration system eliminates the need for a compressor. Figure (1.2) shows a basic absorption unit. Low-pressure vapour from the evaporator is absorbed by the liquid solution in the absorber. If the absorption process were executed adiabatically, the temperature of the solution would rise and eventually the absorption of vapour would cease. To perpetuate the absorption process the absorber is cooled by water or air that ultimately rejects this heat to the atmosphere. The pump receives low-pressure liquid from the absorber, elevates the pressure of the liquid, and delivers the liquid to the generator. In the generator, heat from a high-temperature source drives off the vapor that had been absorbed by the solution. The liquid solution returns to the absorber through a throttling valve whose purpose is to maintain the pressure difference between the generator and absorber. The Coefficient of Performance of the absorption cycle COP is defined as,

$$COP = \frac{\text{Refrigeration rate}}{\text{Rate of heat addition to generator}} \quad (1.3)$$

The heat input to the refrigeration system can be given by various means including solar energy.

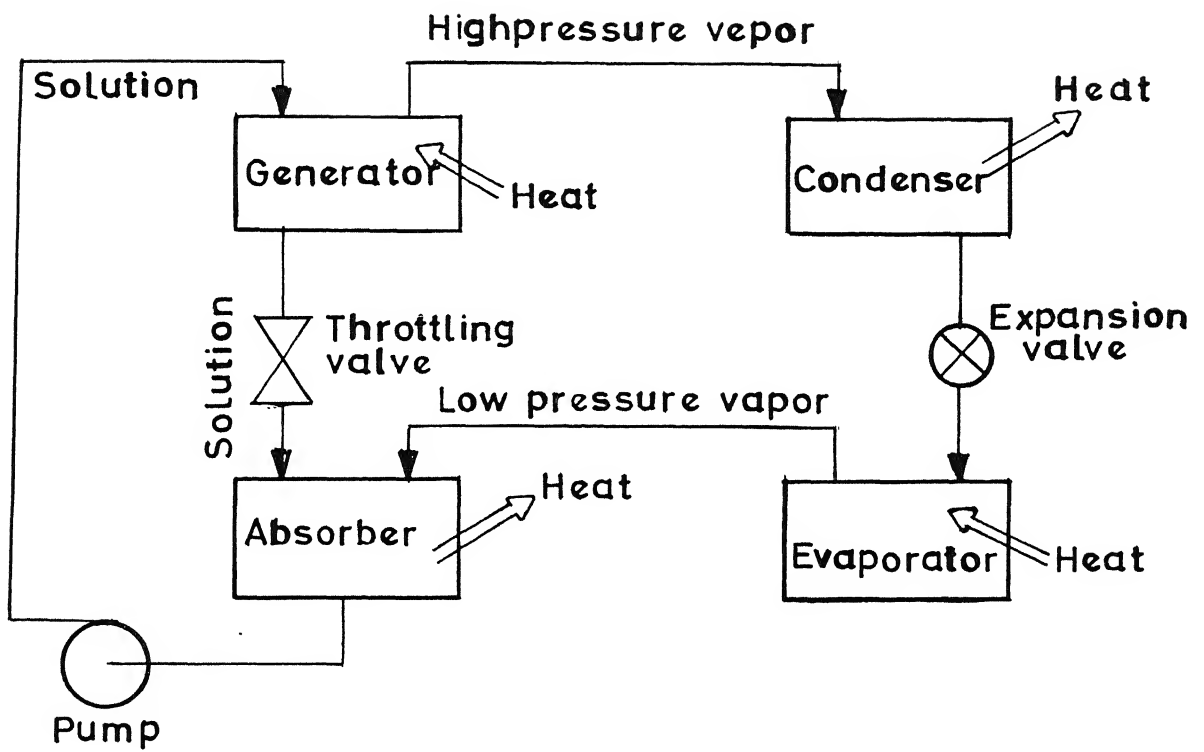


FIG.1.2 THE BASIC ABSORPTION UNITS





Fig. 1.3 100 W Photovoltaic Refrigerator

It is clear from the above description that the air-conditioning, refrigeration and heating systems essentially require energy in the form of heat or work. As the sources of conventional energy are dwindling fast with a corresponding rise in cost, considerable attention is being paid to other alternative sources of energy. The solar energy, which is one of the non-conventional energy resources, has the advantage of being pollution free and being freely available in plenty, particularly in India. It can be converted into thermal energy or directly into electricity (by photovoltaic conversion). A photovoltaic array, called PV array, consists of a number of solar cells arranged in series and parallel. The electrical energy generated in the array can be stored in a battery and can be used to run a compressor of vapour compression system or to heat the generator of vapour-absorption system. Figure (1.3) shows the block diagram of the refrigeration system using PV array. The PV array is a very costly item, therefore its size should be selected judiciously in order to meet the load requirement in the presence of uncertain weather conditions. Also, the effort should be to utilize the PV array most effectively.

The present work investigates the various aspects of photovoltaic air-conditioning, refrigeration and heating. Photovoltaic systems are not being used on a commercial scale due to extremely high cost. It is expected that in the coming century they are expected to attract more attention in view of the global warming and degradation of environment as a result of burning of fossil fuel and depletion of fossil fuel once and for all. The present work aims at providing guidelines for the design of systems using PV array.

## 1.2 Literature Review

There is hardly any literature available on the use of PV array in air-conditioning, refrigeration and heating systems. However, matching of PV array with the loads and

photovoltaic, in general, has been studied by various authors. The present section gives a brief account of the research carried out in this area.

Optimum matching of directly coupled loads to PV array is studied [Khouzam,1990]. Matching of resistive loads coupled directly to PV array is optimized by selecting the load rated power, voltage and resistance with respect to those of the array [Khouzam,1990]. But direct matching of other loads such as D.C. motor has not been studied. Optimum matching for separately excited D.C. motors can be obtained by changing of connections of cells and modules within the solar cell array [Braunstein and Zinger, 1981]. This can only give discrete matching. Two to three different series - parallel arrangements of modules can give up to 15% increase in efficiency. More than three different states (connections) are not economically viable [Zinger and Braunstein,1981] and [Salameh and Dagher,1990]. Continuous optimum matching can be obtained by changing module connections along with field current variation [Faldella et al., 1991].

Choppers are also used for continuous matching purpose. A simple step-up chopper circuit can consist of a single power transistor and an inductor. There exists a unique duty ratio which gives optimum utilization efficiency at all insolation levels. This property makes this technique attractive since it eliminates the continuous adjustment of the duty ratio [Al-humairi, 1992]. Optimum matching can also be obtained by predetermining the flux constant  $K$  of the motor for a particular load type and the location of the installation before placing the order for the same. Due to the losses in the motor, the maximum gross mechanical power characteristic is different from maximum power characteristics of the array. Flux constant  $K$  is determined [Saied,1988] to operate the motor at its maximum mechanical power points for different insolutions and then  $K$  is weight-averaged to adjust for different duration of insolation intervals. D.C. motor with this  $K$  can be directly coupled to PV array for optimum matching.

Similar study is carried on in [Saied,1991] for a D.C. motor connected to PV array via a chopper. Here output energy is plotted with respect to flux constant  $K$  and the optimum range for  $K$  and corresponding value for duty ratio of the chopper is decided. Comparison of operation between various types of D.C. motors shows that separately excited D.C. motors are most suitable for such systems. Efficiency of D.C. motors for part load or at light load is high. Also since the source is D.C., therefore D.C. motors become the obvious choice to be run by PV array. But brushes in D.C. motor need replacement (after 4000 h of operation) otherwise commutator may get damaged.

A D.C. motor can be replaced by (Inverter + Induction motor) with improved part load efficiency arrangement. In reference [Bhat et al.,1987] induction motor/pump system is connected to PV array via a chopper and an inverter (VSI, Voltage Source Inverter). Here maximum power is extracted for any insolation condition and optimum  $V/f$  relationship is used for the motor control which is not quite correct.

As mentioned earlier, maximum mechanical output power characteristic of the motor is different from the maximum electrical power characteristic of the array and also optimum  $V/f$  relation will be different as pump head (load) varies. Induction motor-pump system can also be connected via a chopper and CSI (Current Source Inverter) [OJO,1991] instead of VSI.

Reference [Enslin and Snyman,1991] suggests that traditional cascaded PV power conditioning system, consisting of many stages such as maximum power point tracker, regulator, battery and an inverter can be replaced by a composite circuit comprising all the above functions in a circuit. But the circuit given here is only for constant frequency output whereas for improving part load-efficiency of induction motor, we need variable frequency supply. Proper selection of solar array and battery size, known as sizing problem [Jaboore et al.,1991] is based on annual simulation using actual meteorological (insolation and temperature) and typical load data pertinent to the place of installation.

The procedure determines the useful (effective), dumped (wasted) and commercial energy components in the system. Optimum PV- and battery sizes are selected where effective energy is maximum.

The residential photovoltaic power conditioning system is studied in [Bose et al.,1985]. High frequency link scheme is used here, giving considerable weight reduction of the power converter and maintaining a unity power factor at the AC line terminal. Micro computer is used for array current feedback control, maximum power tracking, sequencing and safe zone steering control.

[Ranade et al.,1989], present islanding problem - a phenomenon in which one or more inverters continue to operate and keep the system energized even after the utility supply is disconnected. It is shown that islanding can be virtually eliminated through the use of destabilized feedback controls for the inverters.

### 1.3 Scope and Objective of the Present Work

As is evident from the review of literature, the load matching of the array has not been studied for air-conditioning, refrigeration and heating. The present work aims at finding the array size for specified design parameters. A code has been developed to calculate load of the system as a function of time. The size of the array is selected seeing the load requirement in a day. As the load as well as the available PV array output keep changing with time, it is advisable to always employ a battery. Thus, load matching problem becomes a problem of a battery connected with PV array.

The present work also incorporates the uncertainties in the weather conditions using fuzzy set theory. A methodology for designing the array size using fuzzy set theory is suggested. This approach will be helpful to produce an economical and reliable design.

For a given size of the array, the cells can be arranged in the series and parallel in

various ways. They should be arranged in a manner to give maximum output over the day. One objective of the work is to find out the optimum arrangement of the cells in the PV array. The PV array should be positioned in a manner such that it gives maximum output and covers the roof properly reducing the load due to radiation. This work addresses these aspects.

Finally, the gain to environment due to use of PV array operated systems is discussed. At present the solar energy may not be competitive with the conventional sources except at remote places where other sources of energy can reach only with difficulty. However, if the pollution aspect is considered, the solar energy may be a good alternative to conventional sources of energy.

It is shown that if in place of conventional electricity photovoltaic energy is used then for a room size as given in Appendix G, CO<sub>2</sub> at the rate of 3.75 kg/s at the peak time can be saved. Also for the same size of room amount of ash particulates saved is 0.8 kg/h.

## 1.4 Organization of Thesis

The thesis is organized in the following manner. Chapter 1 presents introduction, literature review and the objective of the work. The methodology to find out the array size is presented in Chapter 2. The methodology to find out cooling/heating/refrigeration load as a function of time is discussed here. Chapter 3 is on the application of fuzzy set theory for estimation of array size. Chapter 4 is on the optimum arrangement of series and parallel cells in the array. The positioning of array and the environmental issues are discussed in Chapter 5. Chapter 6 is on conclusions and scope for further work.

## Chapter 2

# DETERMINATION OF PHOTOVOLTAIC ARRAY SIZE

### 2.1 Introduction

Airconditioning, refrigeration and heating essentially require same appliances. In these, either a vapour-compression system or a vapour-absorption system is employed [Prasad, 1993]. There is a requirement of electricity for running the compressor in the vapour-compression system and pump in the vapour-absorption system. The required electrical energy may be obtained by photovoltaic array. Since the photovoltaic array is a costly item, its size for a specific purpose has to be selected judiciously.

In this chapter methodology to find out the size of the array is described for airconditioning, heating and refrigeration. Both, vapour-compression and vapour-absorption systems have been considered. A software has been developed for finding the total heat load requirement and the size of the array. The determination of the size of array is the most important part of the photovoltaic airconditioning, heating and refrigeration design as this gives the idea about the space occupied by the array and the cost

required. Subsequent chapters will be dealing with the arrangement of the array.

## 2.2 Characteristics of Photovoltaic Array

The photovoltaic array output varies with solar insolation and temperature. The array characteristics has been described in reference [Khouzam, 1990]. The V-I equation of a solar array generator is expressed by:

$$V = AV_T \cdot \ln\{(I_{Ph} - I + I_r)/I_r\} - I \cdot R_s \quad (2.1)$$

where,  $I$  is the load current,  $I_{Ph}$  is the array photo-generated current,  $I_r$  is the total reverse saturation current,  $R_s$  is the total series resistance and  $AV_T$  is the equivalent thermal voltage of the array. If the array generator is composed of  $N_s$  series cells and  $N_p$  parallel strings, then,

$$I_{Ph} = I_1 \cdot N_p \quad (2.2)$$

$$I_r = I_s \cdot N_p \quad (2.3)$$

$$R_s = R_c \cdot N_s / N_p \quad (2.4)$$

$$AV_T = N_s \cdot V_T \quad (2.5)$$

where,  $I_1$  is the photo-generated current per cell,  $I_s$  is the reverse saturation current per cell,  $R_c$  is the series resistance per cell, and  $V_T$  is the cell thermal voltage.

The effect of the array temperature on the reverse saturation current, the photocurrent, and the thermal voltage is given by [Appelbaum, 1986]

$$I_r(T) = I_r(T_0) \cdot (T/T_0)^3 \cdot \exp\{-b(1/T - 1/T_0)\} \quad (2.6)$$

$$I_{Ph}(T) = I_{Ph}(T_0) \cdot [1 + a(T - T_0)] \quad (2.7)$$

$$AV_T(T) = AV_T(T_0) \cdot T/T_0 \quad (2.8)$$



where,  $T_o$  is the cell reference temperature (at 288.15 K), and  $a$  and  $b$  are coefficients dependent on the type of semiconductor material used and the manufacturing process. The output power of the array depends on the loading and is given by

$$P = I.AV_T. \ln\{I_{Ph} - I + I_r\}/I_r\} - I^2.R_s \quad (2.9)$$

The array photo generated current varies with time over a day. Anis et al. [1985] and Appelbaum [1987] have taken a standard clear sky insolation model in which the following equation holds good:

$$I_{Ph} = I_G. \sin(w) \quad (2.10)$$

where,  $I_G$  is the array photo-generated current at solar noon, and  $w$  is the solar hour angle. Actually the variation of  $I_{Ph}$  over the day is not sinusoidal, rather it is proportional to the radiation falling on the array. In the present model, it is assumed that the following relation holds good for the  $I_{Ph}$ .

$$I_{Ph} = I_G \frac{(\text{radiation at a particular time})}{(\text{radiation at solar noon})} \quad (2.11)$$

The above model is validated by doing the experiments on an inclined photovoltaic array. Figures (2.1-2) compare the power output obtained experimentally and its comparison with the theoretical prediction using the proposed model. It is seen that the power prediction from the model is in good agreement with the experimental results.

The next section describes the procedure for finding the solar radiation at a particular time. The V-I and P-V characteristics of PV array at different level of insolation are shown in Figure (2.3). As  $I$  is varied,  $V$  varies, therefore for a particular  $(V_{mp}, I_{mp})$  power input is maximum for a given insolation. The array maximum power is found by differentiating power ( $P$ ) in equation (2.9) with respect to load current  $I$  and equating to zero. This gives the following equation:

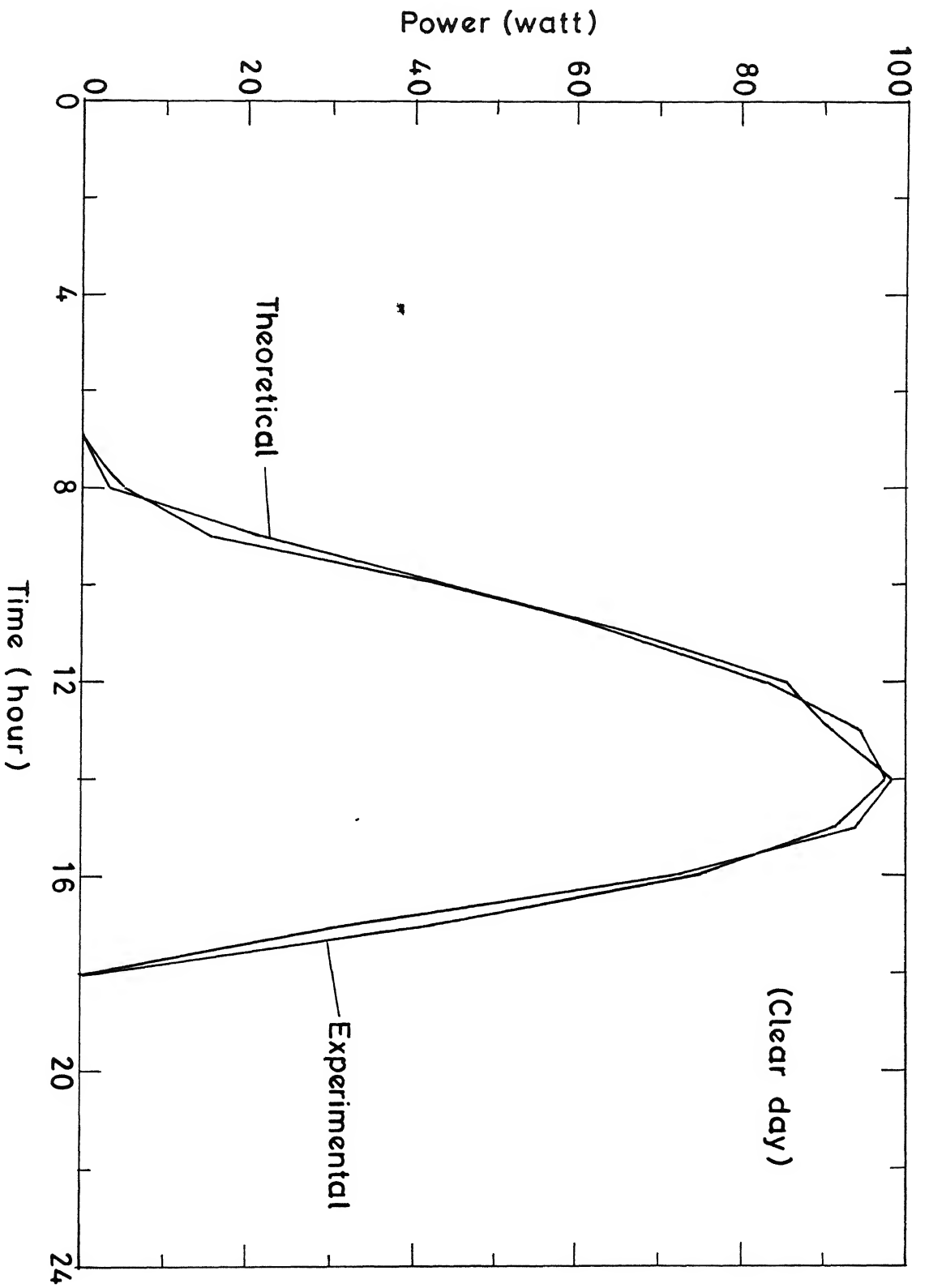


Fig. 2.1 PV array output experimental and theoretical (clear sky day in March)

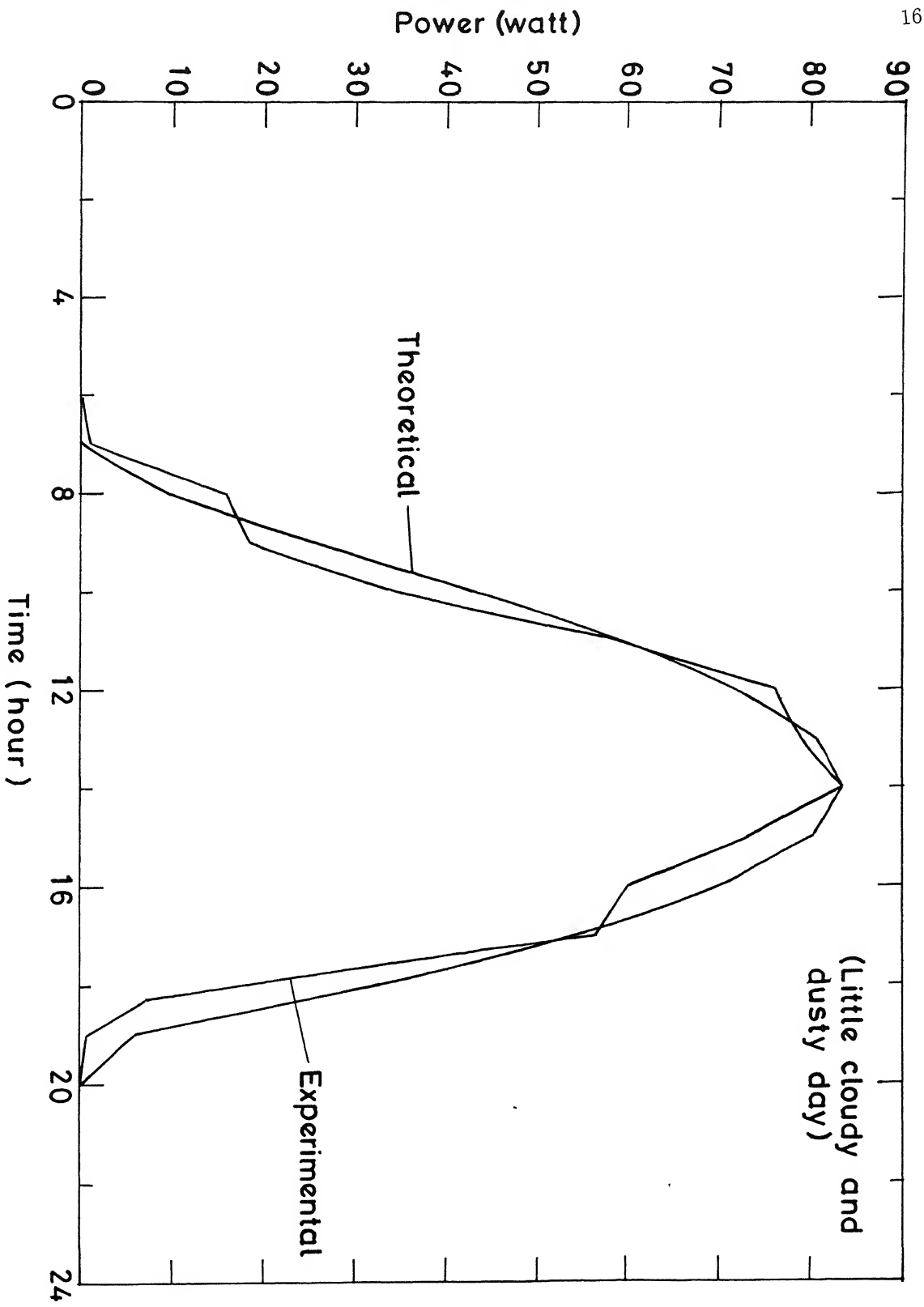


Fig. 2.2 PV array output, Experimental and theoretical (little cloudy and dusty day in May)

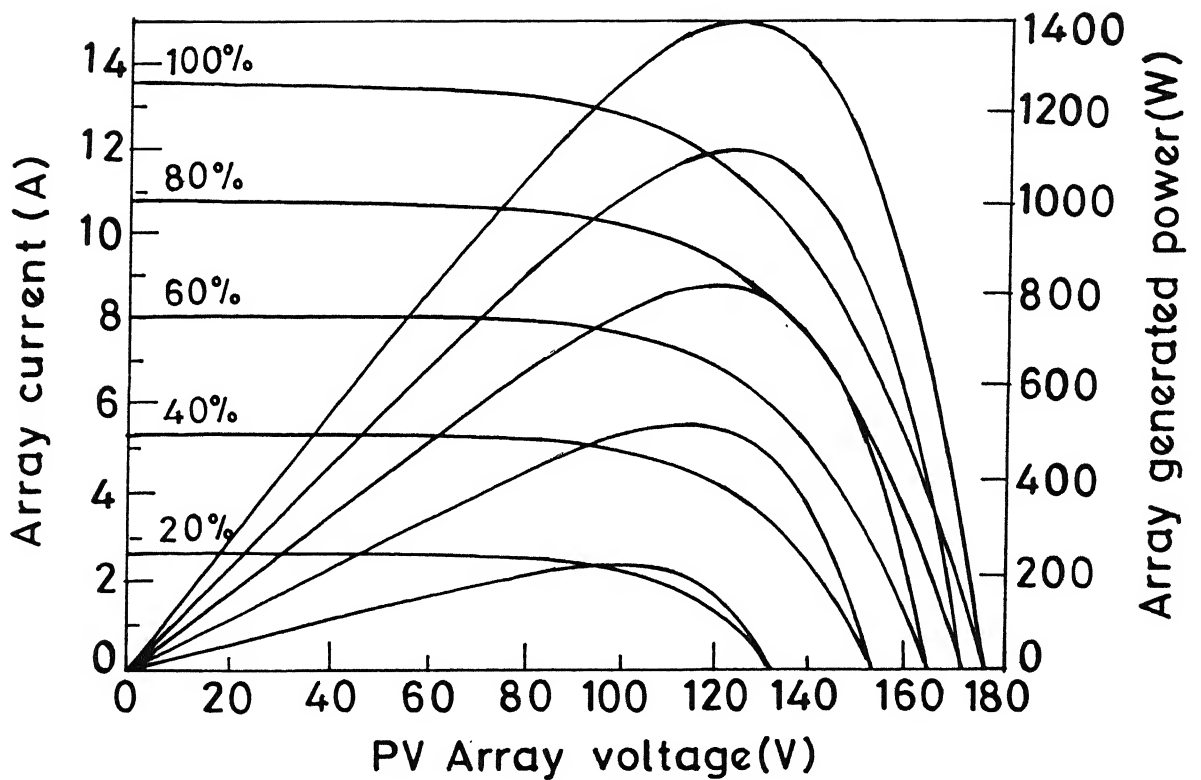


Fig.2.3 Effect of Insolation on the I-V and P-V characteristics of crystalline silicon solar cells.

$$I_{Ph} = I_{mp} + I_r \{ \exp[(2I_{mp}R_s/AV_T) + I_{mp}/(I_{Ph} - I_{mp} + I_r)] - 1 \} \quad (2.12)$$

The maximum power point voltage,  $V_{mp}$  can then be found from equation (2.1) by replacing  $I$  by  $I_{mp}$ . The maximum power,  $P_{mp}$  is then given by:

$$P_{mp} = V_{mp} \cdot I_{mp} \quad (2.13)$$

For the efficient utilization of PV array, the array should be operated at maximum power point voltage.

## 2.3 Radiation Falling on the Surface

Based on an analysis of U.S. data, ASHRAE [1982] has given a method for estimating the hourly variation of global and diffused solar radiation falling on a horizontal surface on a clear day. The relationship may be developed which find the radiation on an inclined surface. It is advantageous to describe some definitions first. If  $\theta$  is the angle between an incident beam of flux  $I_{bn}$  and the normal to a plane surface, then the equivalent flux falling normal to the surface is given by  $I_{bn} \cos \theta$ . The angle  $\theta$  can be related by a general equation to  $\phi$  the latitude,  $\delta$  the declination,  $\gamma$  the surface azimuth angle,  $\omega$  the hour angle, and  $\beta$  the slope. Each of these will first be defined.

The latitude  $\phi$  of a location is the angle made by the radial line joining the location to the centre of the earth with the projection of the line on the equatorial plane. By convention, the latitude is measured as positive for the northern hemisphere.

The declination  $\delta$  is the angle made by the line joining the centers of the sun and the earth with its projection on the equatorial plane. It arises by virtue of the fact that the earth rotates about an axis which makes an angle of approximately  $66.5^\circ$  with the plane of its rotation around the sun. The declination angle varies from a maximum

value of  $+ 23.45^\circ$  on June 21 to a minimum value of  $-23.45^\circ$  on December 21. It is zero on the two equinox days of March 21 and September 22. Cooper [1969] has given the following simple relation for calculating the declination:

$$\delta(\text{in degrees}) = 23.45 \sin \left[ \frac{360}{365} (284 + n) \right] \quad (2.14)$$

where  $n$  is the day of the year.

The surface azimuth angle  $\gamma$  is the angle made in the horizontal plane between the line due south and the projection of the normal to the surface on the horizontal plane. By convention, the angle is taken to be positive if the normal is east of south and negative if west of south.

The hour angle  $w$  is an angular measure of time and is equivalent to  $15^\circ$  per hour. It is measured from noon based on local apparent time (LAT), being positive in the morning and negative in the afternoon. The term ‘local apparent time’ is defined below.

**Local Apparent Time** - This time can be obtained from the standard time observed on a clock by applying two corrections. The first correction arises because of the difference between the longitude of a location and the meridian on which the standard time is based, the correction has a magnitude of 4 minutes for every degree of difference in longitude. The second correction called the equation of time correction is due to the fact that the earth’s orbit and rate of rotation are subject to small perturbation. This correction is based on experimental observation and is plotted in Figure (2.4). Thus,

$$\begin{aligned} \text{Local apparent time} &= \text{Standard time} \mp \\ &4(\text{Standard time longitude} - \text{longitude of location}) \\ &+ (\text{Equation of time correction}) \end{aligned} \quad (2.15)$$

The negative sign in the first correction is applicable for the eastern hemisphere while the positive sign is applicable for the western hemisphere.

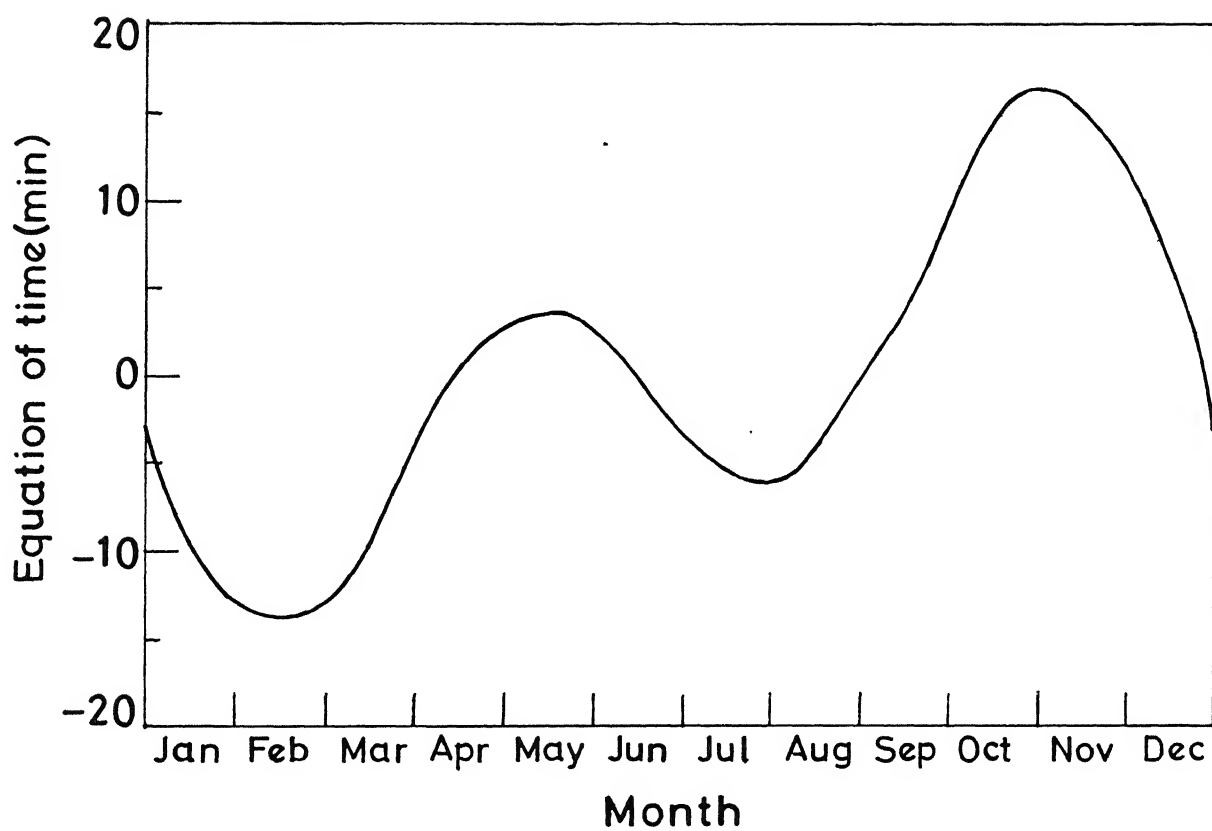


Fig. 2.4 Equation of time correction

Another way of defining solar hour angle is like this,

$$w = 15(t - 6) \quad (2.16)$$

where  $w$  is in degrees,  $t$  is the solar time, which is related to actual time  $t_a$  by:

$$t = 6.0 + \frac{6.0(t_a - t_{sr})}{(t_{ss} - t_{sr})} \quad (2.17)$$

where  $t_{sr}$  and  $t_{ss}$  are the sunrise and sunset times respectively. The sunrise and sunset times at a particular place are given by:

$$t_{sr} = 12 - \frac{1}{15} \cos^{-1}(-\tan \phi \cdot \tan \delta) \quad (2.18)$$

$$t_{ss} = 12 + \frac{1}{15} \cos^{-1}(-\tan \phi \cdot \tan \delta) \quad (2.19)$$

Here  $\phi$  is the latitude of the place and  $\delta$  is declination, given by equation (2.14).

The slope  $\beta$  is the angle made by the plane surface with the horizontal. It is taken to be positive for surfaces sloping towards the south and negative for surfaces sloping towards the north.

The relationship between various angles is :

$$\begin{aligned} \cos \theta &= \sin \phi (\sin \delta \cdot \cos \beta + \cos \delta \cdot \cos \gamma \cos w \sin \beta) \\ &\quad + \cos \phi (\cos \delta \cos w \cos \beta - \sin \delta \cdot \cos \gamma \sin \beta) \\ &\quad + \cos \delta \sin \gamma \sin w \sin \beta \end{aligned} \quad (2.20)$$

For horizontal surface,  $\beta$  is zero and

$$\cos \theta = \sin \phi \cdot \sin \delta + \cos \phi \cdot \cos \delta \cdot \cos w \quad (2.21)$$

The angle  $\theta$  in this case is called the zenith angle and is denoted by  $\theta_z$ .

The global radiation  $I_g$  reaching a horizontal surface on the earth is given by

$$I_g = I_b + I_d \quad (2.22)$$



where

$I_g$  = hourly global radiation

$I_b$  = hourly beam radiation

$I_d$  = hourly diffused radiation

Now,

$$I_b = I_{bn} \cos \theta_z \quad (2.23)$$

where  $I_{bn}$  is the beam radiation in the direction of the rays and  $\theta_z$  is the angle of incidence on a horizontal surface, i.e., the zenith angle. Thus,

$$I_g = I_{bn} \cos \theta_z + I_d. \quad (2.24)$$

In the ASHRAE model, it is postulated that for a clear cloudless day

$$I_{bn} = A \exp[-B / \cos \theta_z] \quad (2.25)$$

and

$$I_d = C I_{bn} \quad (2.26)$$

where A, B and C are constants whose values have been determined from an analysis of data for the U.S.A. and are given in [Sukhatme, 1994], and are reproduced in Appendix A.

**Radiation on a Tilted Surface:** The radiation on a tilted surface is composed of three parts, beam radiation, diffused radiation and the reflected radiation.

- (1) Beam radiation: The ratio of the beam radiation flux falling on a tilted surface to that falling on a horizontal surface is called the tilt factor  $R_b$  for beam radiation and is given by:

$$R_b = \frac{\cos \theta}{\cos \theta_z} \quad (2.27)$$

- (2) Diffused Radiation: The tilt factor  $R_d$  for diffused radiation is the ratio of the diffused radiation flux falling on the tilted surface to that falling on a horizontal surface. It is given by:

$$R_d = \frac{1 + \cos \beta}{2} \quad (2.28)$$

It is to be noted that  $(1 + \cos \beta)/2$  is the radiation shape factor for a tilted surface with respect to the sky.

- (3) Reflected Radiation: Assuming that the reflection of the beam and diffused radiations falling on the ground is diffused and isotropic, and that the reflectivity is  $\rho$ , the tilt factor,  $R_r$ , for reflected radiation is given by

$$R_r = \rho \left[ \frac{1 - \cos \beta}{2} \right] \quad (2.29)$$

The flux  $I_T$  falling on a tilted surface at any instant is thus given by

$$I_T = I_b R_b + I_d R_d + (I_b + I_d) R_r \quad (2.30)$$

## 2.4 Estimation of Cooling/Heating/Refrigeration Load

The design of an airconditioning/heating/refrigeration plant requires corresponding load to be estimated with sufficient accuracy. The load calculation needs the information about climate and inside conditions desired. A generalised computer programme for hourly load has been developed. The procedure is similar to that given in ASHRE [1982].

For the ambient temperature variation, a mathematical model [Alford et al., 1939] has been adopted which gives a close approximation to an average value equal to the mean daily temperature range. Therefore, the final form of the expression comes out

to be a harmonic series of first order.

$$T_o = \left( \frac{T_{min} + T_{max}}{2} \right) + \left( \frac{T_{max} - T_{min}}{2} \right) \cos[15(t - t_{sr} - 1)] \quad (2.31)$$

where  $T_o$  is the outside temperature and  $T_{min}$  and  $T_{max}$  are the minimum and maximum temperature in a day. In deriving the above relation, the assumption is that minimum temperature over the day occurs one hour before the sunrise, and maximum temperature occurs 12 hours after that. This equation has been verified for Kanpur conditions by K. Sekar [1986].

The Sol-air temperature :- For heat transfer calculations, it is convenient to combine the effects of outside air temperature and solar radiation clustered into a single fictitious quantity called sol-air temperature ( $T_s$ ). The rate of heat transfer,  $q$ , from outside to inside surface of a sunlit structure, considering the effect of emissivity ( $\epsilon$ ) of the surface may be written as,

$$q = h_o(T_o - T_{w,o}) + a_t \cdot I_t - \epsilon \Delta R \quad (2.32)$$

where,

$h_o$  is outside air convective heat transfer coefficient ( $W/m^2 K$ ),

$T_o$  is outside air temperature (K),

$T_{w,o}$  is temperature of the outside surface(K),

$a_t$  is absorptivity of the structure, and  $I_t$  is total intensity of solar radiation ( $W/m^2K$ )

$\epsilon$ , emissivity of the surface,  $\Delta R = 63 W/m^2$  for the horizontal surface and zero for the vertical surface. The heat transfer can also be written as

$$q = h_o(T_s - T_{w,o}) \quad (2.33)$$

Comparing the equation (2.32) and equation (2.33), the expression for *sol-air temperature*, considering emissivity of the surface [ASHRE, 1982] is:

$$T_s = T_o + a_t \cdot I_t / h_o - \epsilon \Delta R / h_o \quad (2.34)$$

When emissivity of the surface is considered,  $T_s$  is found to be about 0.3 K less than that of the case when emissivity is ignored. The outside air convection heat transfer coefficient,  $h_o$  is calculated as follows [Kadambi and Hatchinsen,1968]:

$$\begin{aligned}
h_o &= 14.278 + 3.559V_w \quad \text{for very smooth surface} \\
&= 18.423 + 3.81V_w \quad \text{for smooth surface} \\
&= 26.55 + 5.0663V_w \quad \text{for rough surface} \\
&= 28.64 + 6.364V_w \quad \text{for very rough surface}
\end{aligned} \tag{2.35}$$

where  $V_w$  is the design velocity of the outside air in km/h and  $h_o$  is kW/m<sup>2</sup> K.

Selection of Indoor Conditions: - The field studies [Malhotra, 1967] reveal that in India, for hot and humid climates, the comfort zone is between 295 K and 297.5 K effective temperature.

Here the comfort condition is taken as follows:

$$T_{db} = 297K, R_H = 0.65, V = 0.8 \text{ m/min.}$$

The components of cooling load which are considered here are as follows:

- (a) Heat Transfer Through Walls and Roofs - It is calculated by time lag and decrement factor method [Arora,1993]. Combined effect of outside air temperature and incident solar radiation intensity is accounted, as sol-air temperature is used for all calculations. Thus, the structural heat load  $\dot{Q}_{st}$  including solar radiation is found to be

$$\dot{Q}_{st} = \sum_{k=1}^5 \dot{Q}_k = \sum_{K=1}^5 \left\{ (UA)_K \left[ (\bar{T}_{sk} - T_{in}) + \lambda_k (T_{sk}(t_a - \tau)) - \bar{T}_{sk} \right] \right\} \tag{2.36}$$

where  $\bar{T}_{sk}$  is the mean outside sol-air temperature on the  $k^{th}$  surface of the structure,  $\lambda_k$  is the corresponding decrement factor,  $\tau$  is the time lag and  $UA$  is

the product of overall heat transfer coefficient and surface area.  $T_{sk}(t_a - \tau)$  is the sol-air temperature at  $(t_a - \tau)$  time.  $T_{in}$  is the inside design temperature of the room and  $t_a$  is the actual time at which cooling load is being calculated.

To obtain the overall heat transfer coefficient,  $U$ , is found as follows. It has been assumed that the walls and roofs have three layers of materials with thickness  $x_i$  and thermal conductivity  $k_i$  of the  $i^{th}$  layer of the structural material. In the present case, the values are taken from ASHRE[1982].  $U$  is given by

$$U = \frac{1}{\left(\frac{1}{h_o} + \sum_{i=1}^3 \frac{x_i}{k_i} + \frac{1}{h_i}\right)} \quad (2.37)$$

Here,  $h_i$  is the inside convective heat transfer coefficient.

- (b) Heat Transmission Through Glass Windows - Solar radiation, direct and diffused, incident upon a glass surface is, in parts, transmitted, reflected and absorbed. Thus  $\tau$ ,  $r$  and  $a$  represent the respective fractions known as transmissivity, reflectivity and absorptivity, then

$$\tau + r + a = 1 \quad (2.38)$$

The heat gain of a space through glass then comprises:

1. All the transmitted radiations
2. A part of the absorbed radiation that travels to the room, and
3. The heat transmitted due to the temperature difference between the outside and inside.

The direct radiation enters the space only if the glass is receiving the direct rays of the sun. The diffused radiation enters the space even when the glass is not facing the sun.

It can be shown [Arora, 1993] that the heat gain of space is

$$Q = (A_{sun} \tau_D I_D + A \tau_d I_d) + \frac{A_{sun} a_D I_D + A a_d I_d}{1 + \frac{f_o}{f_i}} + UA(T_o - T_{in}) \quad (2.39)$$

where  $A_{sun}$  is the glass area directly exposed to the sun,  $A$  is the total glass area. Subscript  $D$  and  $d$  denote the terms for direct and diffused radiations respectively.  $U$ , the overall heat transfer coefficient is given by

$$\frac{1}{U} = \frac{1}{f_i} + \frac{1}{f_o}$$

The values of transmissivity and absorptivity of ordinary glass are taken from [Arora, 1993] and are reproduced in Appendix B.

- (c) Infiltration Load - Infiltration is the leakage of outdoor air into a building through cracks and opening caused by pressure difference across the boundary surfaces. The exchange of air may lead to both heat and moisture gain for the space. The volume of infiltration is related in terms of the room volume and tabular values are available in [Prasad, 1993] and are reproduced in Appendix C. The expression for the infiltration load is:

$$Q_{infil} = \frac{V_{room}}{v_{air}} \times N_{ACH}(h_a - h_{i,a})/24 \text{ kW} \quad (2.40)$$

where  $V_{room}$  is the volume of the room,  $v_{air}$  is the specific volume of air at outside temperature,  $N_{ACH}$  is the number of air changes/day,  $h_a$  and  $h_{i,a}$  are the enthalpies of outside and inside air, respectively.

- (d) Ventilation Load - Ventilation air requirement can be taken from tables given in Table A.7 of reference [Prasad, 1993], reproduced in Appendix D. The procedure for calculating ventilation load is the same as that of infiltration load.

(e) Internal Heat Gains - It comprises occupancy load, lighting load and appliances load. Occupancy load is calculated from values given in Table 19.1 of Arora [1993] and reproduced in Appendix E. Lighting and appliance load is calculated by adding total wattage of lights and equipments.

In case of refrigerators, internal heat gain consists of loads due to storing of fruits and vegetables and for making ice. The information needed for calculating this is as follows:

- (i) The average amount of commodities present in the refrigerator
- (ii) The average amount of commodities which is replaced at each hour.
- (iii) The per hour ice production.

The heat of respiration of products is given in Table 19.3 of [Arora, 1993] and reproduced in Appendix F.

The total load at a particular time is found by adding all the components of load at that time. Seeing the hourly load, a suitable size of the system may be selected, and components can be designed accordingly. Integrating load with respect to time using Simpson's formula, the energy requirement for 24 hours period is estimated, which is needed for the estimation of PV array size.

## 2.5 Estimation of Size of PV Array

Current  $I_{mp}$  corresponding to maximum power can be found from equation (2.12). The Newton-Raphson method fails to give reasonable results, because first derivative of the function with respect to current is greater than 1. Interval reducing method [Pike, 1986] is used to solve equation (2.12), where absolute value of the function is

minimized for  $I_{mp}$  values between  $.75I_{Ph}$  and  $.95I_{Ph}$ . In this method the convergence is guaranteed. The maximum power,  $P_{mp}$  can then be found from equation (2.13). The  $P_{mp}$  is found at different times in a day and is integrated with respect to time using Simpson's formula to find out energy available in 24 hours.

Using DO loops, energy available in a day is computed for each combination of  $N_s$  and  $N_p$ . The combinations which give total electrical energy in a day close to the electrical load requirement for refrigeration (refrigeration load/coefficient of performance) are printed. A suitable combination of  $N_s$  and  $N_p$  can then be selected to meet refrigeration requirement. Knowing  $N_s$  and  $N_p$  one can find the space needed for PV array.

## 2.6 Results and Discussion

The array size was estimated for airconditioning, heating and refrigeration. The following subsections discuss typical results for the estimation of photovoltaic array.

### 2.6.1 Results for airconditioning

The programme was run for the PV array estimation for airconditioning a room in Kanpur. The particulars of room are given in Appendix G. Figure(2.5) shows variation of cooling load with time for 24 hours period for the month of May (month of maximum heat), that is why May has been taken for design conditions for cooling load calculation [Kadambi and Hutchinson, [1968]] . It is clearly seen that cooling load varies drastically with time. Figure (2.6) shows the electrical energy requirement for vapour-compression and vapour-absorption system. For calculating energy requirement, values of COP for compression and absorption system are taken as 3.84 and 1.2 respectively, from section 7.1.3 and Chapter 7 of reference [Prasad, 1993]. The graph of electrical energy



requirement versus time for vapour-compression system has been obtained by dividing cooling load by COP, while for the vapour-absorption system it is assumed that starting from 3 hours after sunrise upto 2 hours before sunset all the power required can be obtained by solar collectors and therefore electrical power requirement is zero. Rest of the time, electrical power required is obtained by dividing cooling load by COP. The total electrical energy requirement in a day is found from the area under the electrical power requirement curve. From Figure (2.6), we find that total energy required is 15.91 kWh for the vapour-compression system and 23.80 kWh for vapour-absorption system. A 1730 W array in the case of vapour-compression system and 2630 W array in the case of vapour-absorption system is needed in order to meet electrical energy requirement. The powers available from 1730 W and 2630 W arrays are shown for the month of May in Figure (2.7). The PV cell data are given in Appendix H. It is found from the computer program that 320 series cells and 22 parallel strings will be required for 1730 W array. For 2630 W array 320 series cells and 33 parallel strings are needed. The size(area) of the array required is estimated referring [Tata BP Solar India Ltd. Product Catalogue]. The array size for 1730 W array is 12m x 12m. For 2630 W array, it is 12m x 20m. Figure (2.8) shows the cooling load at different times in the month of September and Figure (2.9) is electrical power needed in that month for the two systems. The powers available from the 1730 W and 2630 W arrays are shown for the month of September in Figure (2.10). It is seen that powers available in this month are more than the requirement. The excess power is stored in the battery.

Table (2.1) shows total energy required and energy available from PV array from April to October, for both vapour-compression as well as vapour-absorption systems. The energy required for vapour-compression systems is much lower than that of vapour absorption system because COP of vapour-compression system is higher than that of vapour-absorption system. It is seen that when array is selected on the basis of the

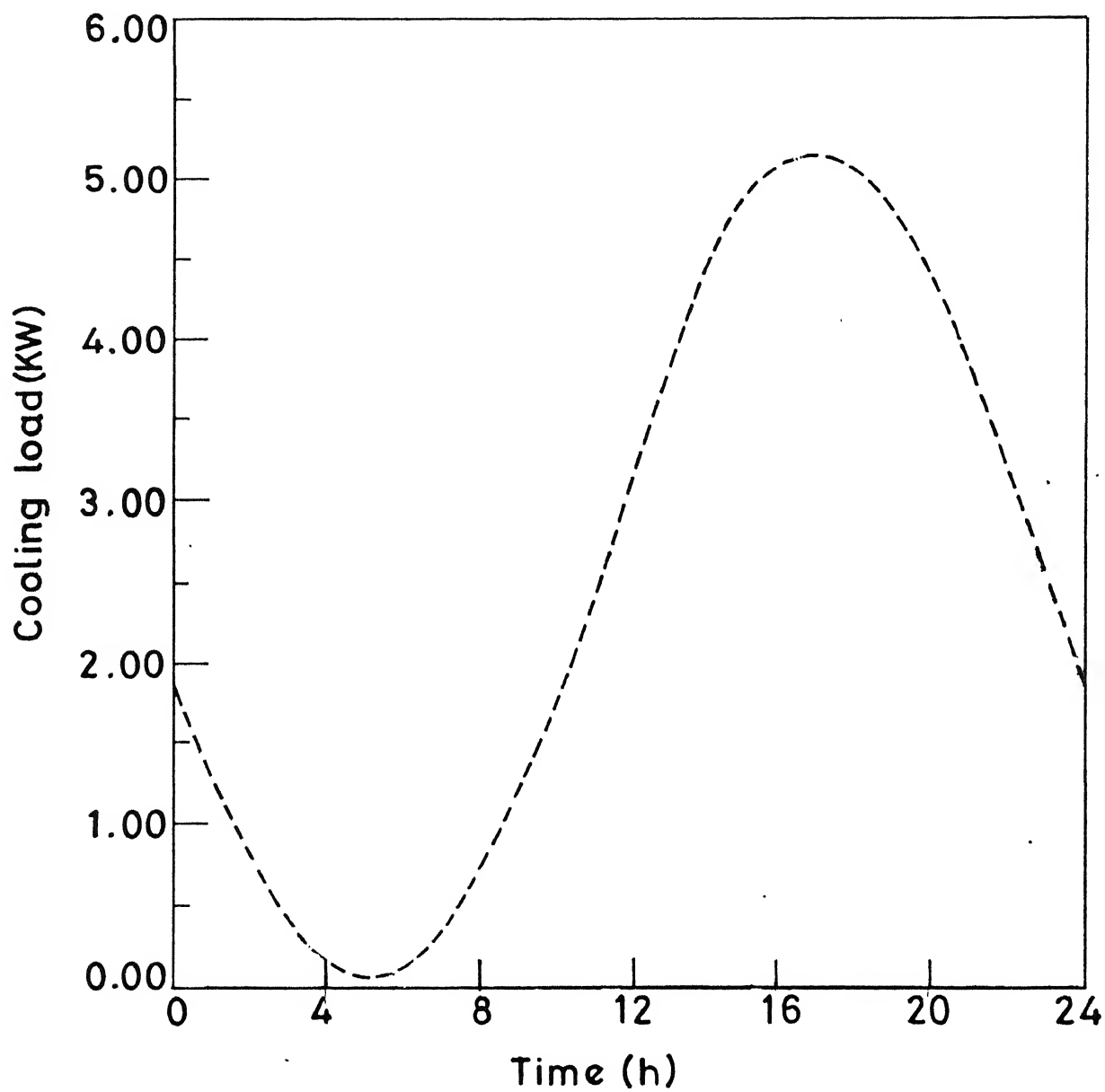


Fig.2.5 Cooling load in May .

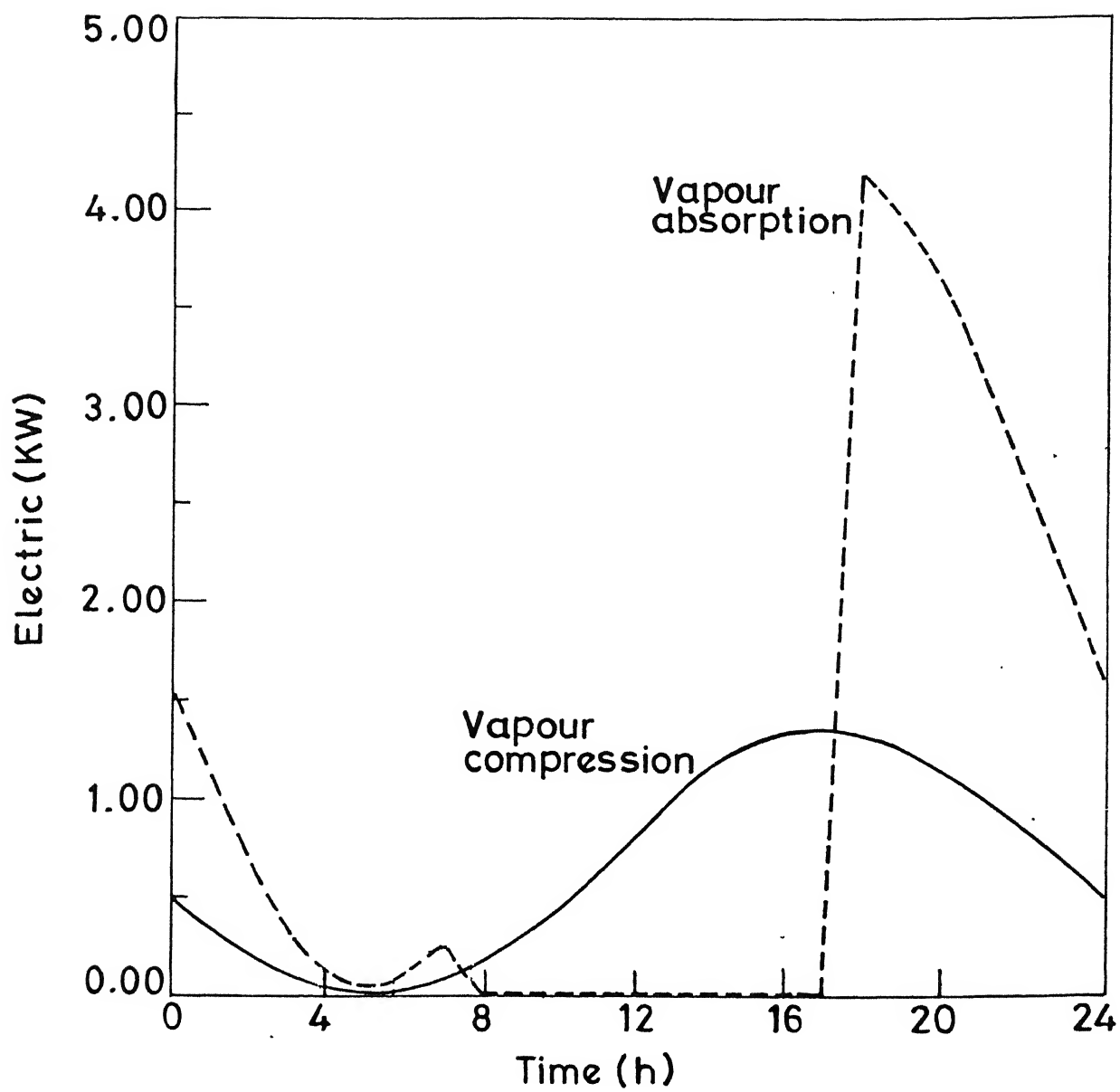


Fig.2.6 Electric power requirement

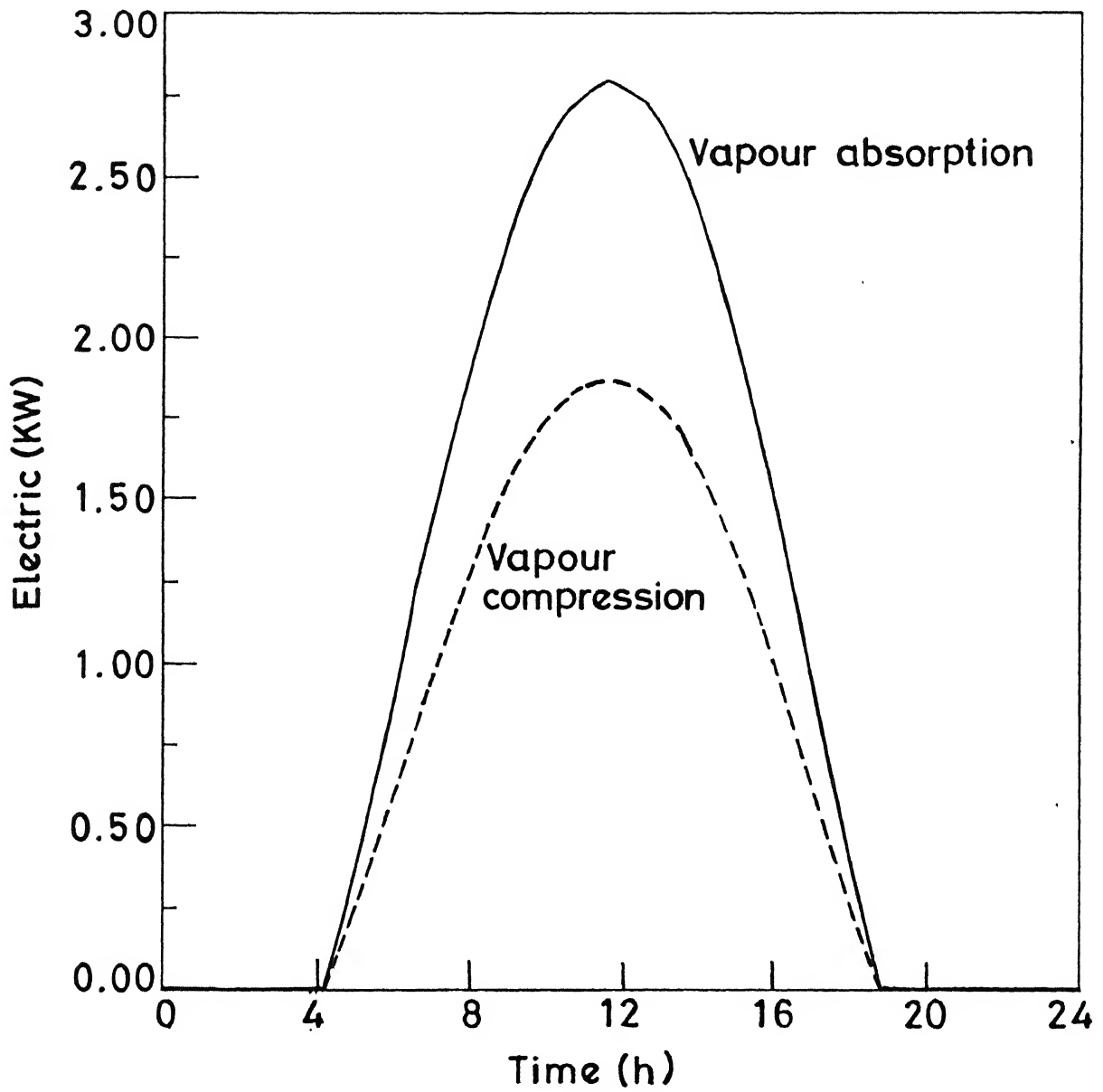


Fig.2.7 Electric power available in May.

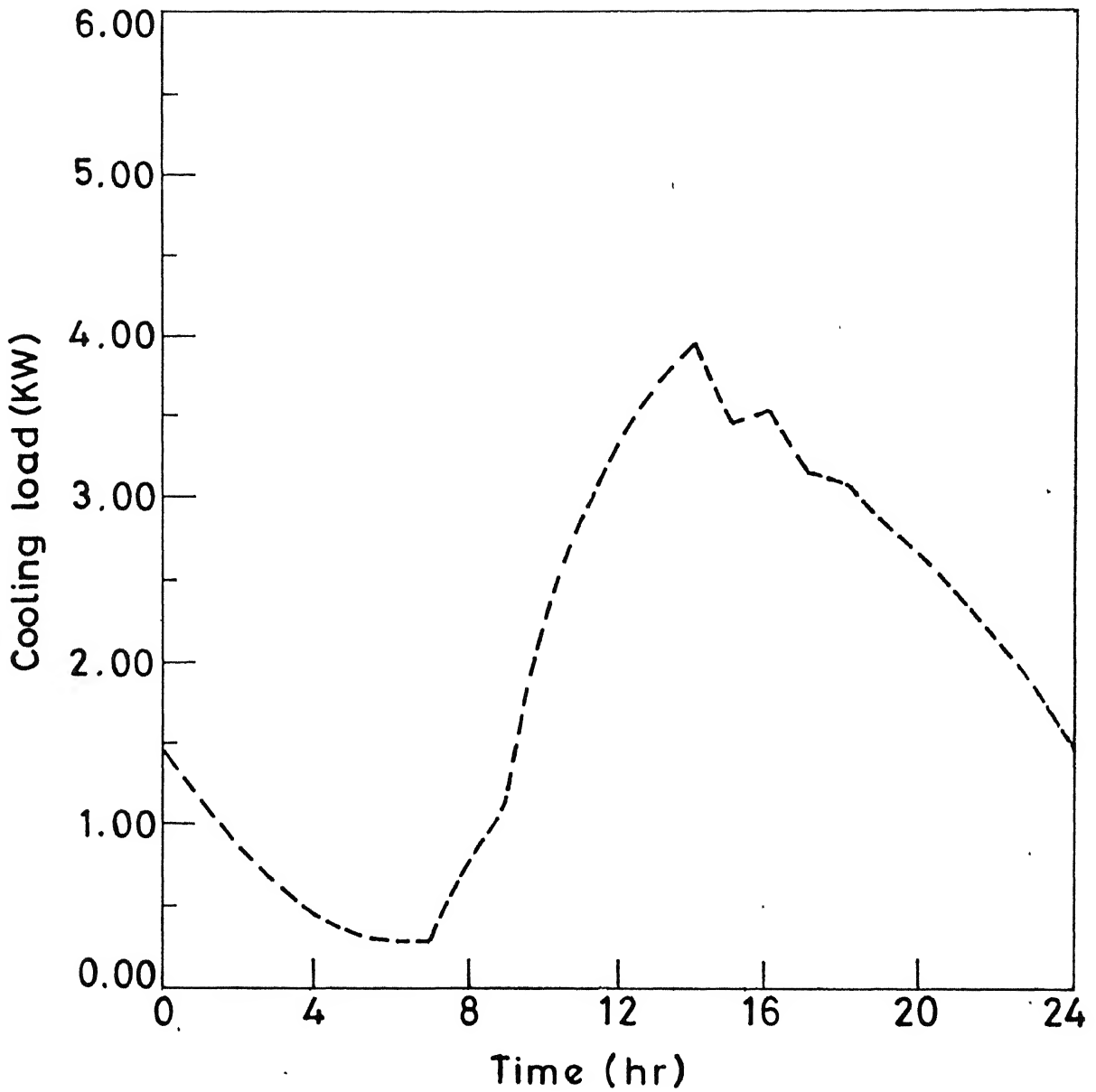


Fig.2.8 Cooling load in September.

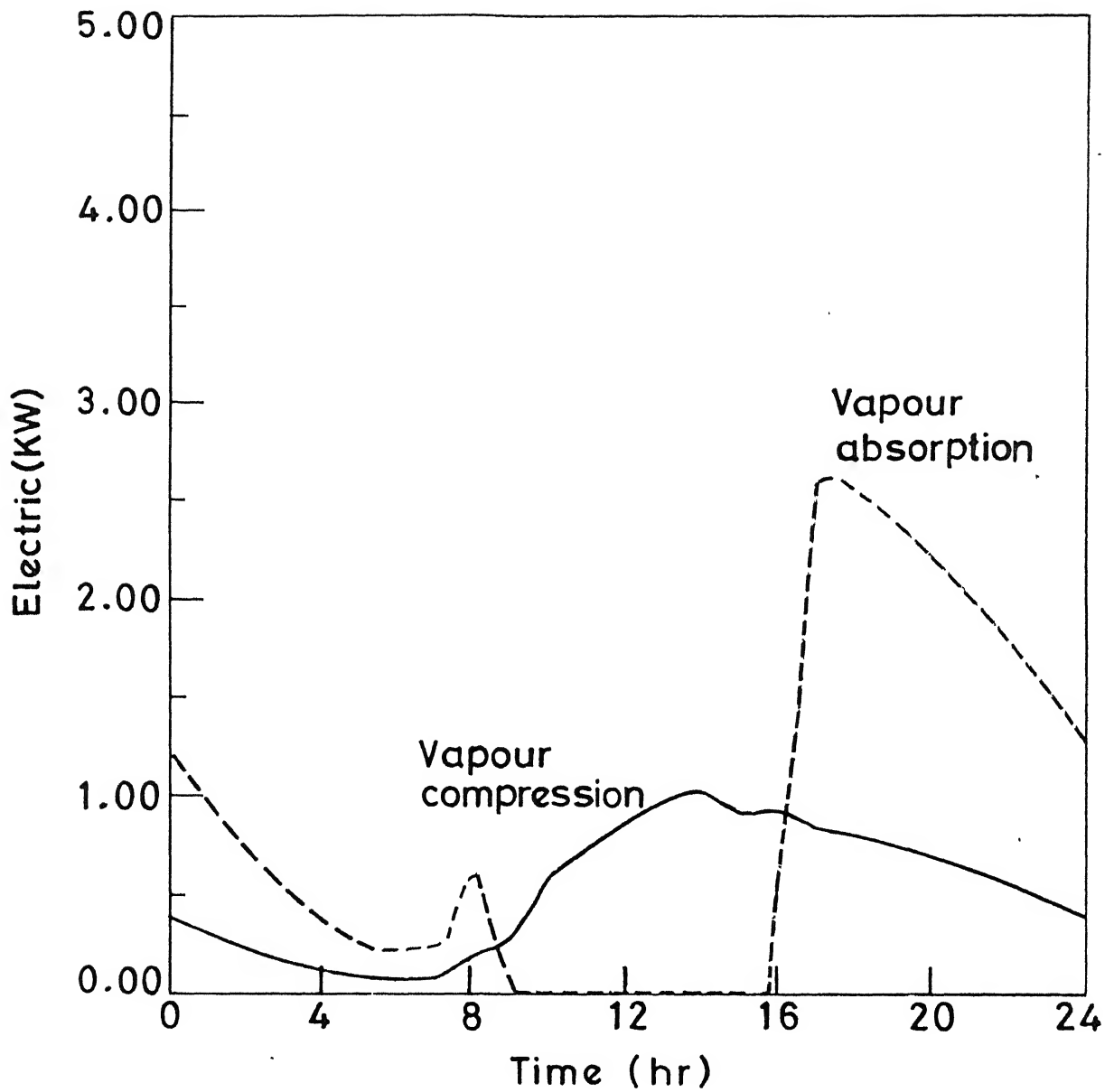


Fig.2.9 Electric power requirement for september.

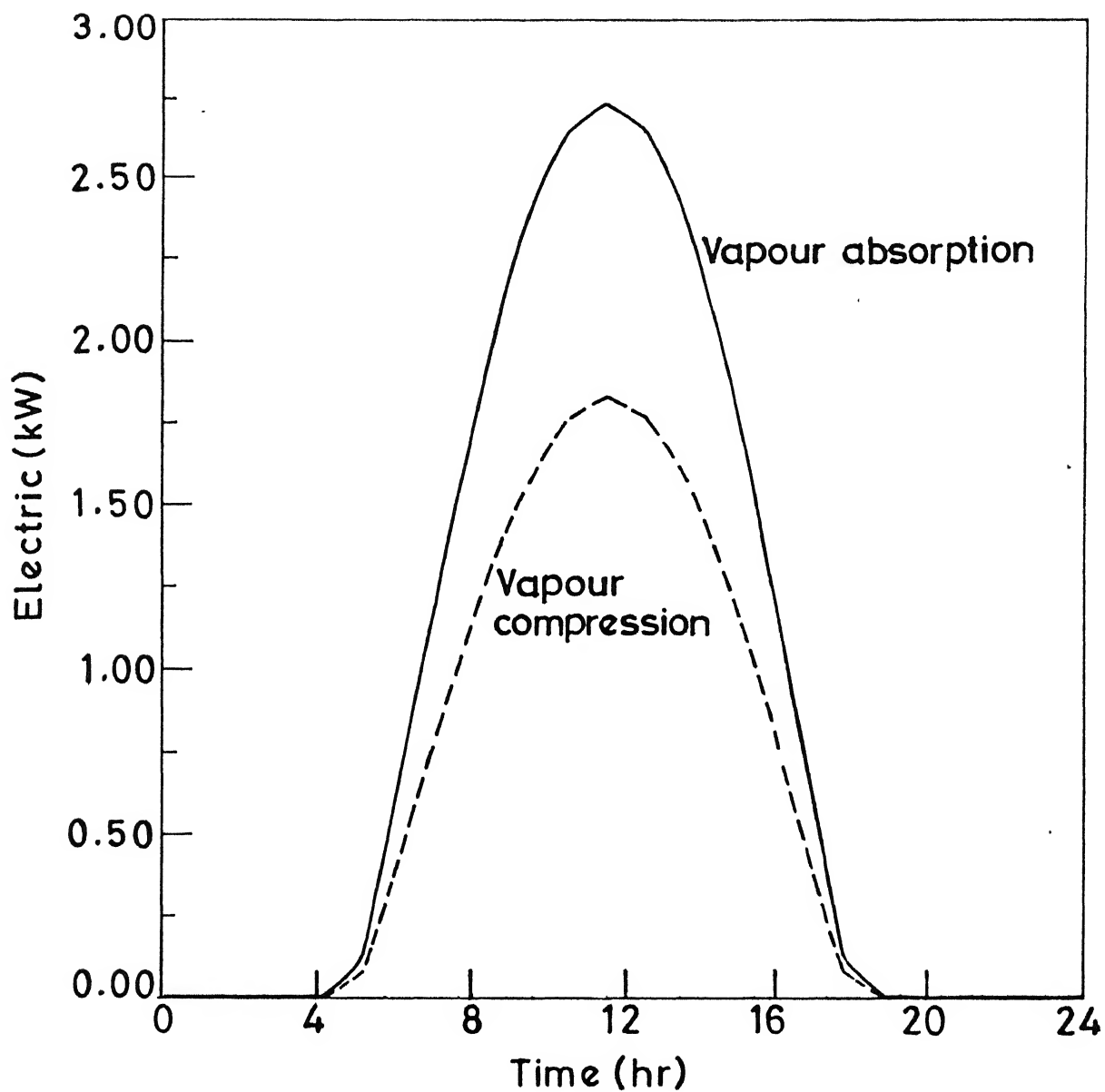


Fig.2.10 Electric power available in September.

Table 2.1: Total Energies (in kWh) per day required and available in different months for airconditioning.

Month	Vapour Compression System		Vapour Absorption System	
	Energy required	PV energy available	Energy required	PV energy available
April	10.44	14.99	15.19	22.48
May	15.91	15.90	23.80	23.81
June	12.71	16.12	18.89	24.18
July	13.59	15.83	22.21	23.74
August	11.47	15.04	20.95	22.57
September	12.59	14.00	20.14	21.00
October	4.93	12.81	4.75	19.21

month of May, in other months power available is more than the requirement. This takes care of the uncertain weather conditions in those months.

## 2.6.2 Results for Heating

Programme was run for the PV array estimation for heating a room in Kanpur. The particulars of room are given in Appendix G. The variation of heating load with time of 24 hour period for the month of January (the coldest month) is shown in Figure (2.11). It is clearly seen that heating load varies drastically with time. Figure (2.12) shows the electrical energy requirement for the vapour-compression system. For calculating energy requirement the values of COP for heating system is taken as 4.84. In section 7.1.3 and chapter 7 of reference [Prasad, 1993] a typical COP value of a practical airconditioning system based on vapour- compression system is given as 3.84. Performance Index(PI) of heat pump is one plus COP of airconditioner. That's why the value 4.84 is taken here. The total electrical energy requirement in a day is found from the area under the electrical power requirement curve. It comes out to be 11.9 kWh. A 1796 W array is needed in order to meet this requirement. The PV cell data



are given in Appendix H. The array size(area) for this array is about 160 m<sup>2</sup>. Power available from this array is shown in Figure (2.12).

Figure (2.13) shows the electrical energy requirement for vapour-absorption system for heating. Based on the COP value of 1.2 for airconditioner of vapour absorption type, PI here has been taken as 2.2. It is also assumed that starting from 3 hours after sunrise upto 2 hours before sunset all the power required can be obtained by solar collectors and therefore electrical power requirement is zero. Rest of the time electrical power required is obtained by dividing cooling load by COP. the total energy requirement in a day is 23.9 kWh. A 3615 W PV array is found to meet this array requirement. The size(area) of the PV array is 325 m<sup>2</sup>. The power output from such an array is shown in Figure (2.13).

Figure (2.14) shows heat load for the month of November. It is observed that heat load is less compared to January. Consequently, the power requirements in vapour-compression and vapour-absorption systems are less (Figures (2.15-16)). The PV arrays have already been chosen based on the requirements in the month of January. Their outputs for the two systems are also shown in Figures(2.15-16). It is seen that PV array output is not much different from the output for the month of January. That means when the array is designed on the basis of the coldest month, in other months the system is highly over designed. Table (2.2) clearly shows this. In this table energies required and available for all months of winter are shown. It is seen that in photovoltaic heating, there is an inverse relation between required and available power which is obvious because increasing solar radiation increases PV array output but decreases heat load. Therefore it is not economical to design the system based on the coldest month requirement.

In the places where all the year-round airconditioning is employed, the array size which is sufficient for cooling the space can be used for heating also. In the previous

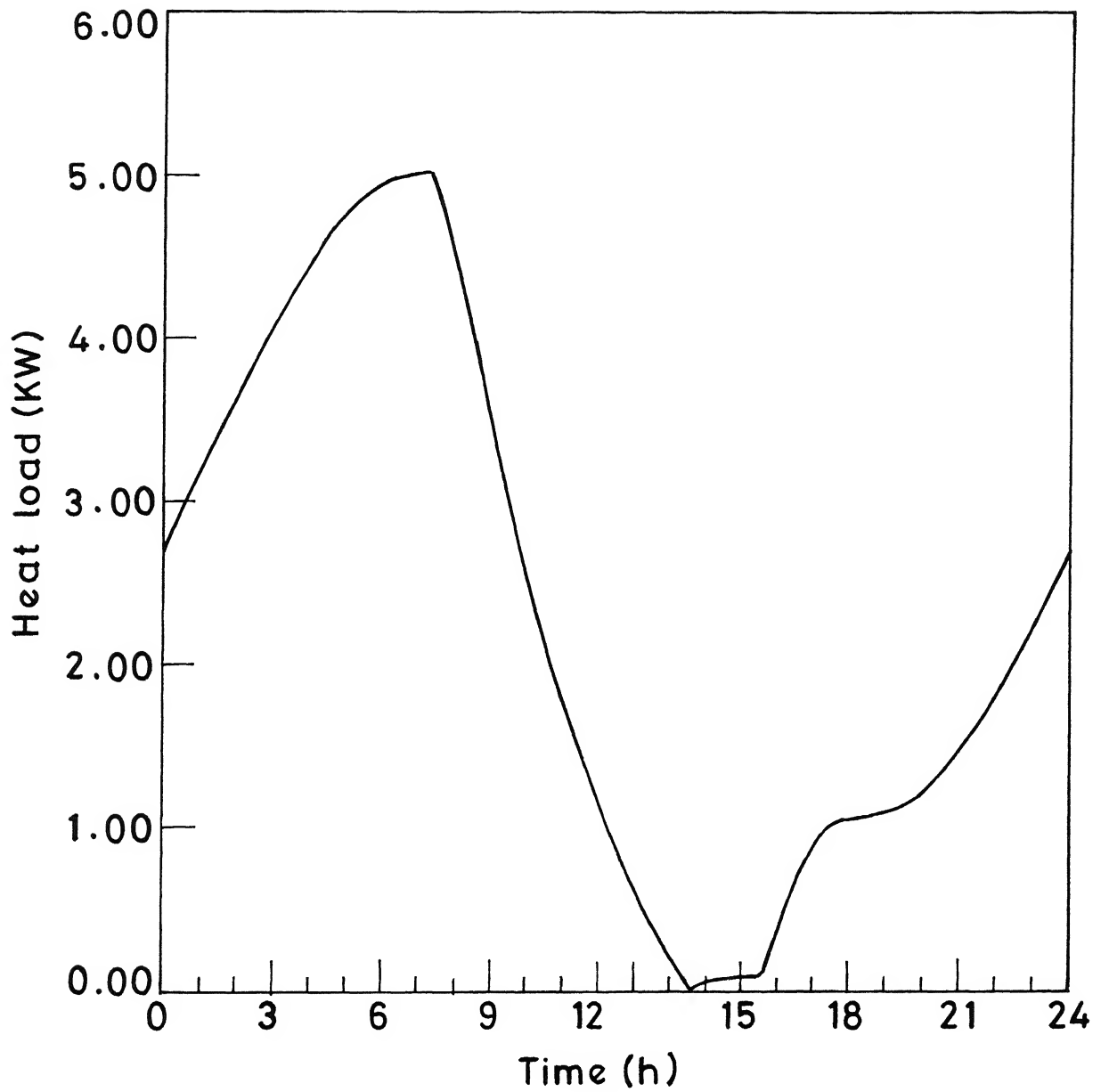


Fig.2.11 Heat load in the month of January.

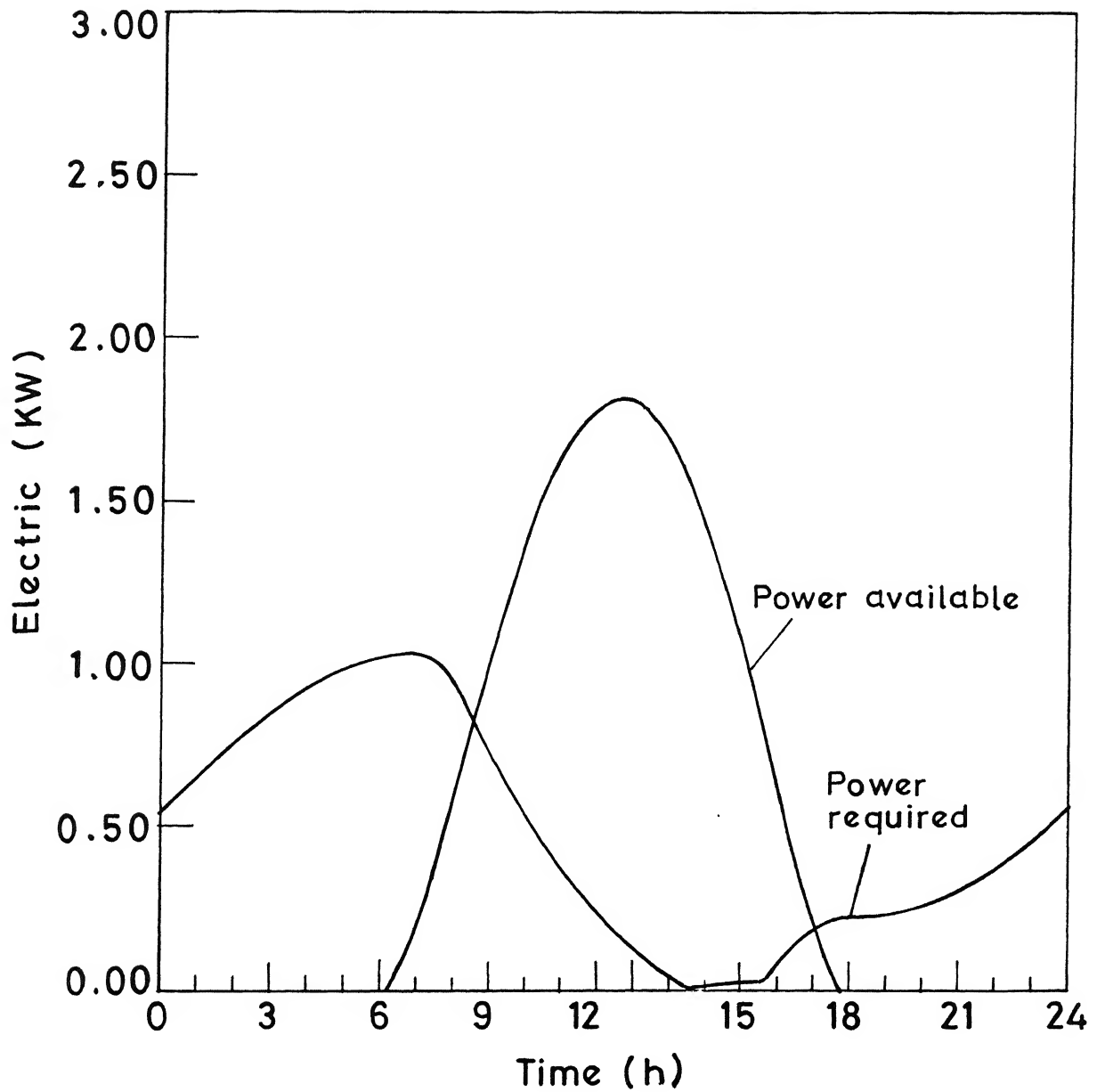


Fig.2.12 Power required and available in the month of January for vapour compression system.

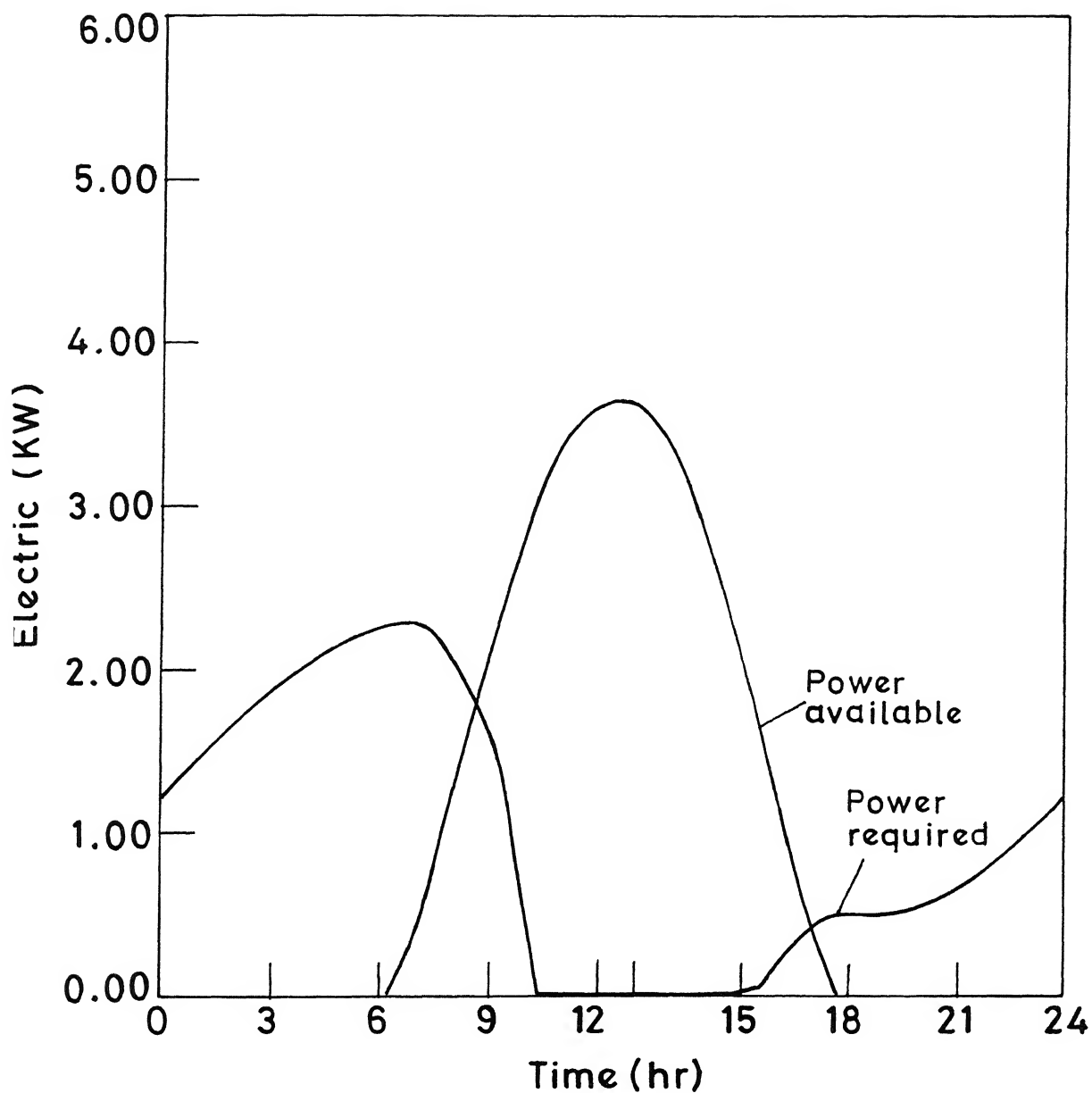


Fig.2.13 Power required and available in the month of January for vapour absorption system .

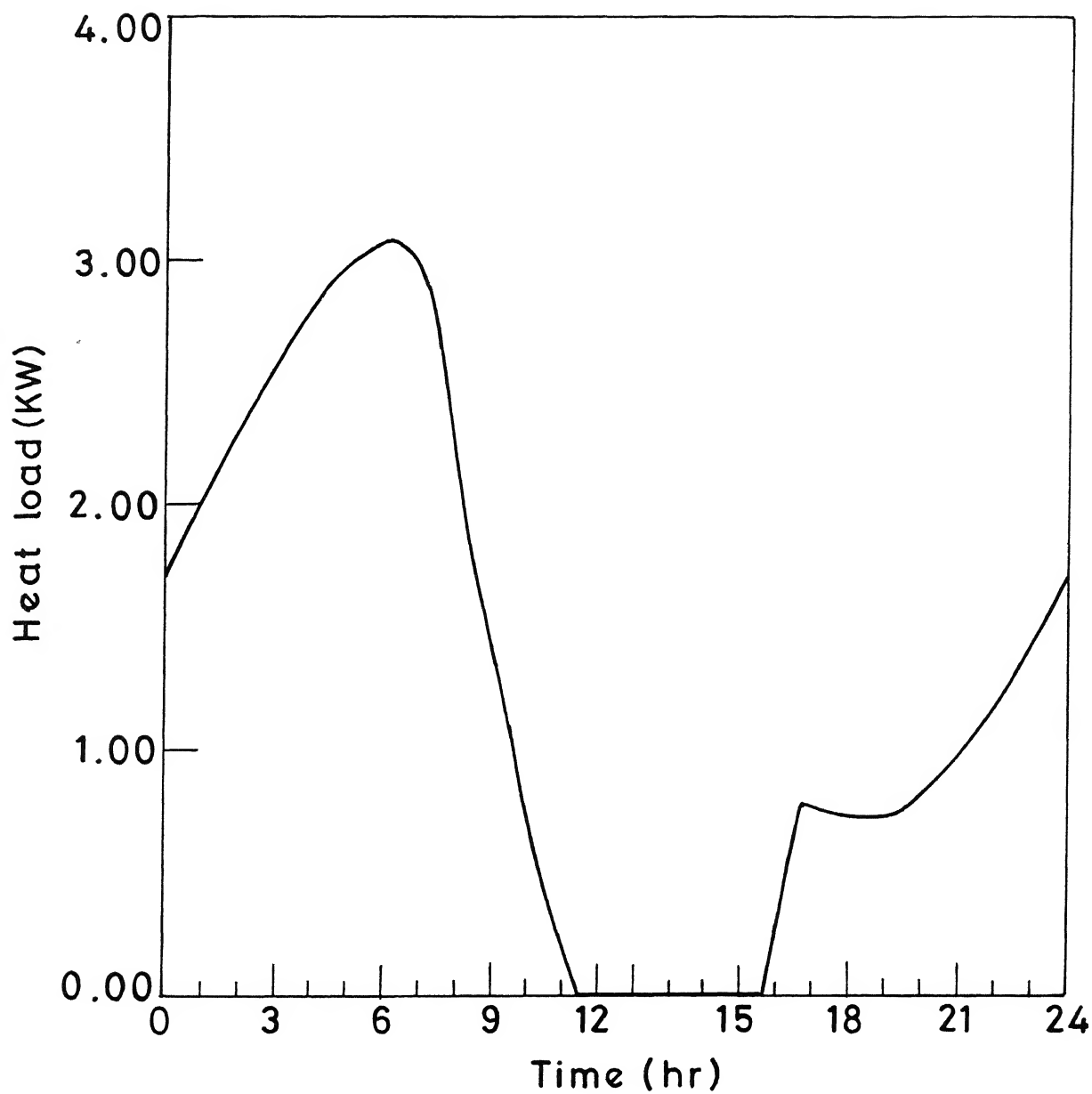


Fig.2.14 Heat load in the month of November.

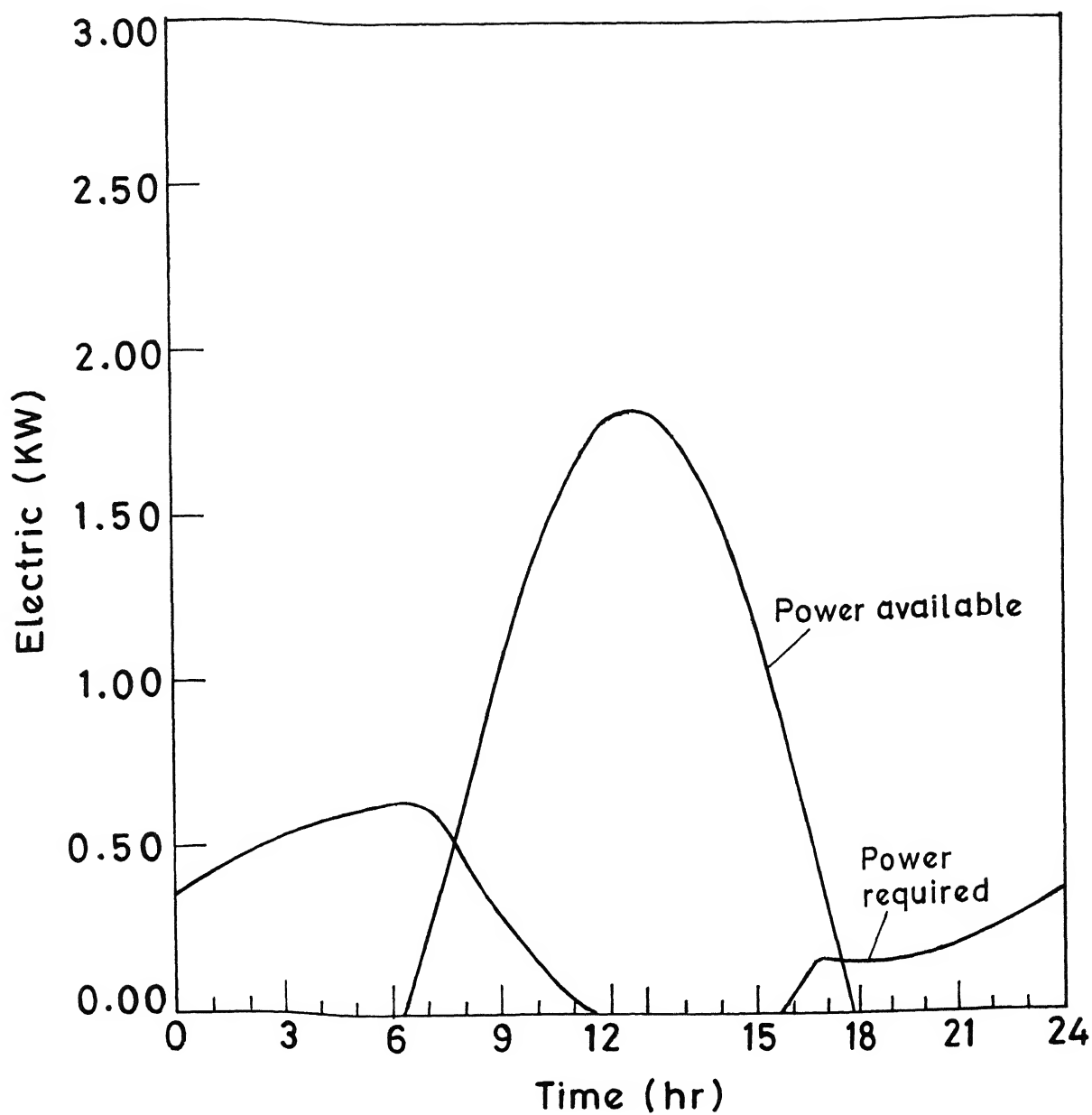


Fig.2.15 Power required and available in the month of november for vapour compression system .

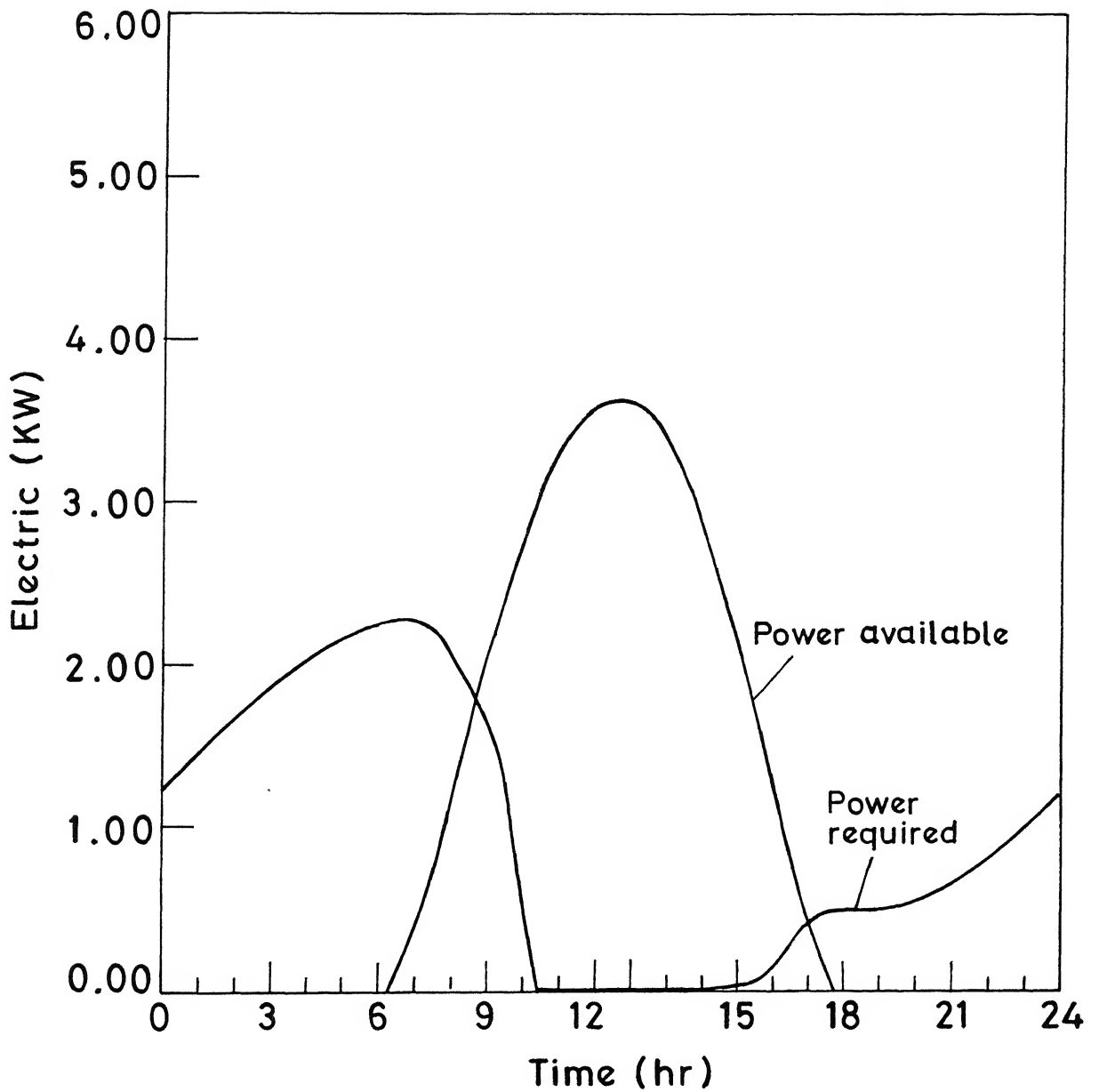


Fig.2.16 Power required and available in the month of November for vapour absorption system.

Table 2.2: Total Energies (in kWh) per day required and available in different months for heating

Month	Vapour-Compression System		Vapour-Absorption System	
	Energy required	PV energy available	Energy required	PV energy available
January	11.9	11.9	23.9	24
February	11.3	13.3	22.3	26.8
March	8.4	14.0	15.4	28.1
November	6.7	12.9	14.5	25.8
December	9.7	12.6	19.5	25.4

example, the array size was computed for the airconditioning of the same room in the hottest month. Interestingly, the array size for the vapour -compression system comes out to be very close to the array size selected here. Therefore, it is advisable to employ the same size of array for the airconditioning and heating purpose. In that case, in some months, array will be supplying more power than the requirement. Whenever the available power is more than the required power, the excess power is stored in a battery which takes care for the peak requirement periods.

### 2.6.3 Results for Refrigeration

The programme was run for the PV array estimation for a refrigerator of 45 liter capacity. The particulars of refrigerator are given in Appendix I. The variation of refrigeration load with time for 24 hour period for the month of May (month of maximum heat) is shown in Figure (2.17). It is clearly seen that refrigeration load varies with time. Figure (2.18) shows the electrical energy requirement for the refrigerator. The refrigerant chosen here is R-12. For calculating energy requirement the values of COP for refrigeration system is taken as 3.5 as calculated in Appendix J. The graph of electrical energy requirement versus time for refrigerator has been obtained by dividing refrigeration load by COP.



The total electrical energy requirement in a day is found from the area under the electrical power requirement curve. From Figure (2.18), we find that total energy required is 897 Wh. A 100 W array is found to meet this energy requirement. The power output from this array is shown in Figure (2.19). This array gives 904 Wh in a day. The 40 series cells and 10 parallel strings will be required for this array and space required is  $0.96\text{m}^2$ . The PV cell data are given in Appendix H.

Figure (2.20) shows the refrigeration load at different times in the month of January (the coldest month) and Figure (2.21) is electrical power needed in that month. The power available from the 100 W is shown in Figure (2.22). It is seen that power available in this month is more than the requirement. The excess power is stored in the battery.

Table (2.3) shows total energy required and energy available from PV array for all months. It is seen that when array is selected on the basis of the month of May, the same array is sufficient for meeting the energy requirement in other months also. The code was run for the environmental conditions of Bombay also. The electrical energy required in the month of May comes out to be 784 Wh there, while the array is able to supply 850 Wh in a day there. In the month of January energy required is 715 Wh and array supplies 716 Wh in a day. Thus the same 100 W array is able to supply the required power in Bombay also. The two cities selected here are the representative cities where environmental conditions and latitude differ much from each other. It is, therefore, expected that in other cities too the 100 W array is expected to be sufficient. The specifications of refrigerator is given in Appendix I. It is considered as maximum capacity specifications. The refrigerator is not used to its full capacity all the time. Moreover, the heat of respiration, frequency of door opening for replacing the food items etc. have been taken on higher side. In practice the energy requirement is expected to be less than calculated here. The excess energy will be stored in battery to be used during uncertain weather conditions.

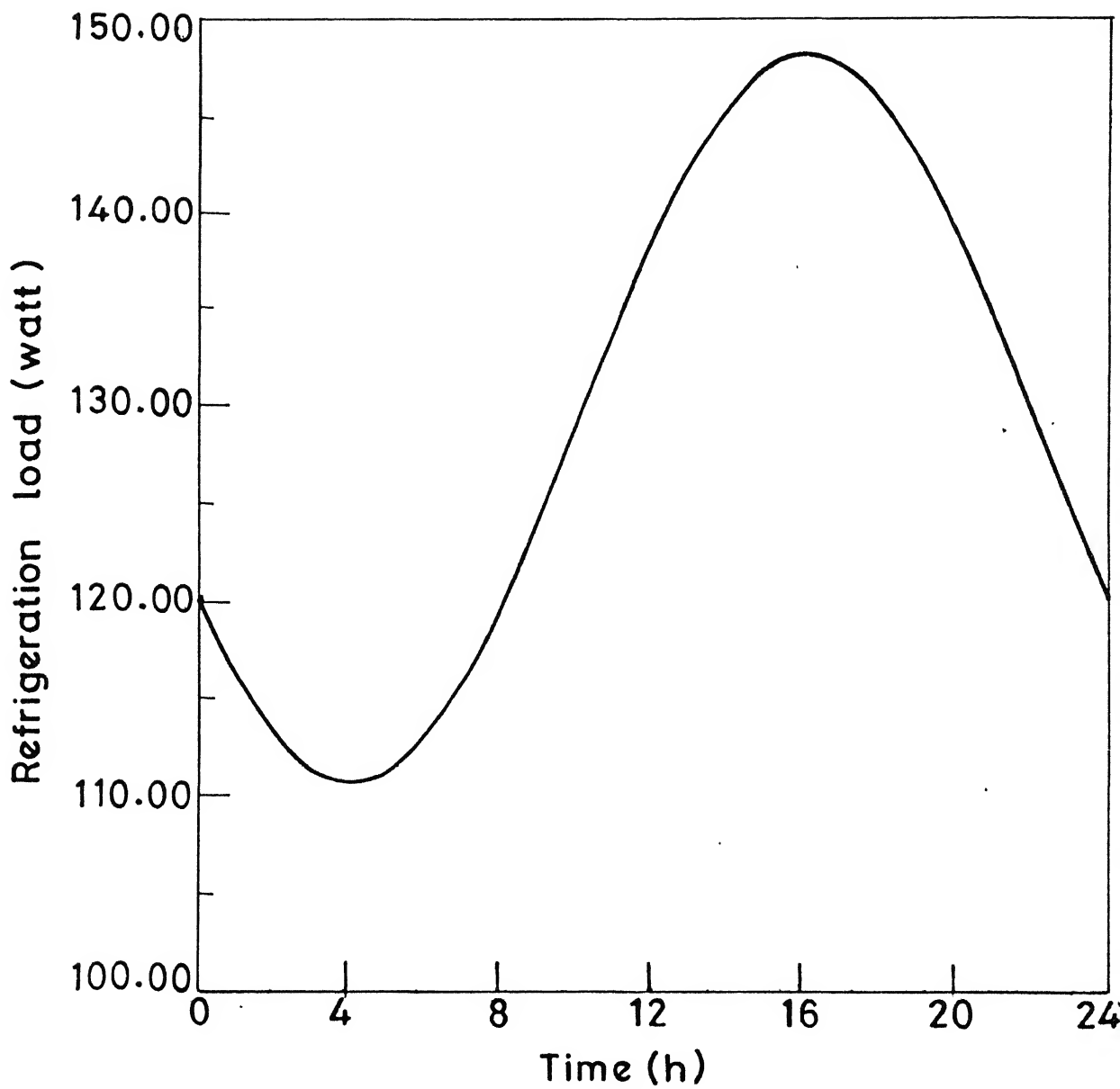


Fig.2.17 Refrigeration load in May .

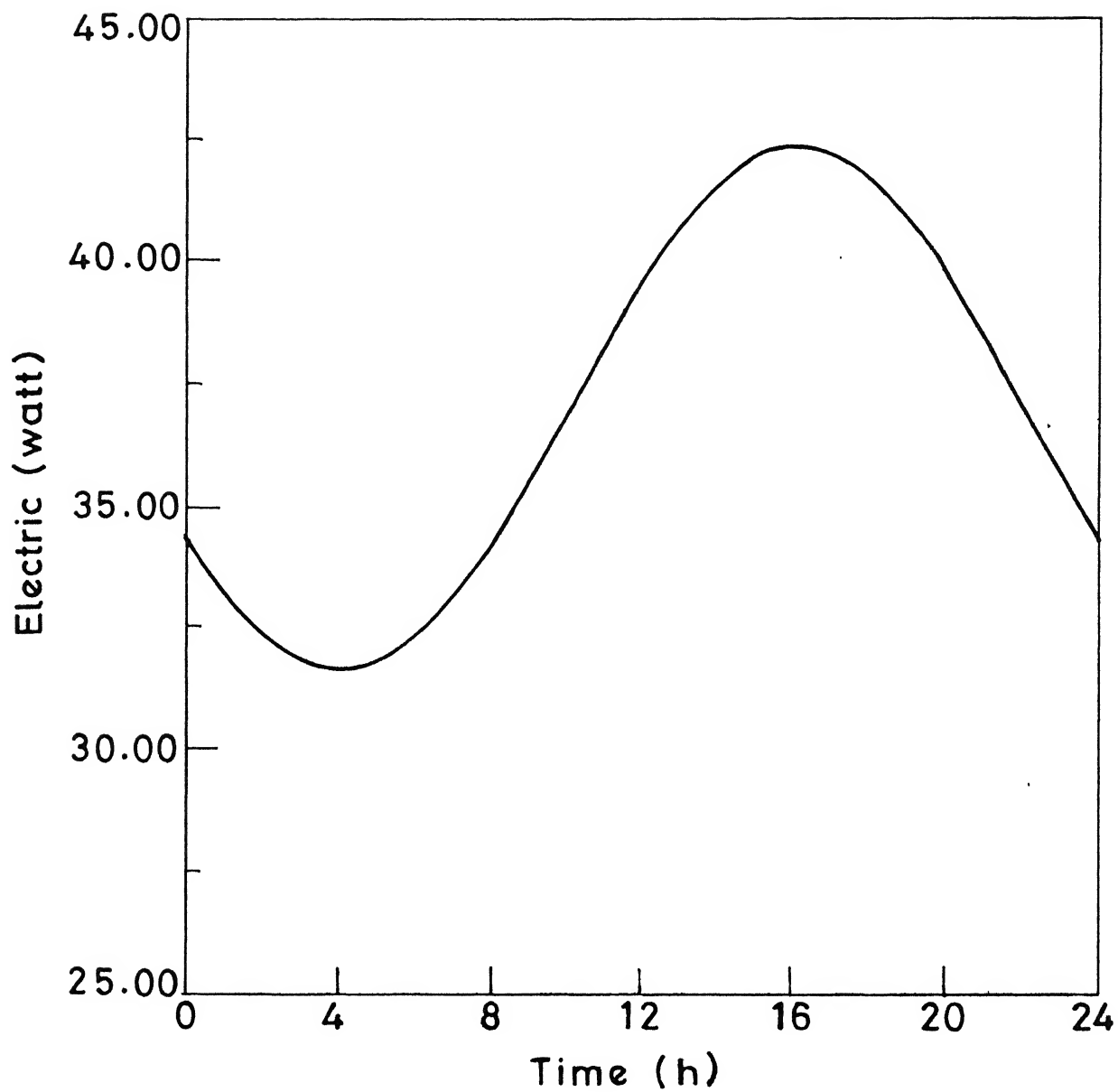


Fig.2.18 Electric power required in May.

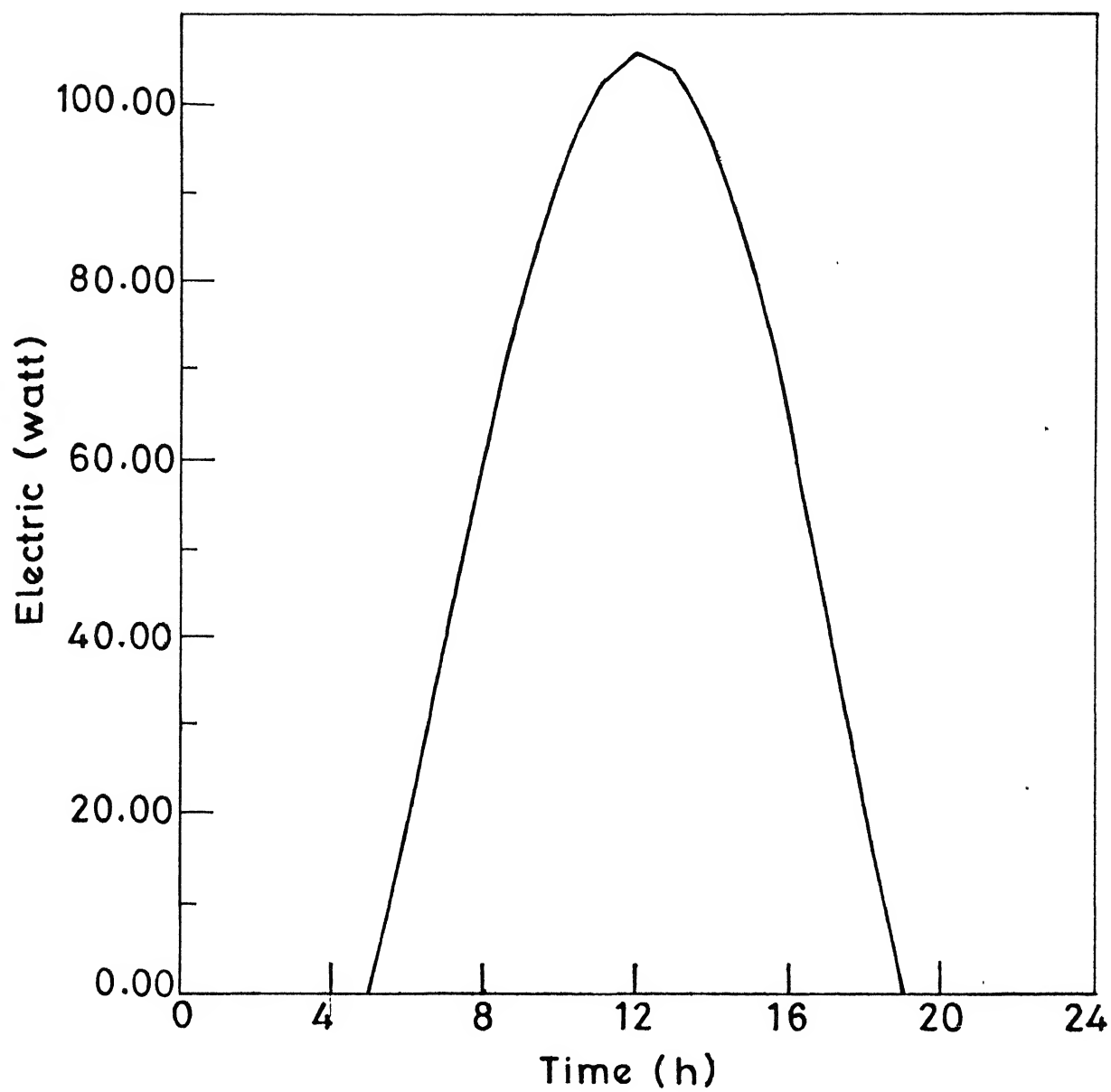


Fig.2.19 PV array output in May.

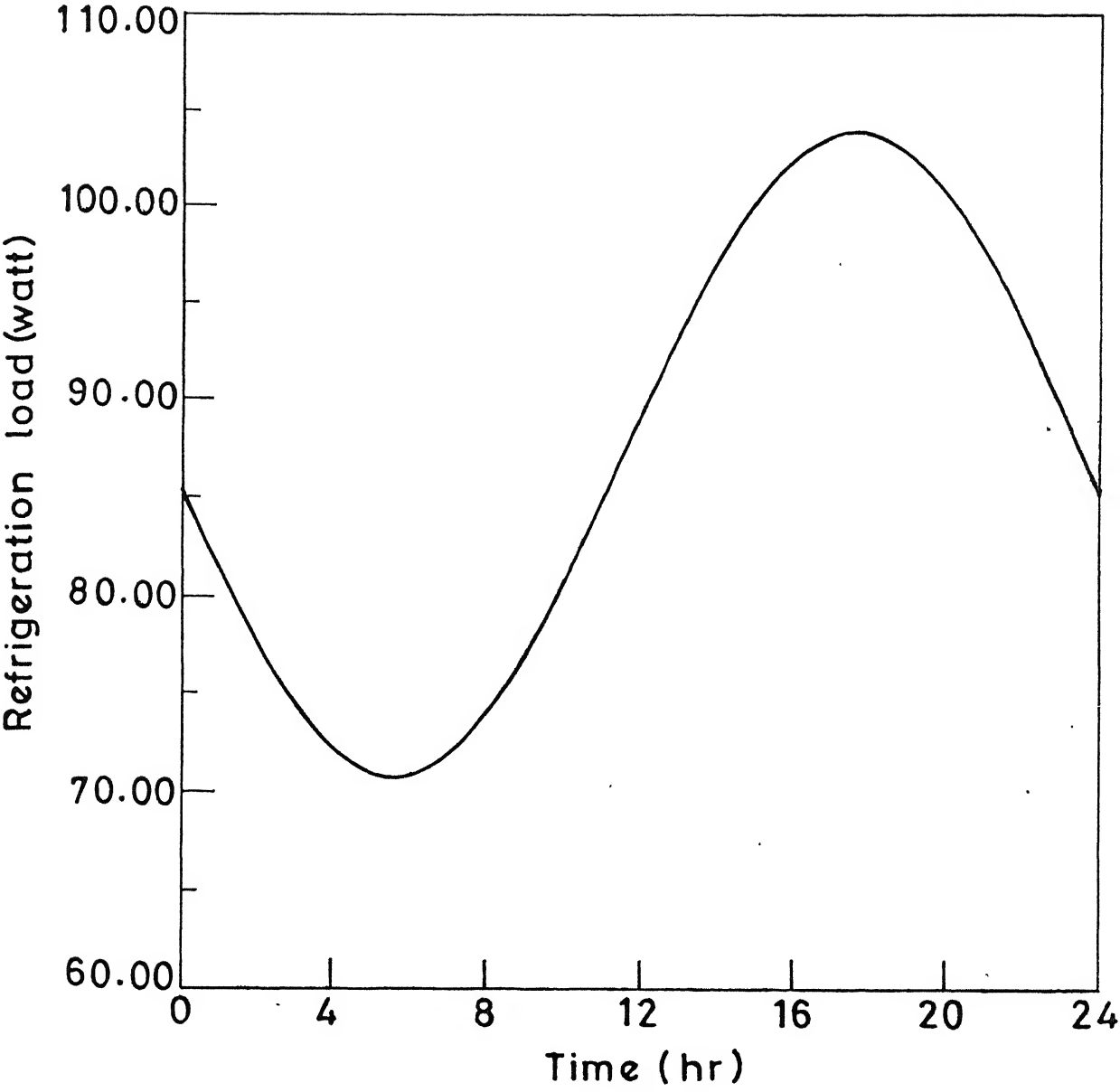


Fig.2.20 Refrigeration load in January .

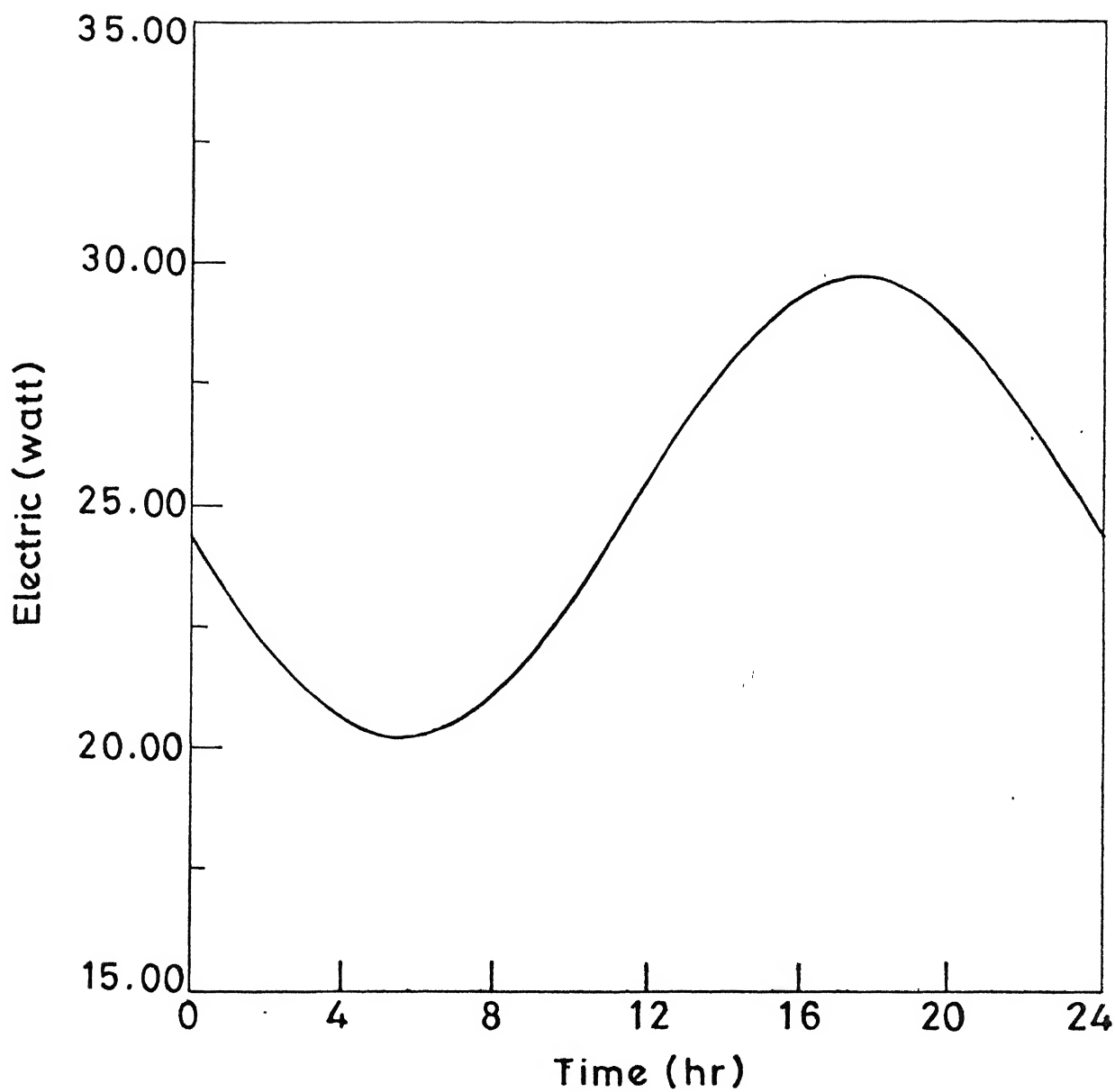


Fig.2.21 Electric power required in January .

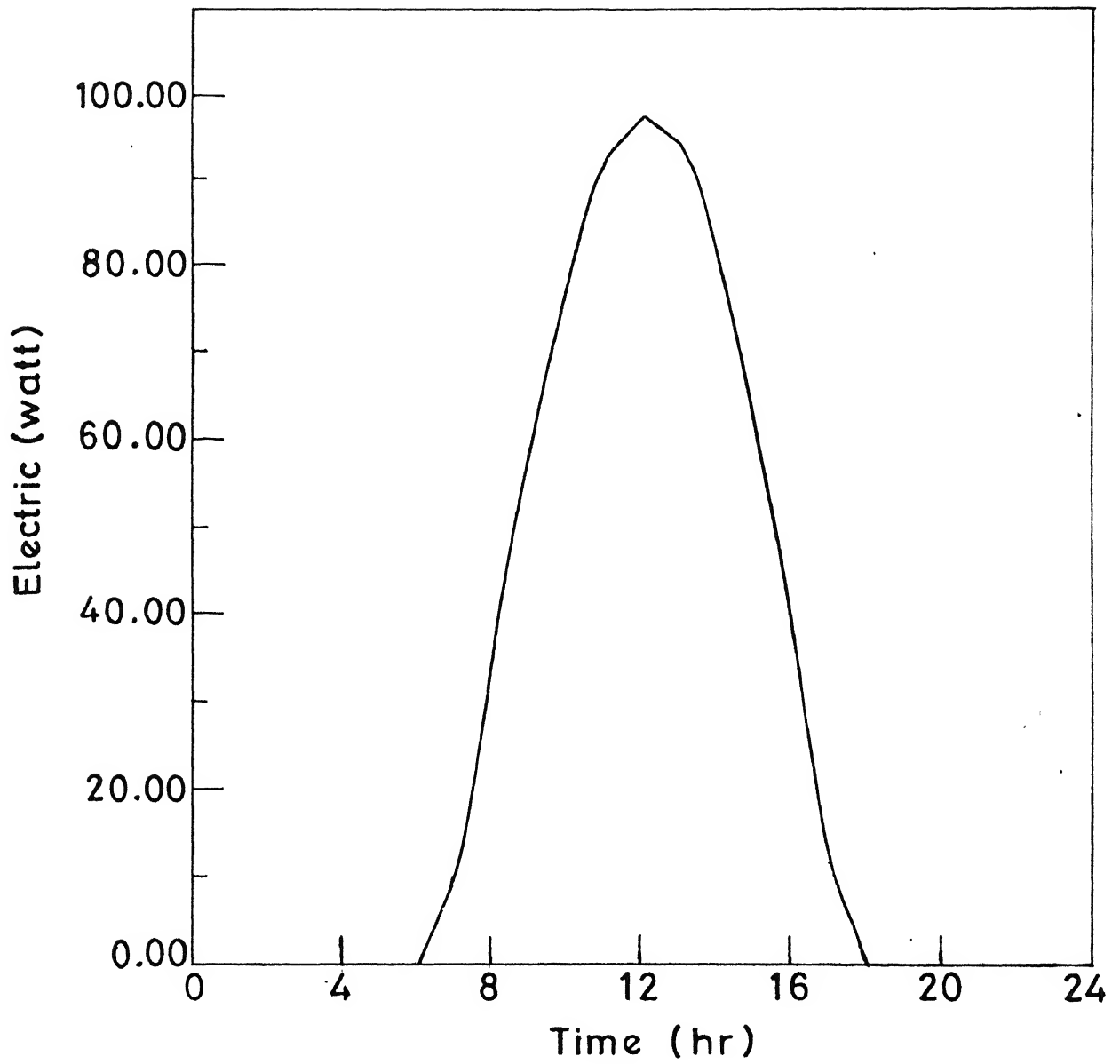


Fig.2.22 PV array output in January.

Table 2.3: Energies required and available per day for 100 W refrigerator.

Month	Energy Required(Wh)	PV Energy Available(Wh)
January	599	663
February	622	710
March	683	771
April	835	839
May	897	904
June	864	916
July	872	900
August	852	855
September	814	816
October	725	727
November	659	672
December	621	647

## 2.7 Summary

A method to estimate array size for airconditioning, heating and refrigeration system is presented and computer code has been developed for this purpose. For each of these cases, examples have been taken for estimating array sizes. For airconditioning and heating both vapour-absorption and vapour- compression systems were considered. It is observed that array size requirement is much more in the case of vapour-absorption system than in the case of vapour-compression system for both airconditioning and heating. This is due to the low COP of the vapour-absorption system.

For the case of a refrigerator, 100 W, 45 liter capacity refrigerator can be developed which can successfully operate at Kanpur and Bombay, the two representative cities of India where environmental conditions differ much more from each other.



## Chapter 3

# APPLICATION OF FUZZY SETS TO THE ARRAY SIZE ESTIMATION

### 3.1 Introduction

As discussed in Chapter 2, the array size is dependent on the cooling load required and the solar energy available. Environmental conditions constitute major uncertainties apart from other type of uncertainties, such as number of occupants inside the room. To account for uncertainties, we are familiar with two types of theories : probability theory and fuzzy set theory. Probability theory is used when an event is precisely defined and an adequate statistical data are available. Various parameters are tested as stochastic variables and it is assumed that uncertainty and imprecision are of random nature. However, most of the meteorological phenomena have another kind of uncertainty referred to fuzziness due to imprecision or lack of data and subjectivity of opinion or judgement. These are sources of uncertainty which are caused by vague definition

rather than by chance. Fuzzy sets deal with the membership or non-membership of an object in a set with imprecise boundaries.

In meteorology, vague informations often arise, for example, the sentence ‘today is hot’ consists in fuzziness. In this case, there is no exact definition about which degree of temperature is considered as ‘hot’. For weather forecasting, especially for long range forecasting, we usually do not ask about the detail but instead the tendency of future weather. Therefore, it seems more reasonable to treat the array size determination problem from the fuzzy set theory [Zadeh, 1965; Kaufmann and Gupta, 1985; Klier and Folger, 1993]. Some of the relevant aspects of fuzzy set theory are presented in Appendix K.

In this chapter a parametric study is carried out to study the influence of various parameters on the array size determination. The parameters which play dominating role, are taken as fuzzy. The possibility distribution of array size is obtained for different months. If an array is designed on the basis of worst expected conditions, it will be a reliable design. But the cost of the airconditioning system will be exorbitant. On the other hand if it is designed on the basis of best expected conditions, the cost will be much less but reliability will be poor. Therefore, it is prudent to design at some intermediate operating conditions which provide an optimal solution. A method to select an optimum array size obtained from the fuzzy solution is discussed.

## 3.2 Parametric Study

The array size is dependent on the cooling load and power generated by photovoltaic array. Cooling load and array output are dependent on a number of factors. Some of these factors play dominating role, while other influence only slightly. A parametric study is done to find out the effect of various parameters, so as to enable us to find out

critical parameters. These parameters will then be taken as fuzzy parameters. The output for different values of parameters can be found by changing the input variables in the input file of cooling load estimation.

- (a) Effect of Maximum Temperature: From Figure (3.1), it is clear that the maximum temperature of the day has much influence on cooling load. A  $10^{\circ}\text{C}$  temperature increase, causes cooling load to increase by a factor of 1.7. However, from Figure (3.2), it is seen that array output increases insignificantly with increasing maximum temperature.
- (b) Effect of Minimum Temperature: Figure (3.3), shows that like maximum temperature of the day, minimum temperature of the day also influences cooling load. Increase in the minimum temperature of the day increases cooling load. However, Figure (3.4), exhibits that increase in array output is not significant. This aspect should be kept in mind while adopting the use of photovoltaic airconditioning system.
- (c) Effect of Humidity: Figure (3.5) shows an increase in cooling load with increasing humidity. Humidity associated with ventilation and infiltration air increases the cooling load only. But humidity does not have any influence on array output.
- (d) Effect of clouds: Figure (3.6) shows that increasing cloud cover decreases cooling load only slightly. This is because firstly with clouds only beam radiation reduces, diffused radiation being slightly increased and secondly since the most of the portion of the room is already covered, radiation in itself accounts for small fraction of cooling load. However, from Figure (3.7), it is seen that increasing cloud cover decreases array output drastically.

- (e) Effect of Number of Occupants: It is seen from Figure (3.8), that as the number of occupants increases, cooling load also increases.
- (f) Effect of Sunrise and Sunset time: The sunrise and sunset times on the first and the last day of month are different. However, due to change in sunrise and sunset timings, cooling load and array output do not change much. Therefore, taking average values of sunrise and sunset timings in a month is appropriate.
- (g) Effect of Door Openings: It is observed that cooling load during normal and heavy door openings are not much different. From the above discussion it is clear that critical parameters are: maximum and minimum temperature of the day, humidity, cloud cover and number of occupants.

### 3.3 Fuzzy Set Modeling of Various Parameters

Maximum and minimum temperatures of the day, humidity, number of occupants in the room and fractional cloud cover are five parameters which have been considered fuzzy. These parameters are characterized by their membership functions. There are various ways to construct a membership function [Vallipan and Pham, 1995], however, for simplicity only linear triangular membership function is considered here. Triangular membership function is given by,

$$\mu(x) = \begin{cases} 0 & x \leq l', \\ \frac{x-l'}{m-l'} & l' \leq x \leq m, \\ \frac{h'-x}{h'-m} & m \leq x \leq h', \\ 0 & x \leq h' \end{cases} \quad (3.1)$$

where

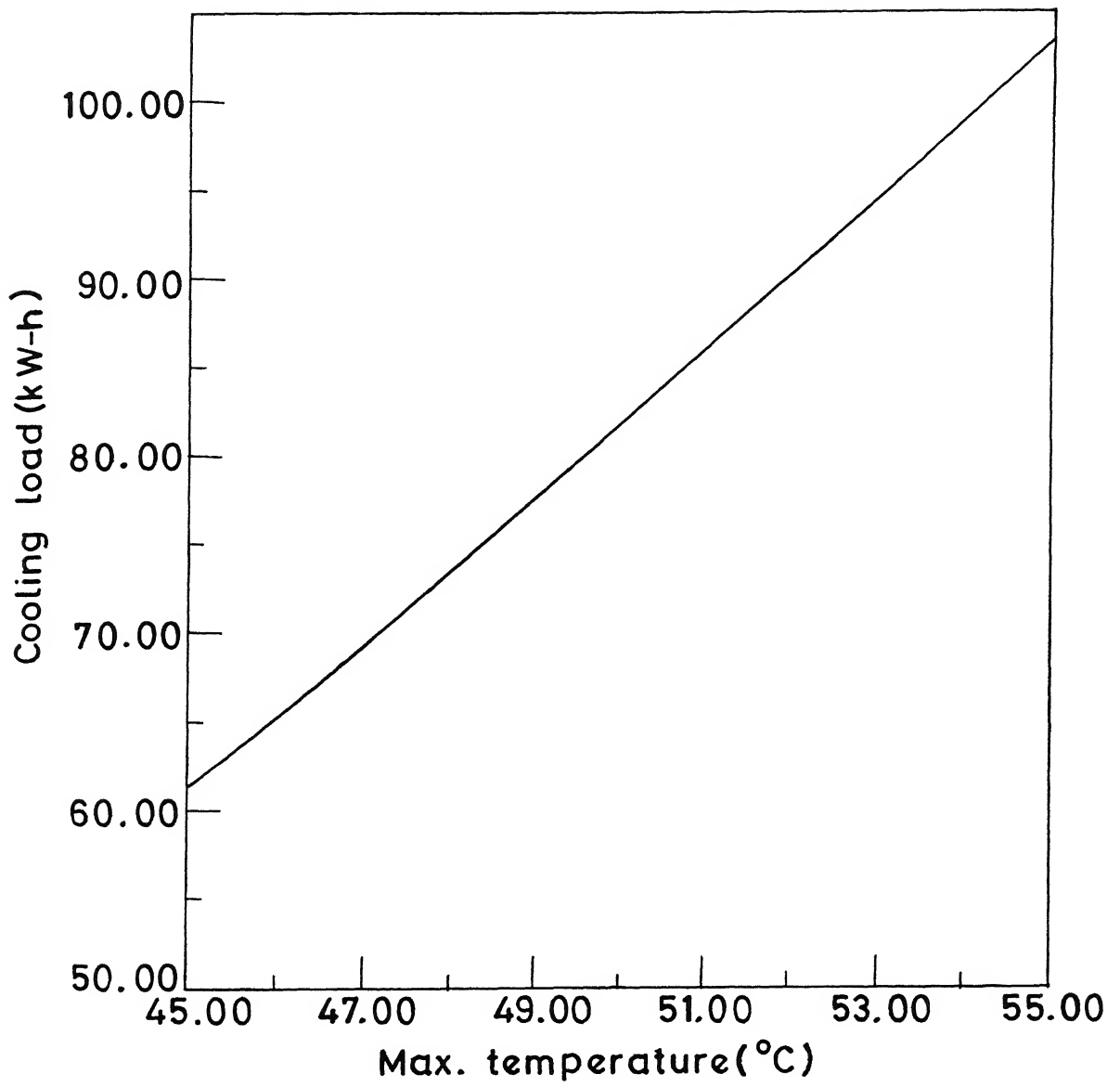


Fig.3.1 Effect of max. temperature on cooling load.

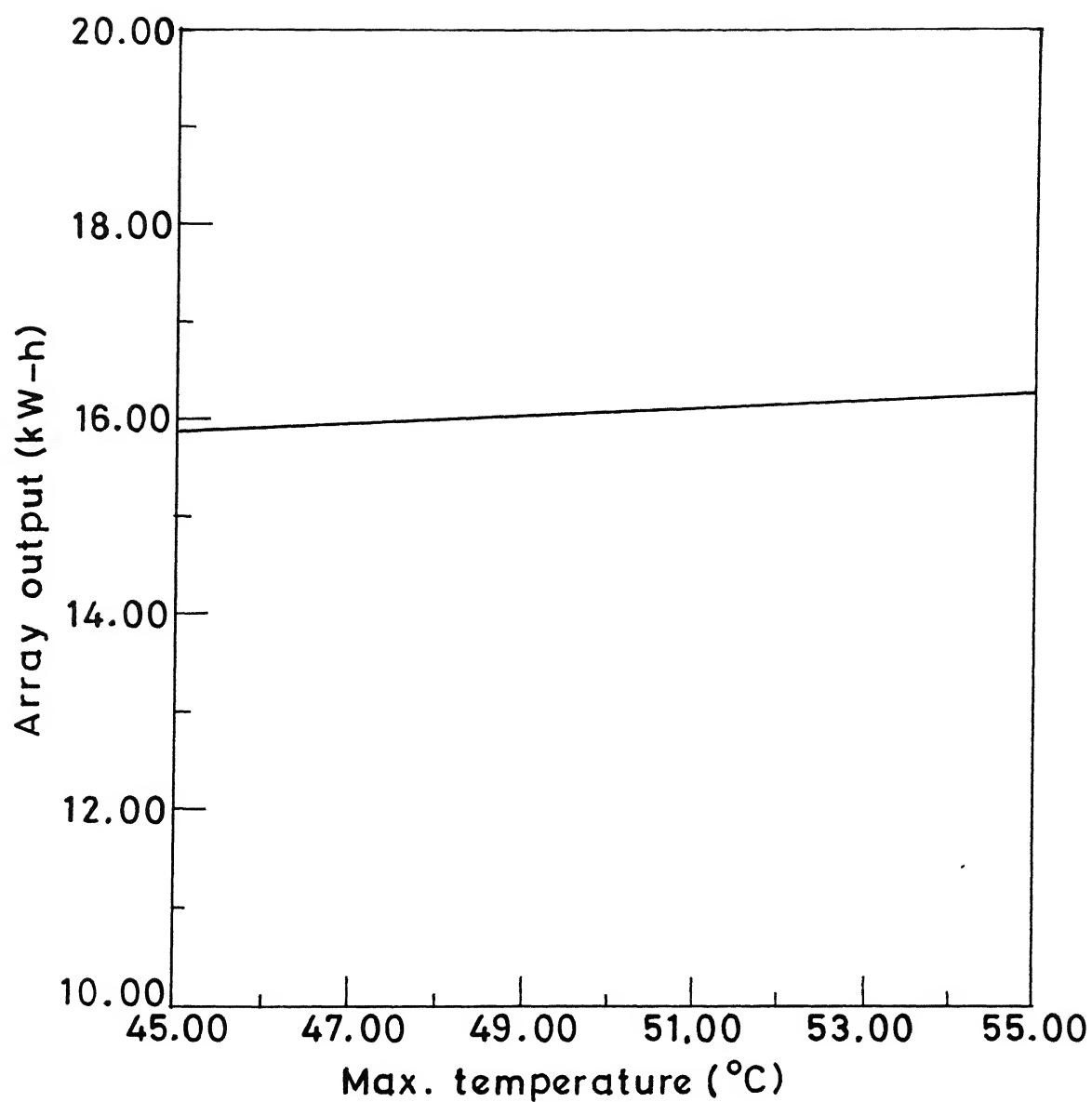


Fig.3.2 Effect of max. temperature on array output.

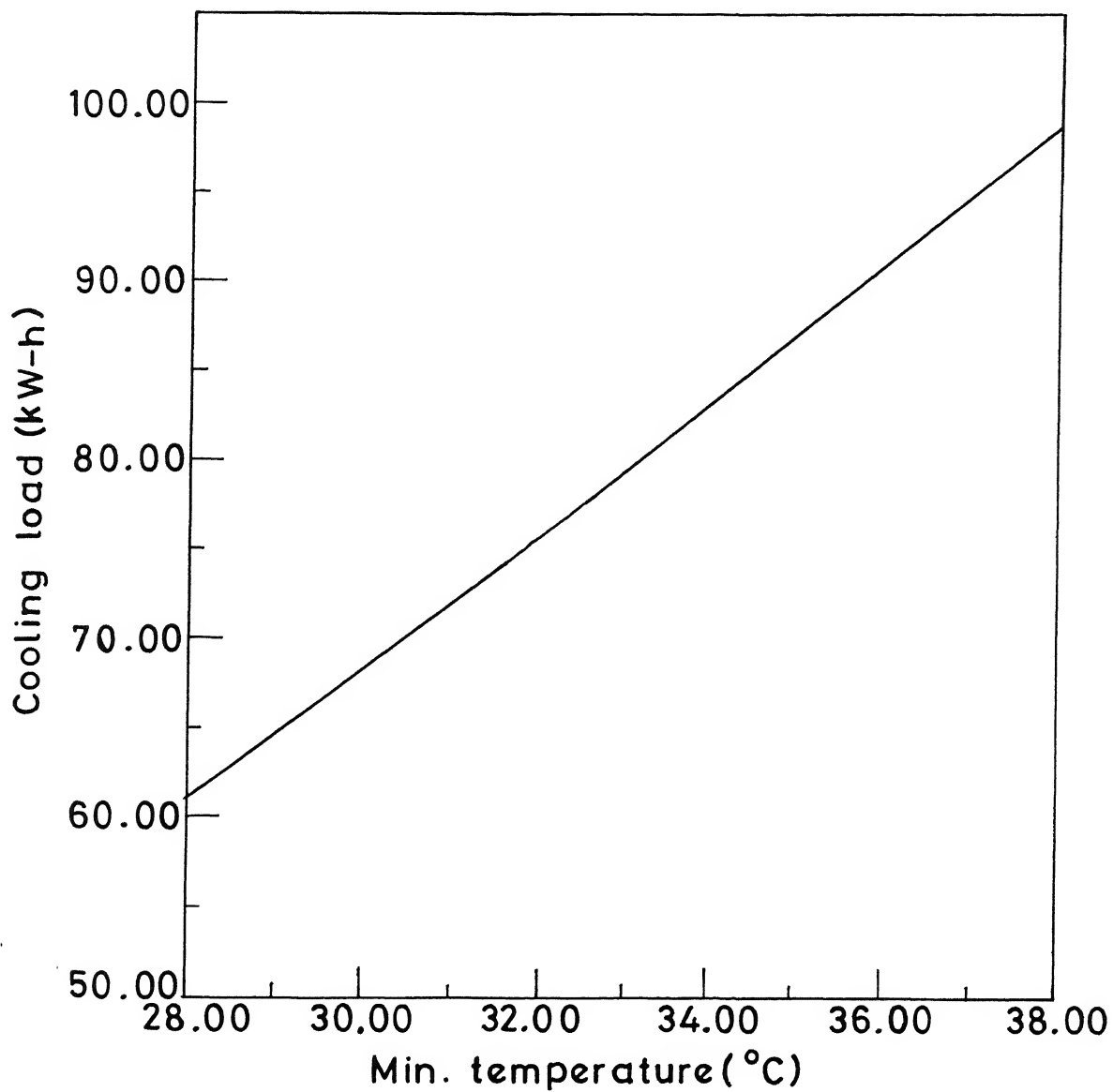


Fig.3.3 Effect of min. temperature on cooling load.

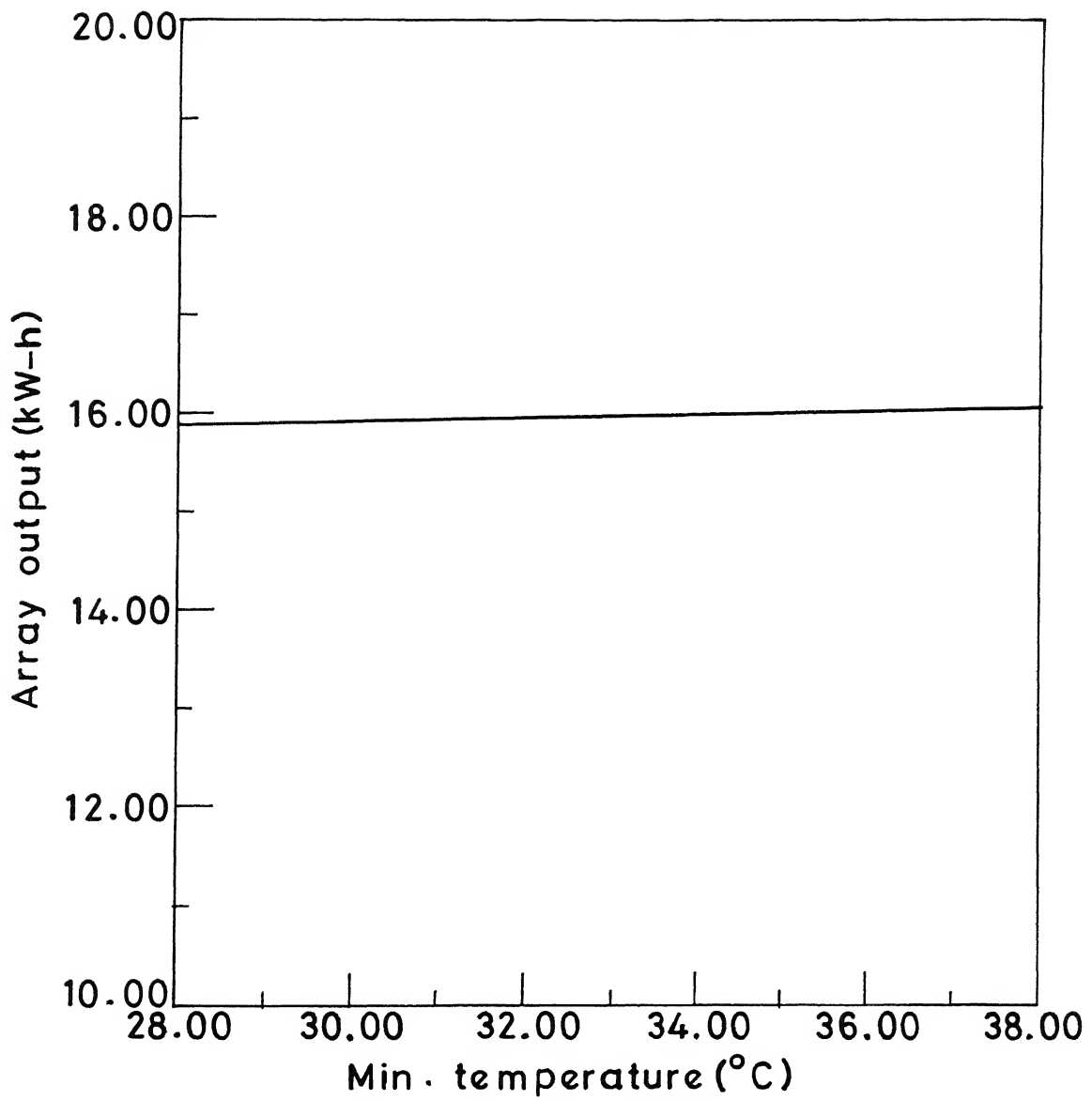


Fig.3.4 Effect of min. temperature on array output.



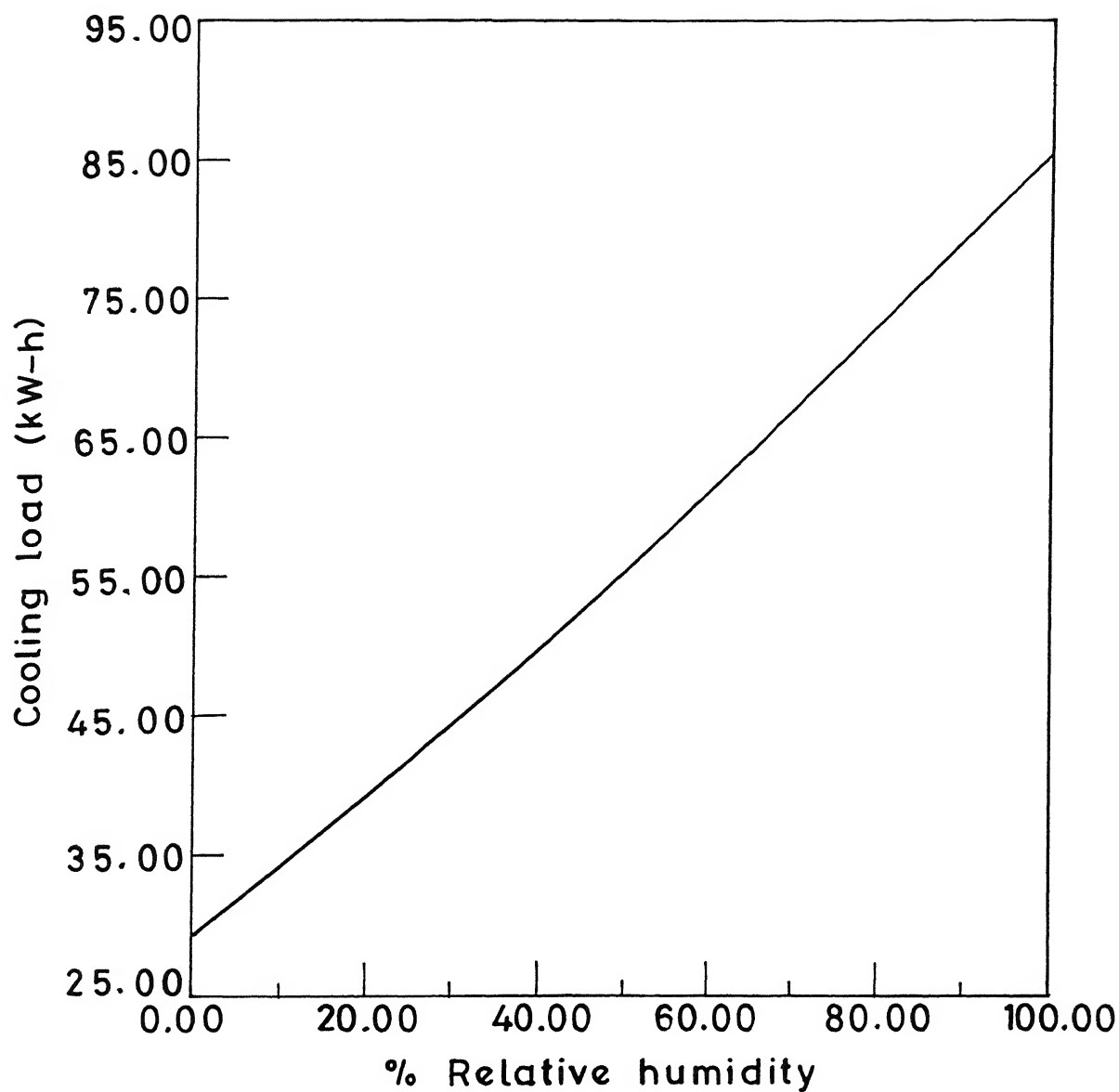


Fig. 3.5 Effect of relative humidity on cooling load.

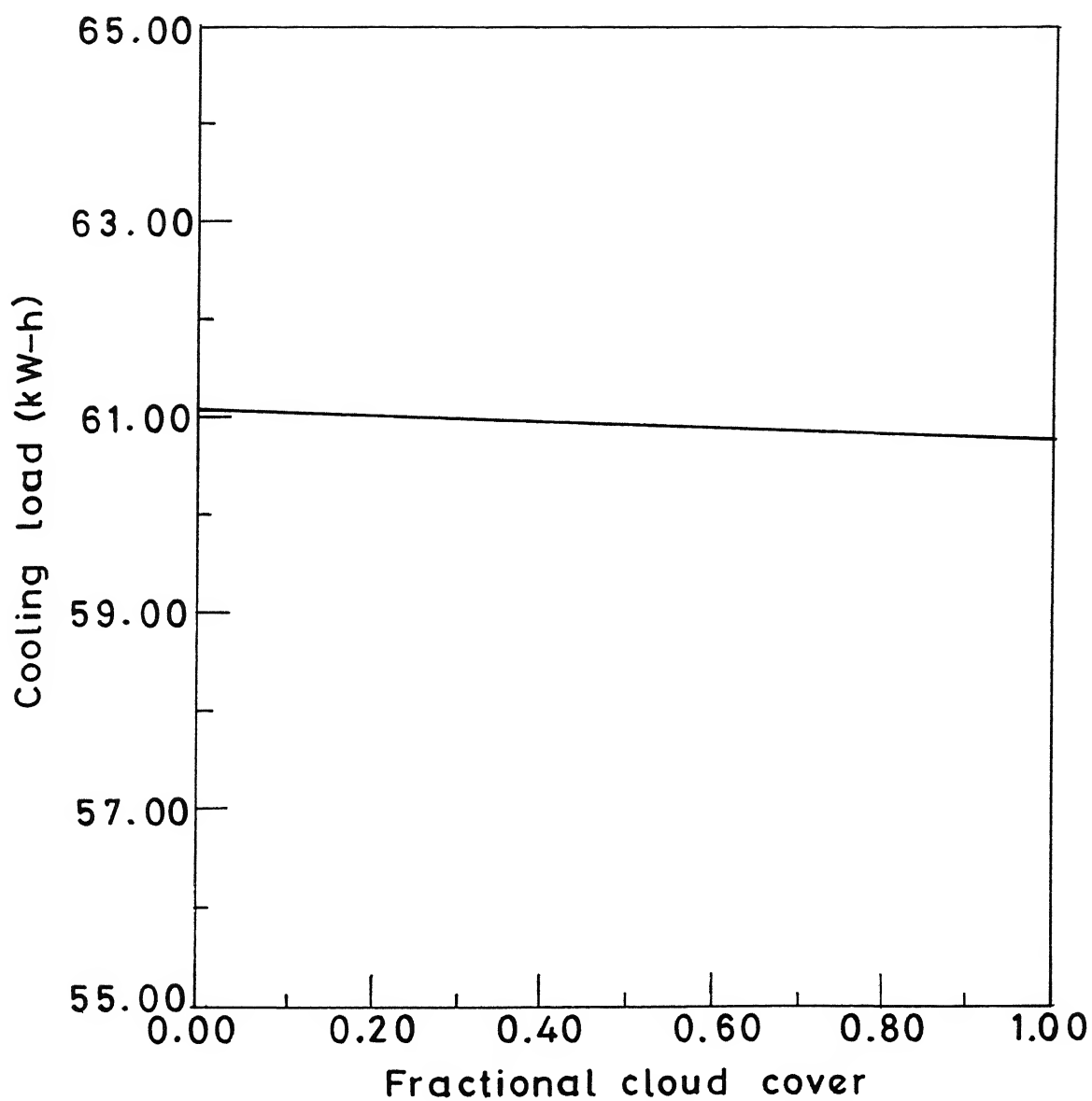


Fig. 3.6 Effect of Fractional cloud cover on cooling load.

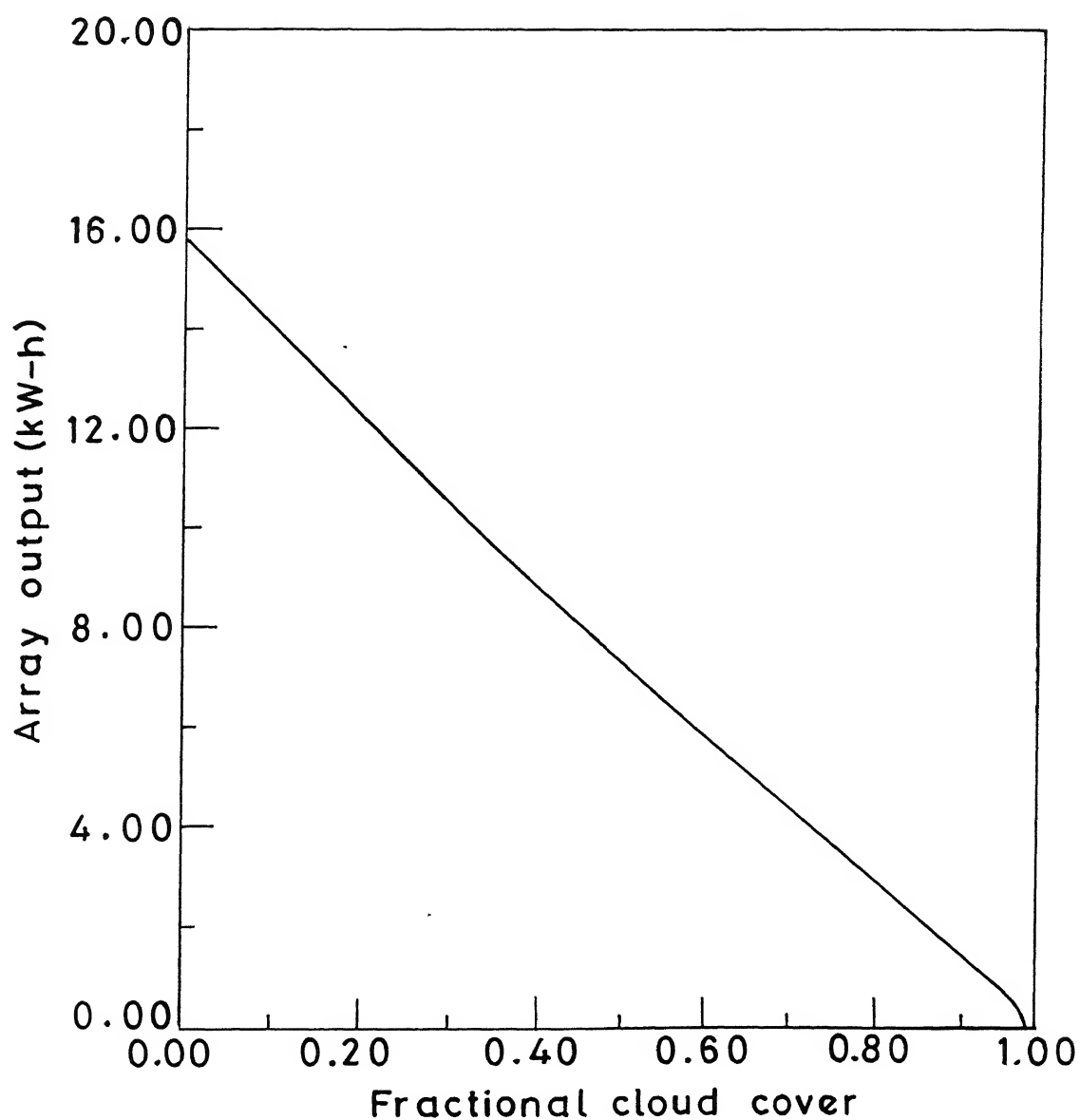


Fig.3.7 Effect of Fractional cloud cover on array output

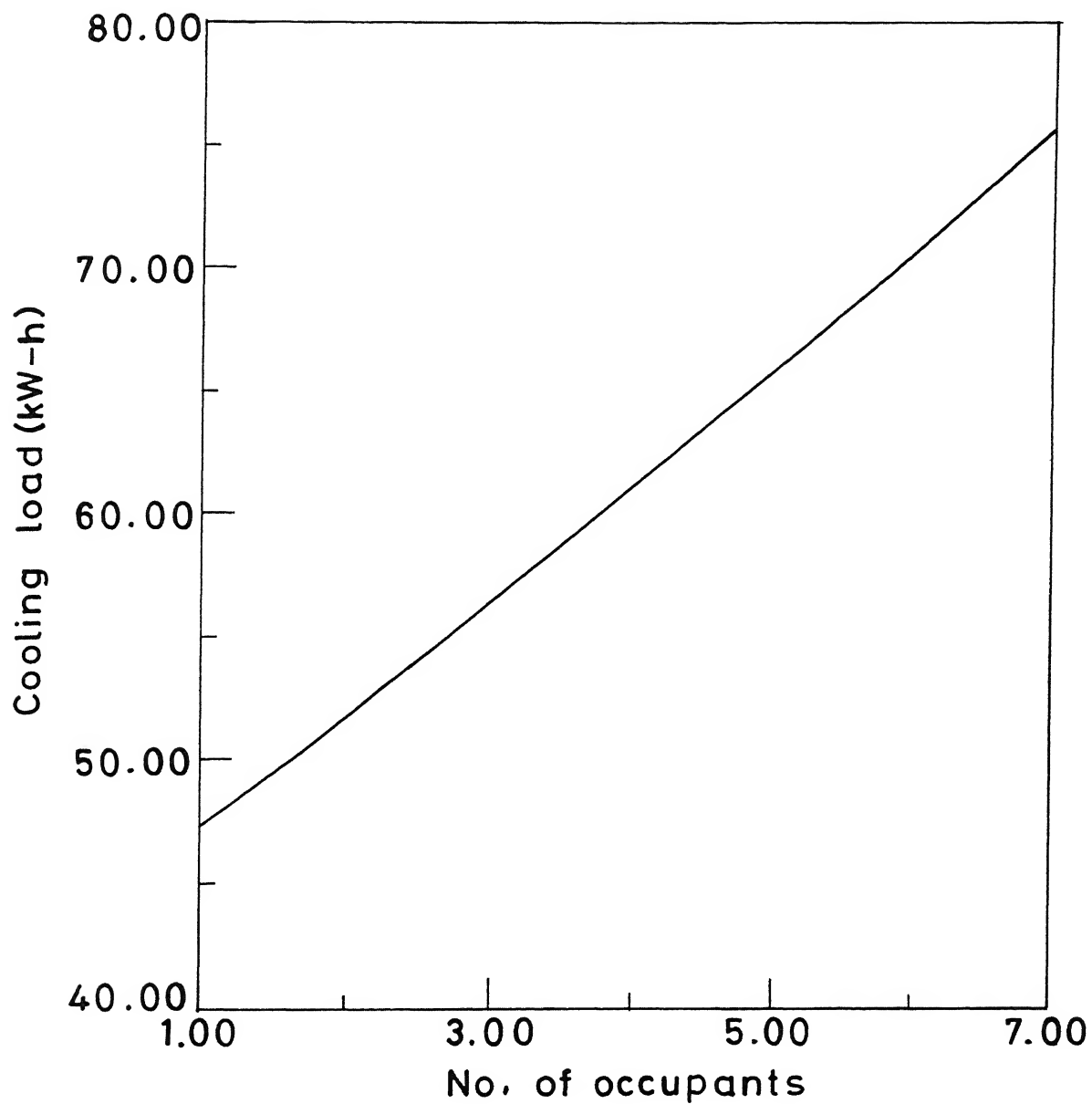


Fig.3.8 Effect of No. of occupants on cooling load .

$$l' = \begin{cases} m - 2(m - l) & m \geq 2(m - l), \\ 0 & m \leq 2(m - l) \end{cases} \quad (3.2)$$

and

$$h' = m + 2(h - m). \quad (3.3)$$

Here  $l$ ,  $m$  and  $h$  are experts estimates of a parameter for low, most likely, and high values respectively. The value of  $\mu$  is taken to be 0.5 at  $x = l$  and  $h$  and 1 at  $x = m$ . These fuzzy parameters lead to the fuzzy arithmetic computations at each  $\alpha$ -cut. Design parameters can be obtained then as fuzzy numbers.

For each parameters, different membership functions are constructed for different months. Average values of each month are considered most likely values, while 0.9 times average value is considered low and 1.1 times average value is considered high.

### 3.4 Results with Fuzzy Parameters

The programme was run for estimation of PV array size for airconditioning a room in Kanpur. The particulars of room are given in Appendix G. COP of the airconditioning system is taken as 3.84 based on section 7.1.3 and Chapter 7 of reference [Prasad, 1993]. PV cell data is given in Appendix H. Figures (3.9-15) show the possibility distributions of cooling load for different months (from April to October). There is a great variation in the cooling loads of various months. Figures (3.16-22) show the possibility distribution of array wattage required for different months. It is to be noted that there is not a direct correlation between cooling load and wattage of array, as the cloud cover is having much influence on the array output.

The question arises that given possibility distributions of array wattage for different months, which wattage of array should be selected. This is a subjective decision.

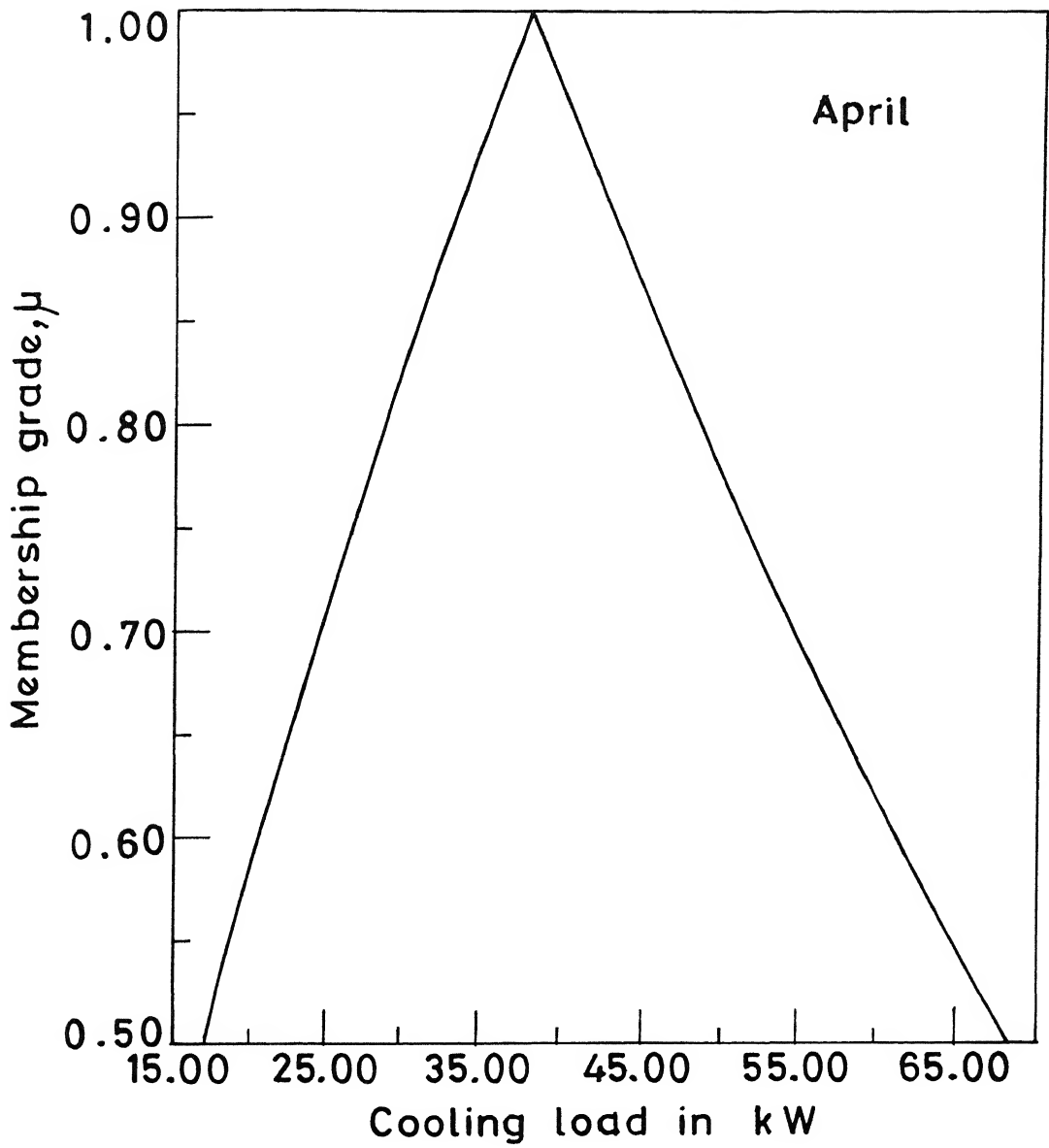


Fig.3.9 Possibility distribution of cooling load.

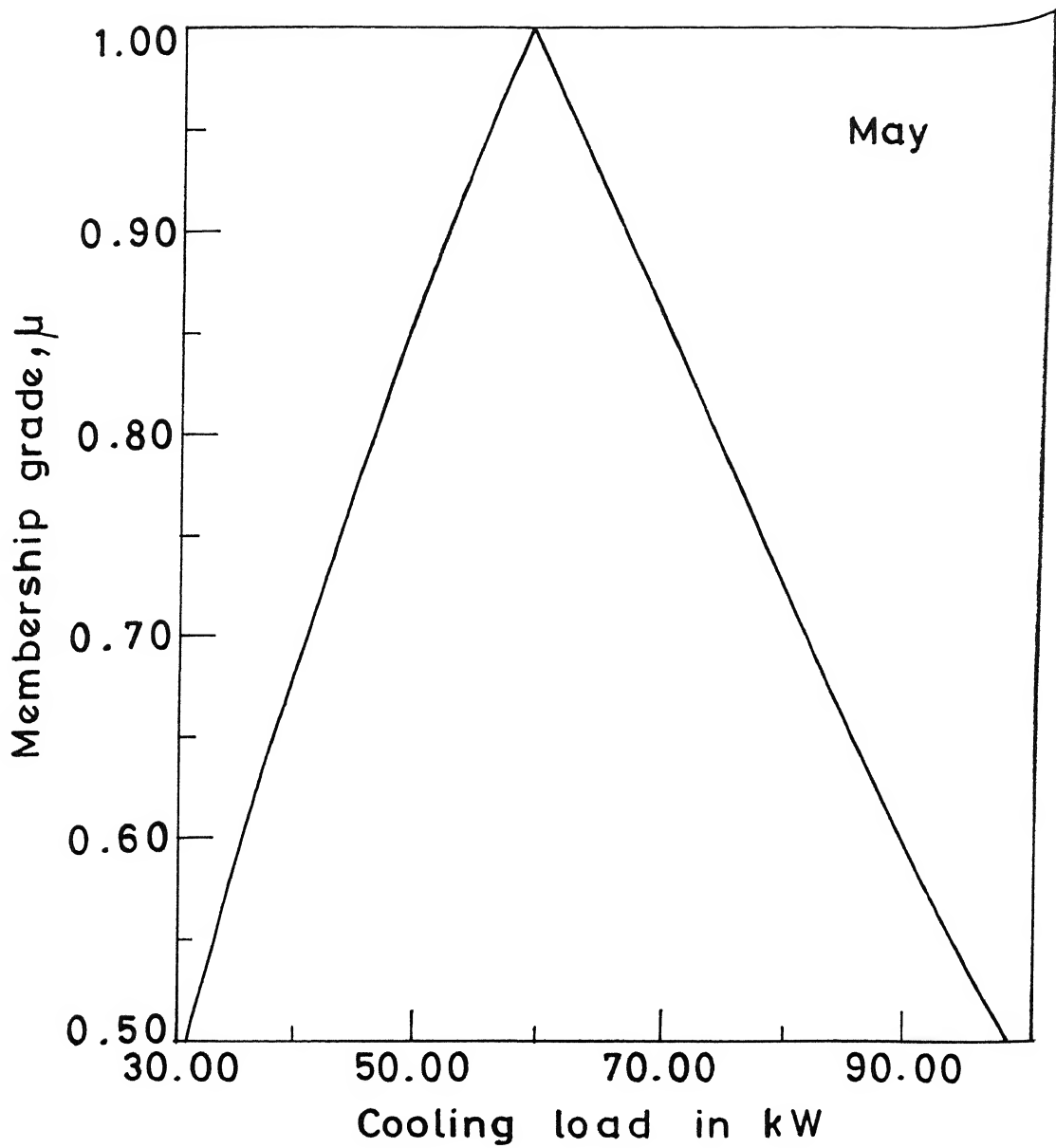


Fig. 3.10 Possibility distribution of cooling load.

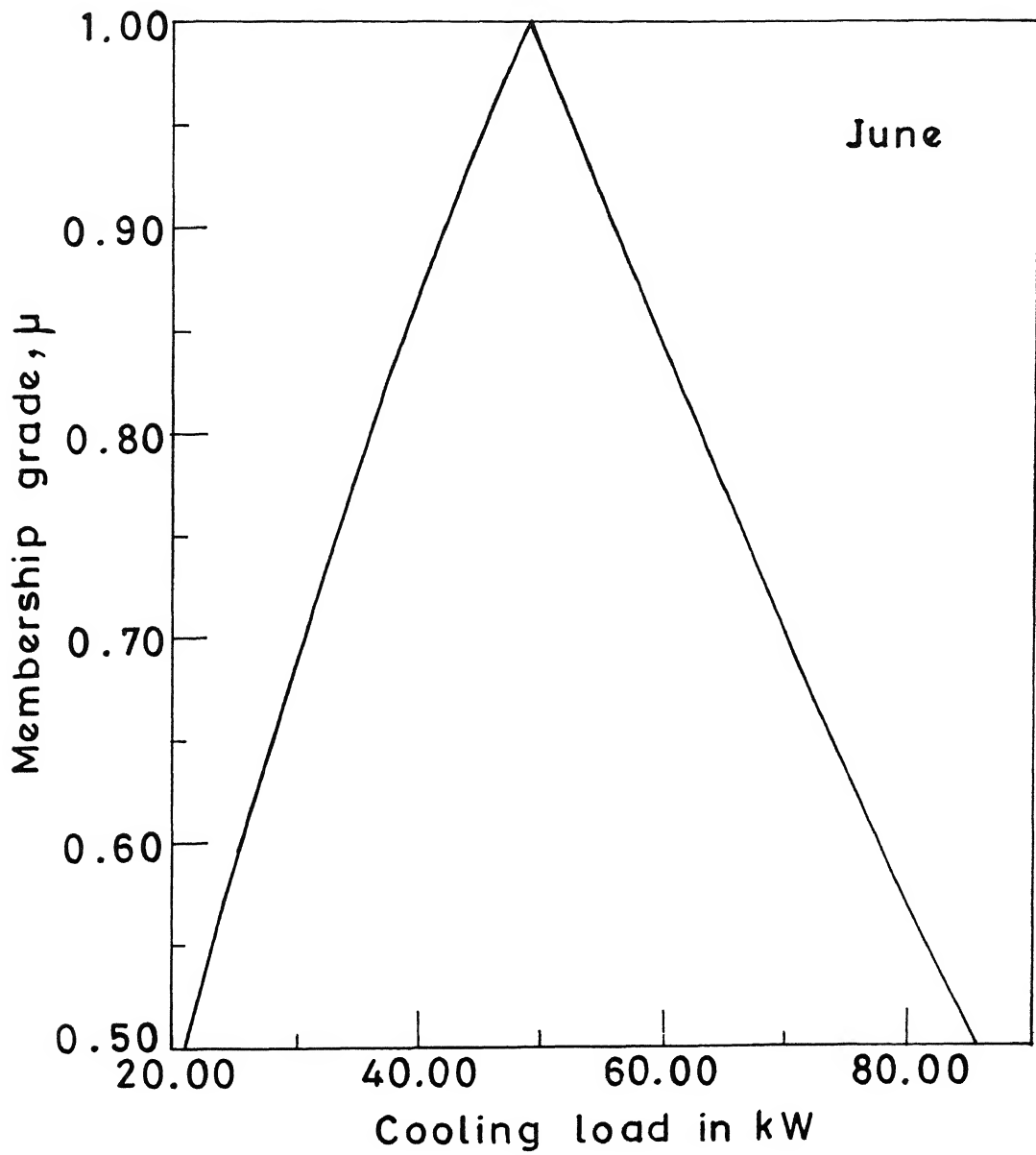


Fig.3.11 Possibility distribution of cooling load .



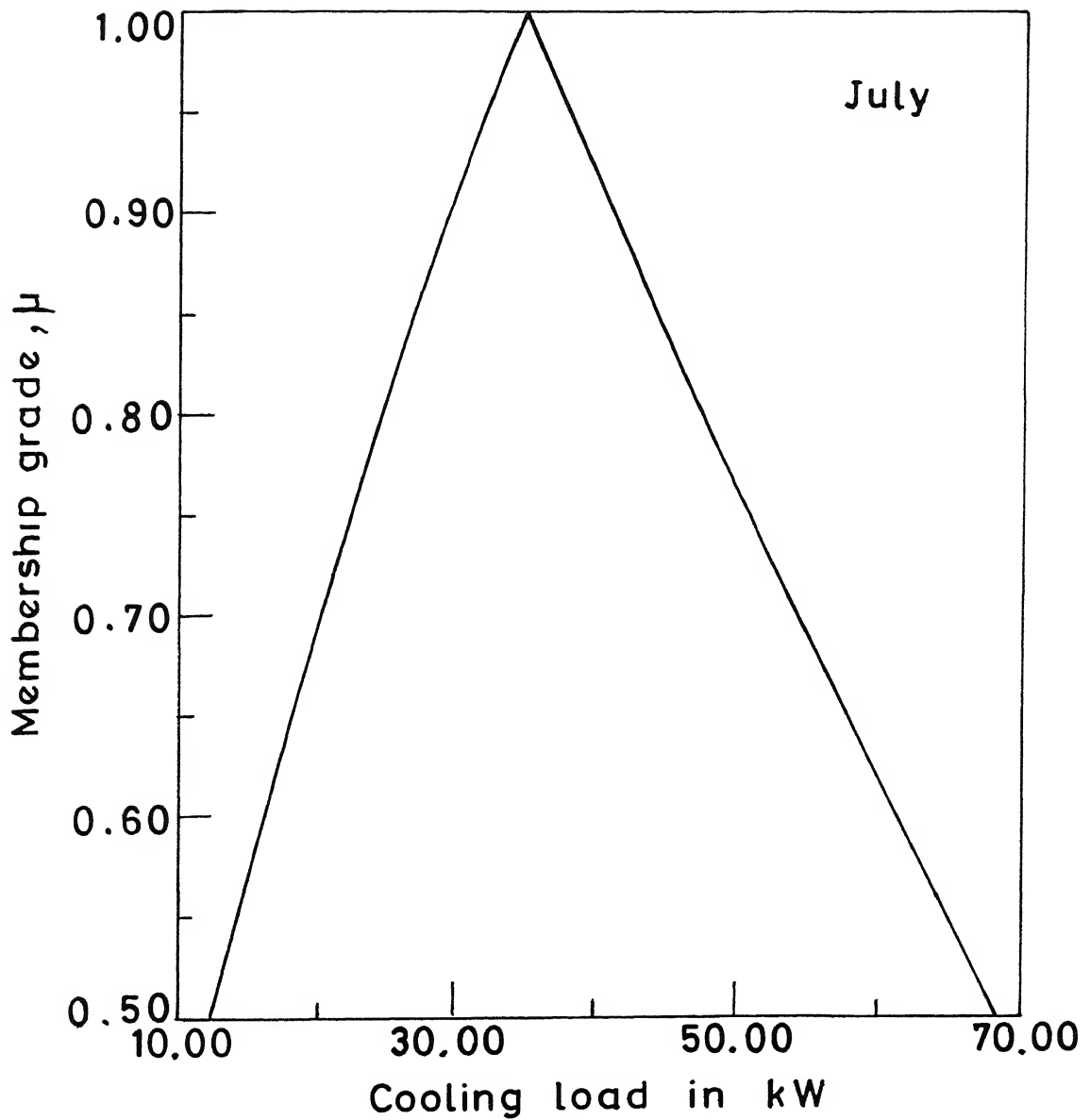


Fig .3.12 Possibility distribution of cooling load .

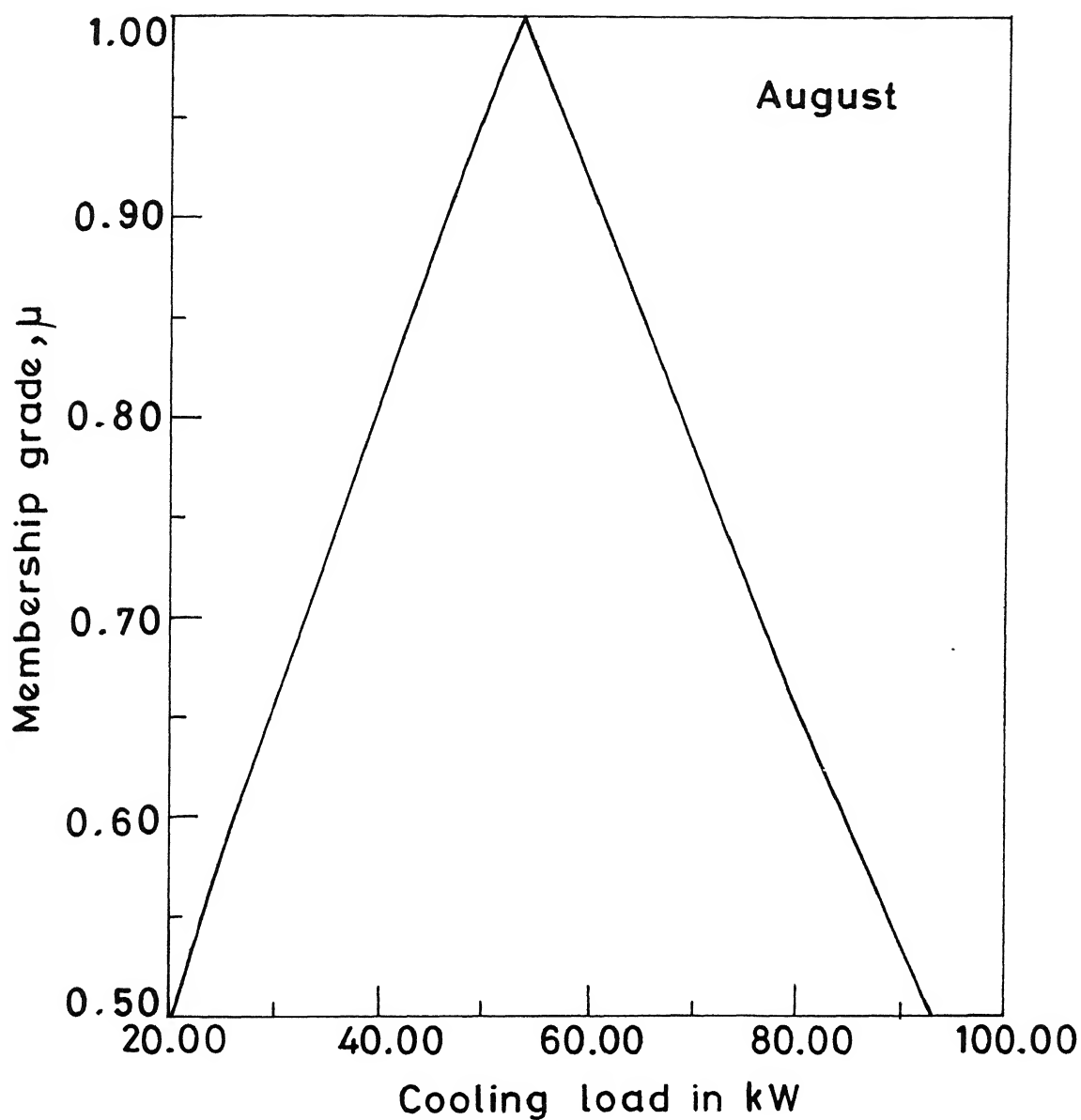


Fig.3.13 Possibility distribution of cooling load.

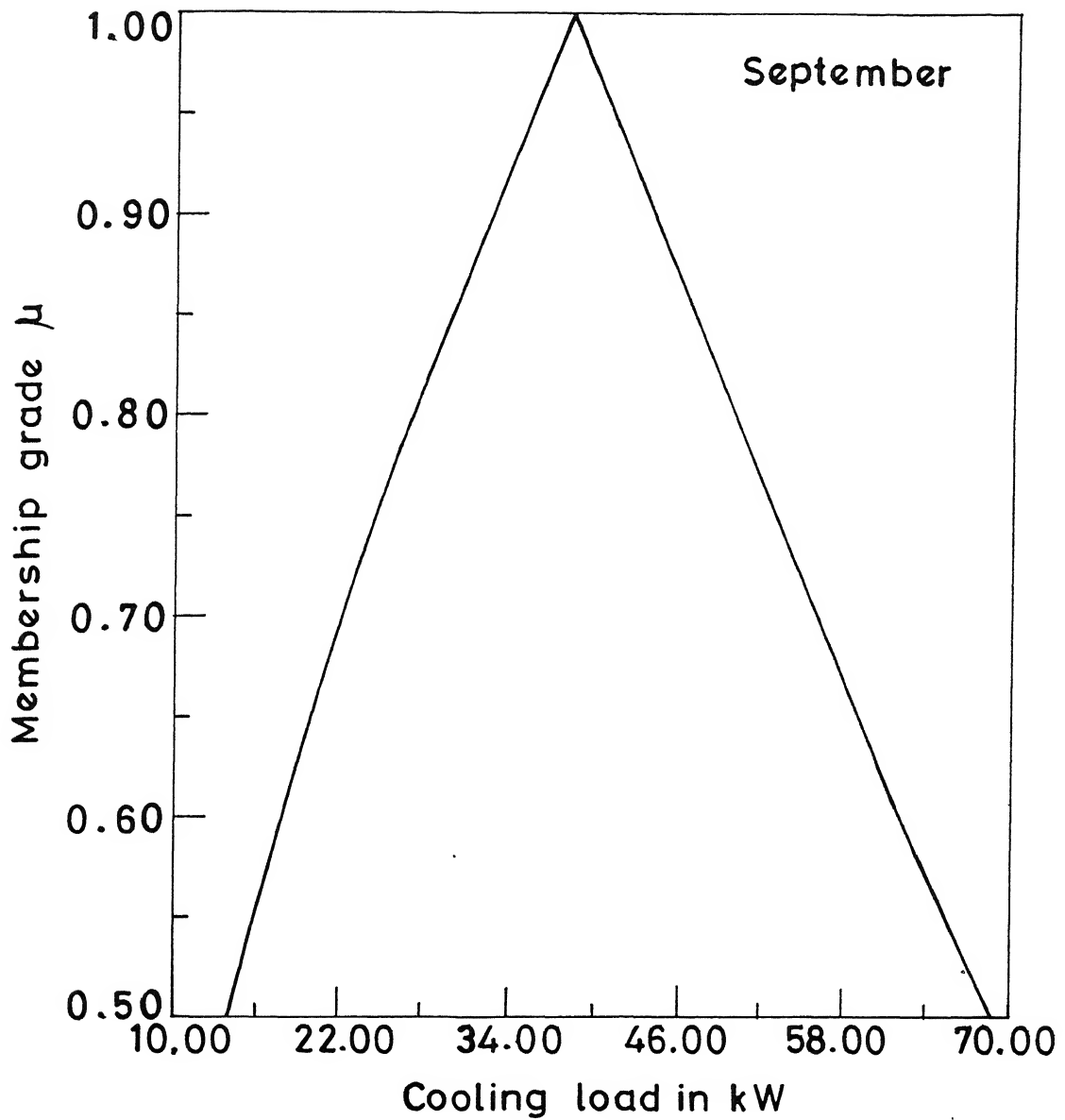


Fig.3.14 Possibility distribution of cooling load.

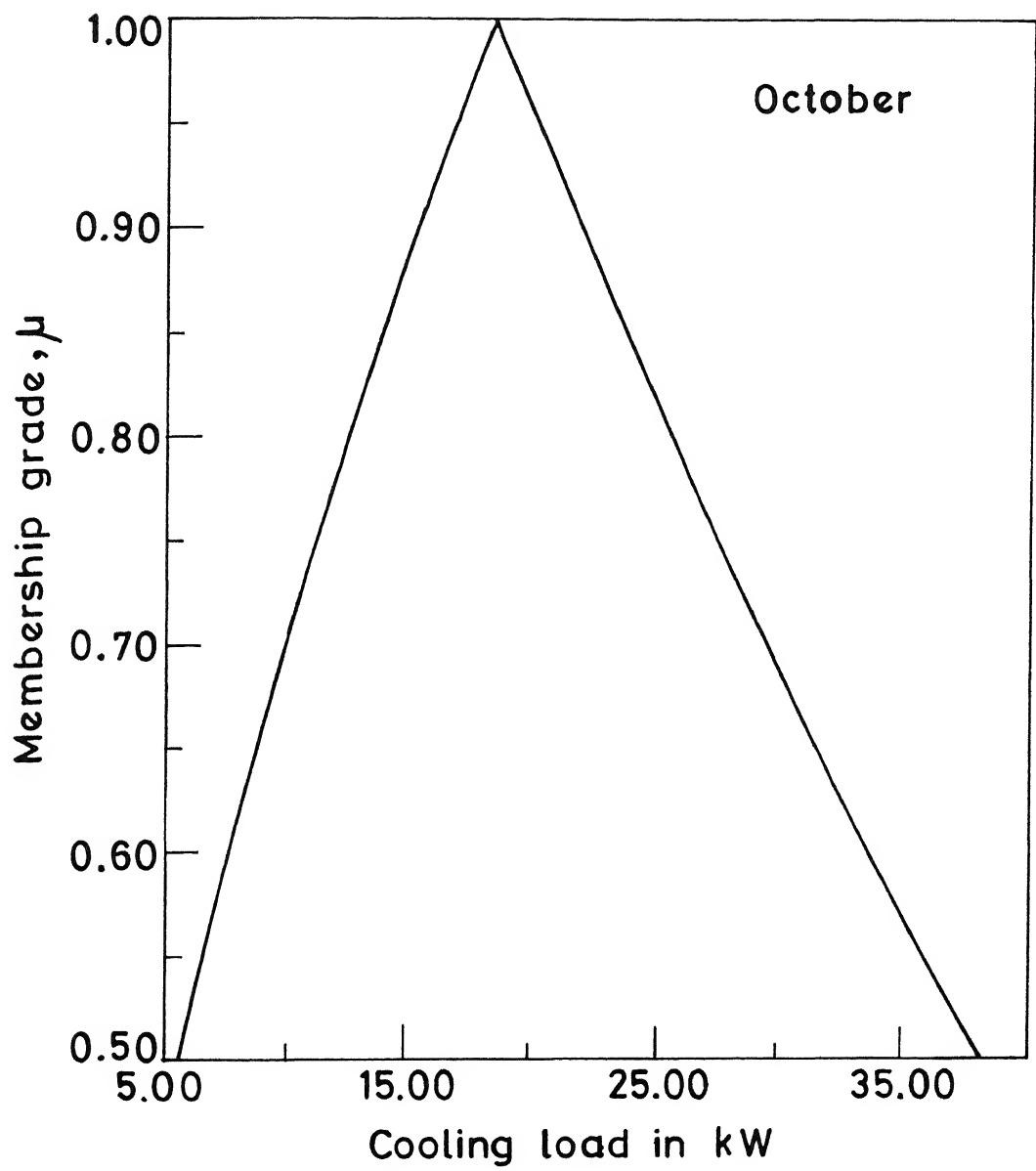


Fig.3.15 Possibility distribution of cooling load.

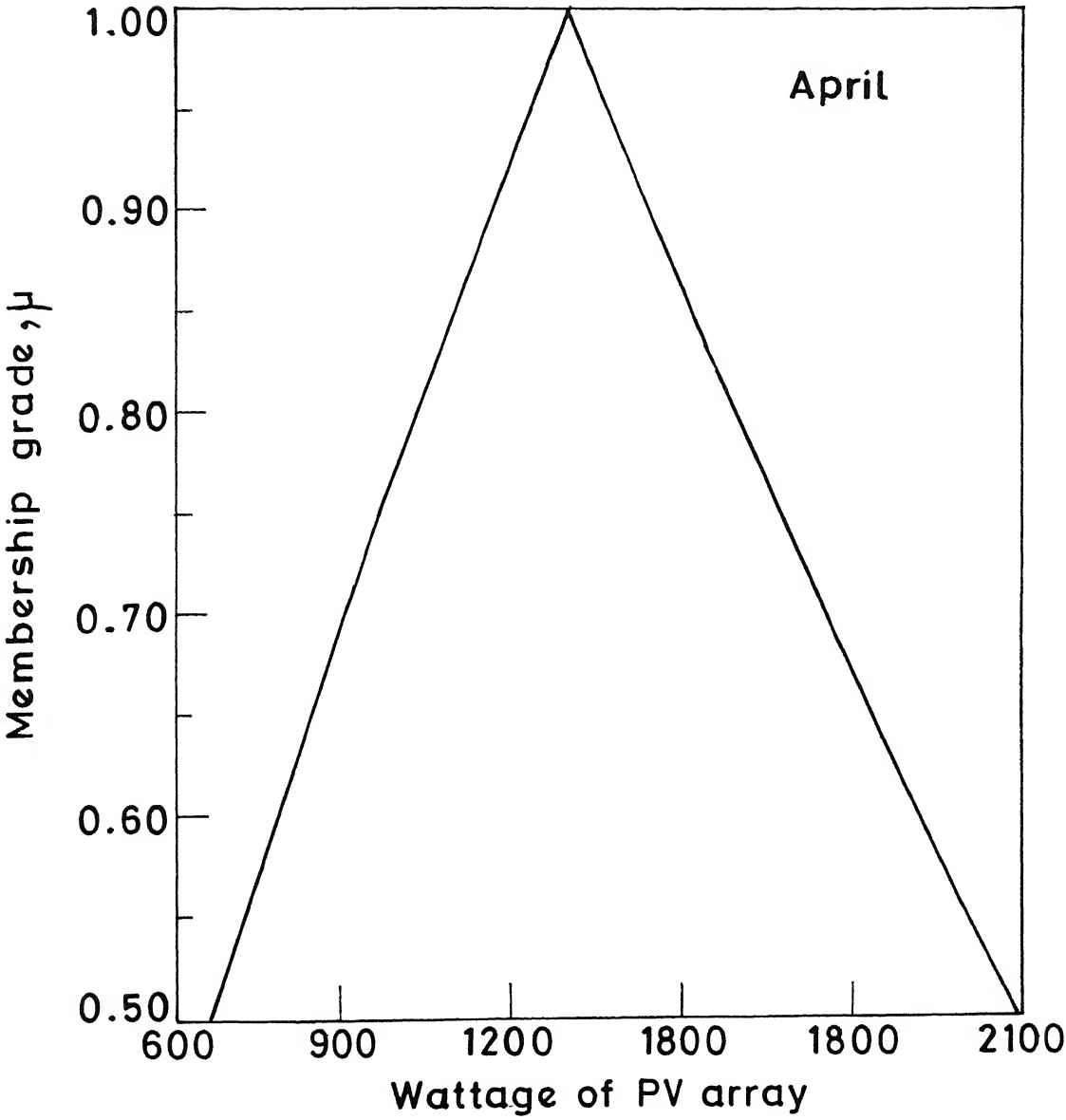


Fig.3.16 Possibility distribution of array wattage.

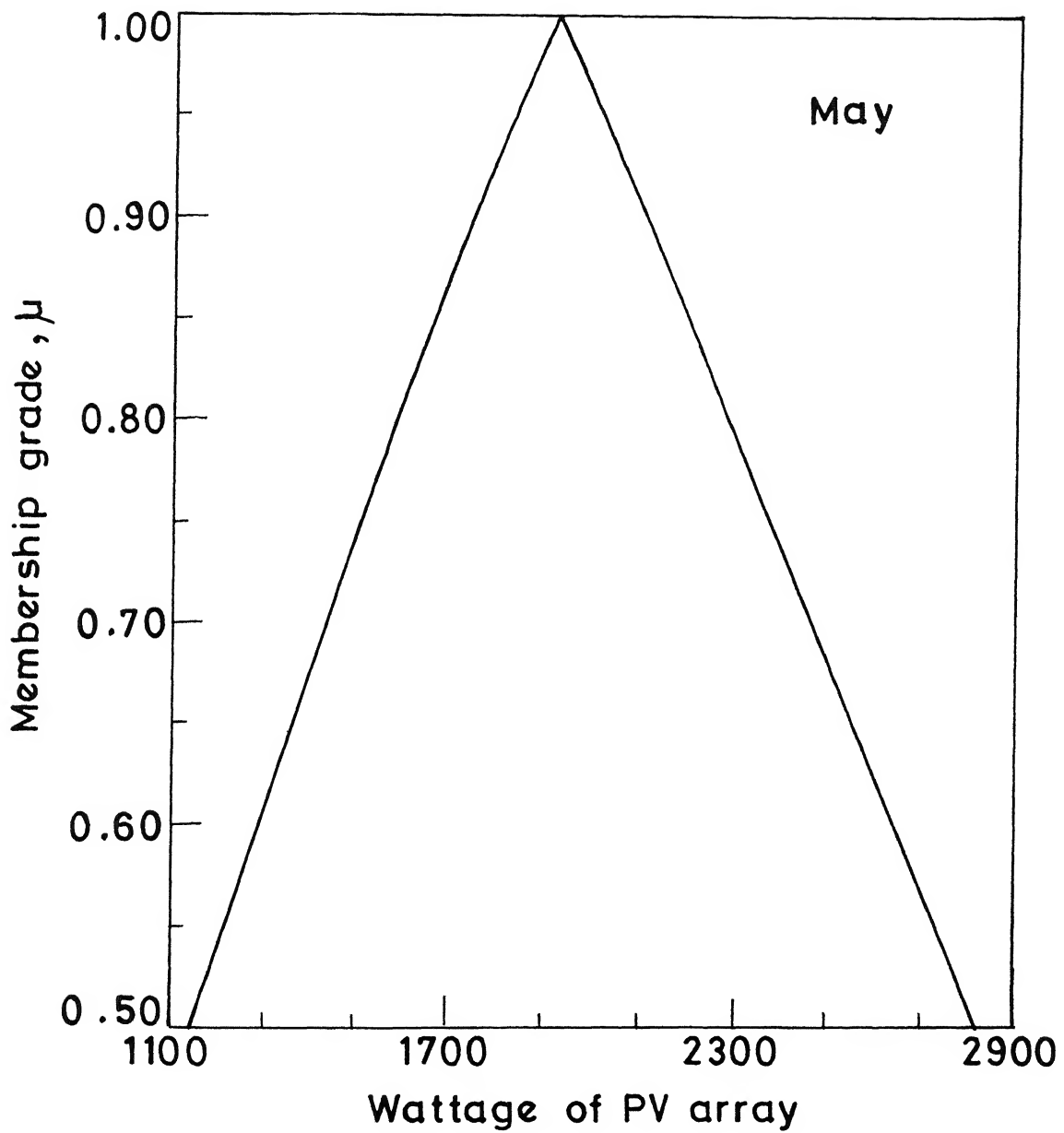


Fig.3.17 Possibility distribution of array wattage

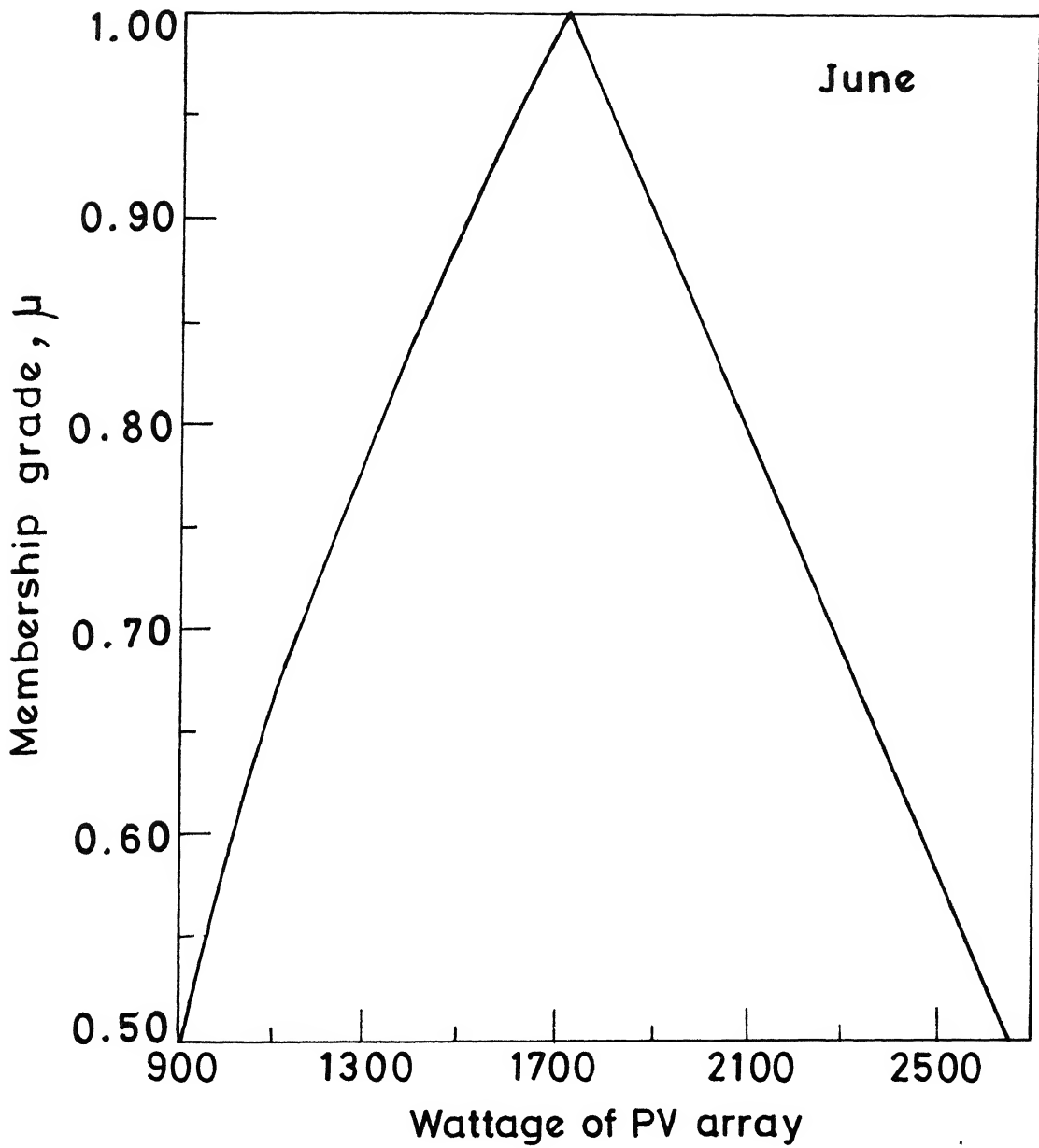


Fig.3 18 Possibility distribution of array wattage

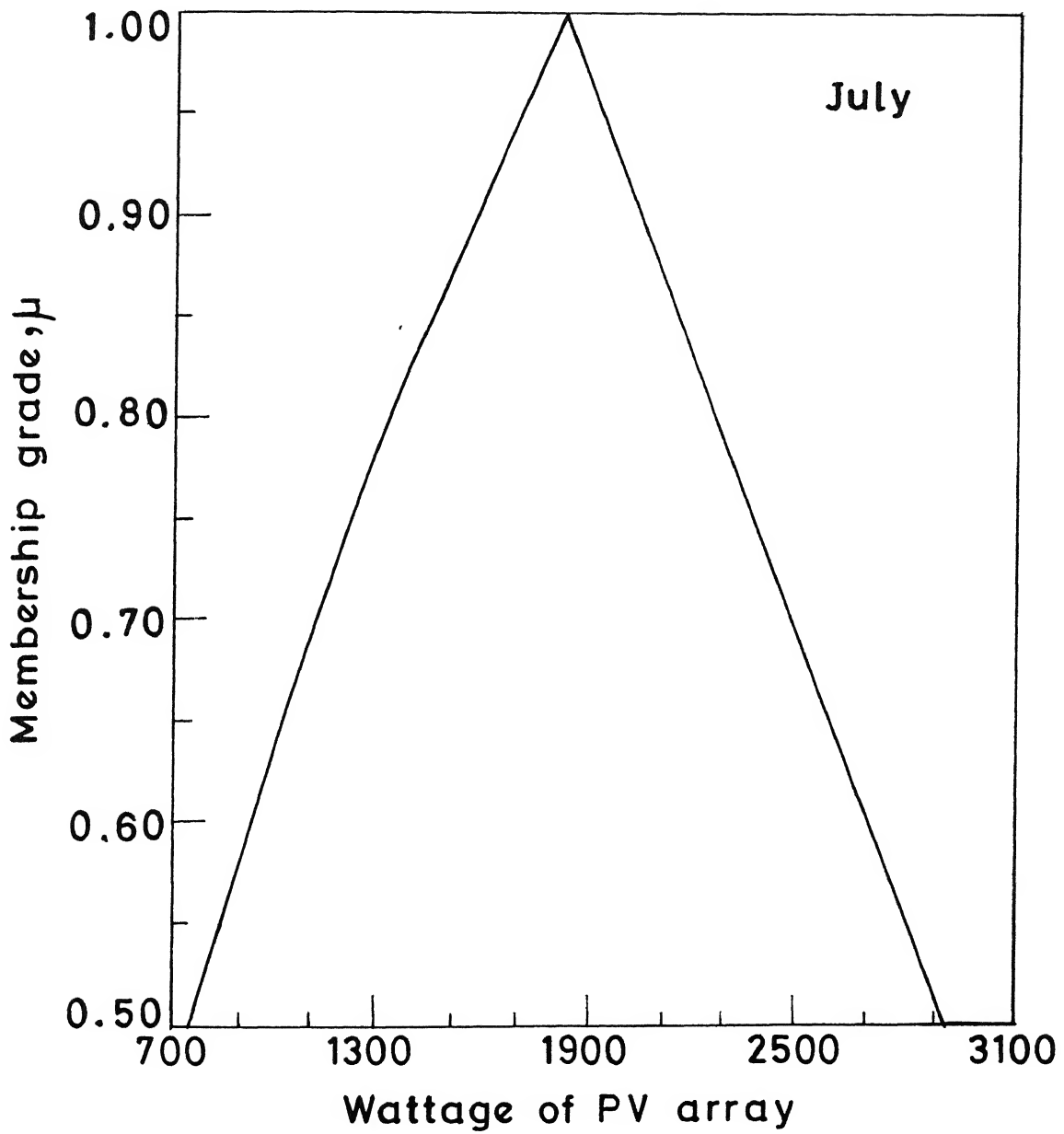


Fig.3.19 Possibility distribution of array wattage.



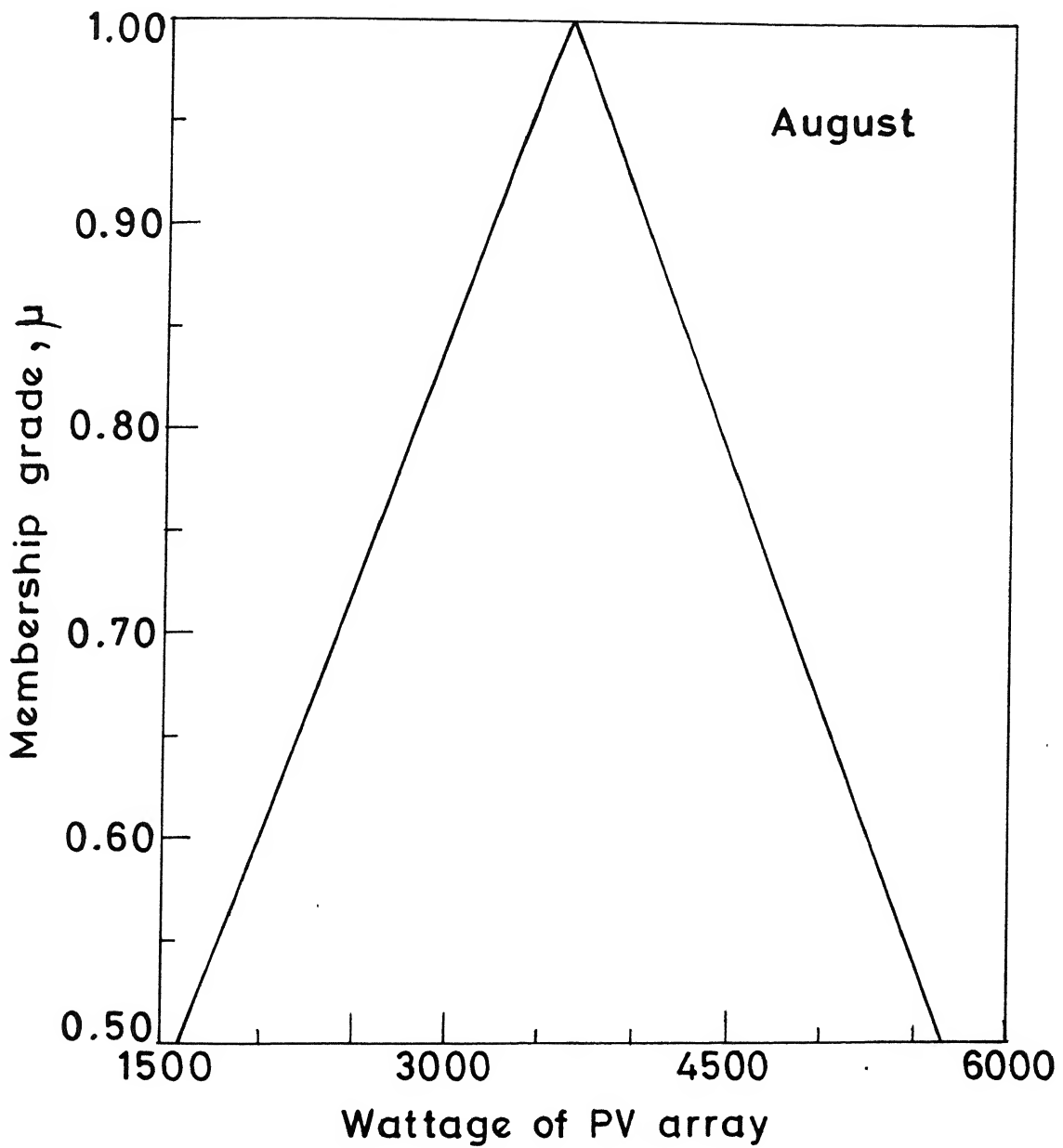


Fig. 3.20 Possibility distribution of array wattage.

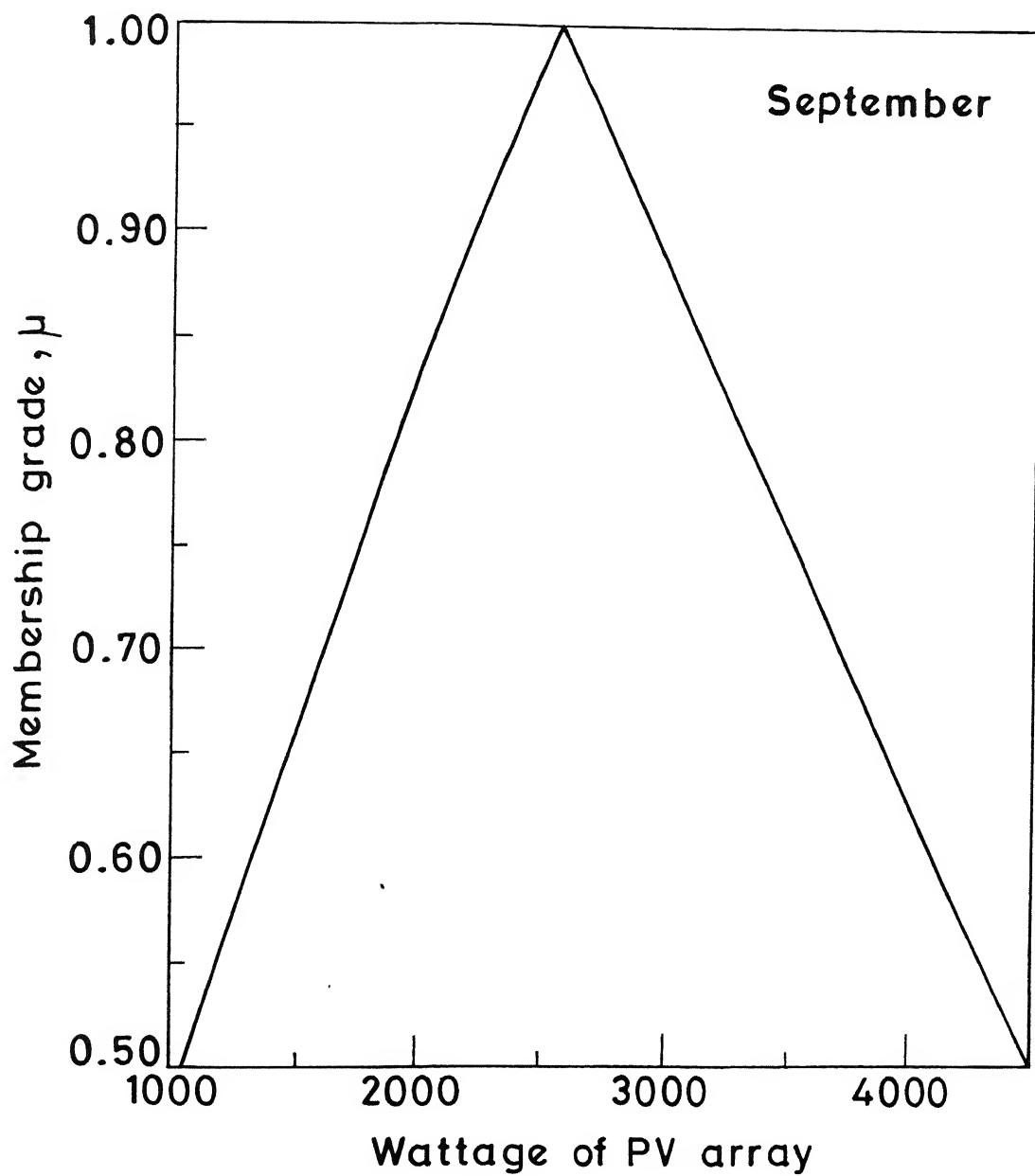


Fig.3.21 Possibility distribution of array wattage.

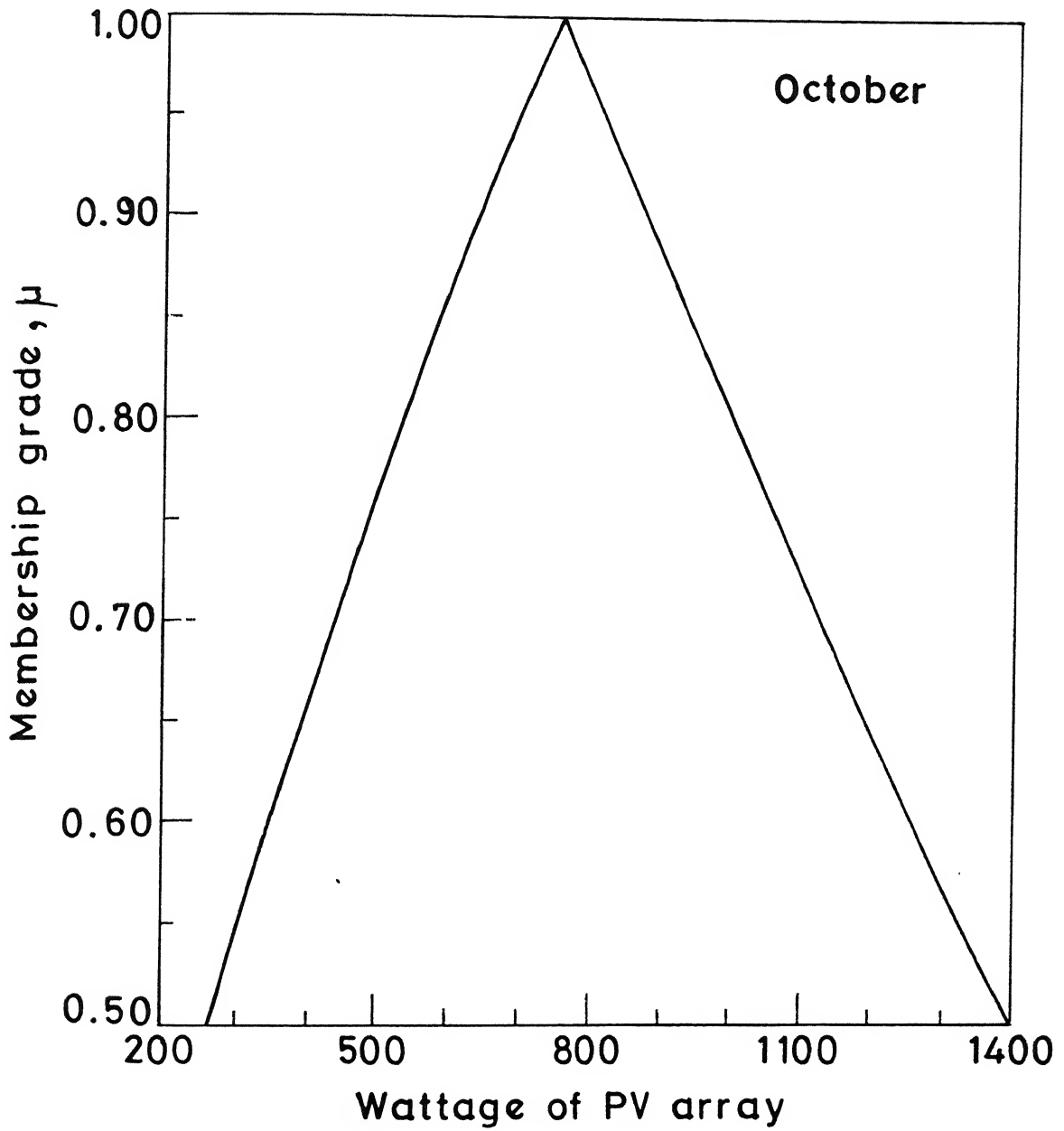


Fig.3.22 Possibility distribution of array wattage.

There can be various methods for it. One method is to give linguistic expressions to membership grades. For example, if the array is selected on the basis of upper limit of 0.5 membership grade, the design performance can be called excellent, because it is based on the worst weather conditions. The design based on the upper limit of 0.6 membership grade is very good and those based on the upper limit of 0.7, 0.8 and 0.9 will be called good, satisfactory and poor respectively. The design based on the membership grade of 1, will be called very poor. Once a particular array is selected, it will fall in the different categories of design in different months. To assess the overall effectiveness of the design, grade points are allotted to design categories as follows:

Design category	Grade point
Excellent	10
Very good	8
Good	6
Satisfactory	4
Poor	2
Very poor	0

Then the average grade point for all months can be found and is converted back into linguistic expression.

The procedure is similar to the evaluation of overall performance of a student in all the courses, he has taken. He is awarded a letter grade in each course, and each grade has corresponding points. To evaluate his overall performance, cumulative performance index is obtained by adding all the points, he has obtained in his various courses and dividing it by the number of courses, he has taken. Similar to that we obtain here, average grade point for the photovoltaic array, over the various months for the array.

#### **Examples:**

Suppose an array of 4500 W is selected. This design will be satisfactory in the month of August and in the rest of months, from April to October, it will be excellent.

The average grade point is given by,

$$\text{av. g. p.} = \frac{10 + 10 + 10 + 10 + 4 + 10 + 10}{7} = 9.14 \quad (3.4)$$

which is between excellent and very good design.

Suppose an array of 3000 W is selected. This design is excellent in April, May, June and July, very poor in the month of August, poor in the month of September and excellent in the month of October. Therefore,

$$\text{av. g. p.} = \frac{10 + 10 + 10 + 10 + 0 + 2 + 10}{7} = 7.43 \quad (3.5)$$

This shows that this design is between good and very good, more inclined towards very good design . The cost of 4500 W array is about 1.5 times that of 3000 W array. Therefore a designer may decide to choose 3000 W array, as the quality of design is not drastically sacrificed.

As a last example, suppose a 2300 W array is selected which gives satisfactory performance in the month of May (month of maximum heat). This design is excellent in the month of April, good in the month of June, satisfactory in the month of July, very poor in the months of August and September and excellent in the month of October. Then,

$$\text{av. g. p.} = \frac{10 + 4 + 6 + 4 + 0 + 0 + 10}{7} = 4.86 \quad (3.6)$$

which is between satisfactory and good design. This design may be opted where cost is the primary consideration.

### 3.5 Summary

A method to estimate array size for airconditioning the space, using fuzzy set theory, is presented and computer code has been developed for this purpose. An example has

been taken for estimating array sizes for a typical room at IIT Kanpur. It is highlighted that use of fuzzy set theory in the array size determination may be much helpful in selecting a optimum array size.

## Chapter 4

# OPTIMUM LOAD MATCHING OF A BATTERY CONNECTED PHOTOVOLTAIC ARRAY

### 4.1 Introduction

In a photovoltaic system it is desirable to extract the maximum amount of energy output from the array connected to the battery having proper matching. This matching is usually done by the suitable choice of number of series modules and number of parallel strings of the photovoltaic array. In addition to this battery parameters may also be decided suitably in order to have maximum energy transfer.

In the past researchers [Khouzam, 1990; Appelbaum, 1987], have concentrated on optimum array for photovoltaic power. In this chapter, a method to select optimum layout for PV cells and battery parameters is presented. The importance of proper load matching for airconditioning and refrigeration is highlighted.

In the present work, the photovoltaic power generated by the array at any instant is

considered to be proportional to the solar radiation falling on it, unlike the assumption of sinusoidal variation of the photovoltaic current with solar time, made by earlier researchers [Khouzam, 1990; Appelbaum, 1987]. A comparison with the experimental results validates our model. Using this model a parametric study is carried out.

Alternatively, to extract the maximum energy output from the PV array, a maximum power point tracker (MPPT) can also be employed in between PV array and the load. The maximum power point tracker is an electronic circuit which can be used to operate the load at the maximum power point of the array. However, MPPT is a costly and use of an additional circuit needs frequent maintenance. Therefore, attempt should be made to avoid its use by proper load matching as discussed here.

## 4.2 Load Characteristics

The battery is directly connected to PV array. The load equation for the battery is given as

$$V_L = I.R_e + V_e \quad (4.1)$$

where  $V_L$  is the load voltage,  $I$  is the load current,  $V_e$  is the induced emf of the battery and  $R_e$  is the internal resistance of the battery. If the small potential drop from array to battery is neglected, then

$$V_L = V \quad (4.2)$$

where  $V$  is the output voltage of the PV array. Substituting the expression for  $V$  from equation (4.1) into the equation (2.1), one gets

$$V_e = AV_T \cdot \ln\{(I_{Ph} - I + I_r)/I_r\} - I(R_s + R_e) \quad (4.3)$$



The power stored in the battery is given by

$$P_B = I.V_e = AV_T.I \ln\{(I_{Ph} - I - I_r)/I_r\} - I^2(R_s + R_e) \quad (4.4)$$

while the power available at the array is given by

$$P_A = I.V = AV_T.I \ln\{(I_{Ph} - I + I_r)/I_r\} - I^2R_s \quad (4.5)$$

The total daily energy which can be stored in the battery, assuming that the battery is connected to the array during the entire period, is then calculated from :

$$E_B = \int_{t_{sr}}^{t_{ss}} P_B dt \quad (4.6)$$

### 4.3 Load Matching Factor

Each array possesses a maximum power line. If the array operates at maximum power point voltage at all the time, the energy output from the array will be maximum. Denoting the maximum possible energy storage in the battery by  $E_{Bmax}$ , a load matching factor is defined as

$$M = E_B/E_{Bmax} \quad (4.7)$$

The closer is the value of M to 1, the better is PV array matching.

The procedure to calculate  $E_{Bmax}$  is described here briefly. The maximum power is found by differentiating power (P) in equation (2.9) with respect to load current I and equating the same to zero. This gives the following equation:

$$I_{Ph} = I_{mp} + I_r \{\exp[(2I_{mp}R_s/AV_T) + I_{mp}/(I_{Ph} - I_{mp} + I_r)] - 1\} \quad (4.8)$$

This equation is solved numerically to find  $I_{mp}$ .

The maximum power point voltage,  $V_{mp}$  can be found from equation (2.1) by replacing  $I$  by  $I_{mp}$ . The maximum power,  $P_{mp}$  is then given by:

$$P_{mp} = V_{mp}.I_{mp} \quad (4.9)$$

The maximum electrical energy which can be generated from the solar energy over one day period is given by the integral:

$$E_{Bmax} = \int_{t_{sr}}^{t_{ss}} P_{mp} \cdot dt \quad (4.10)$$

which is a characteristics of the array. Here,  $t_{sr}$  and  $t_{ss}$  are the sun-rise and sun-set times respectively.

## 4.4 Selection of Battery Voltage and Capacity

It is observed that most of the refrigerators require fractional horse power motors. A permanent magnet D.C. motor powered by 12 volt battery source may be employed as the D.C. motor is inherently efficient for part load operation. For airconditioners and heaters requiring high power motors either brushless D.C. motor or induction motor along with optimal flux control circuit (to make it part load efficient) may be employed. For this purpose a 24-volt battery along with inverter may be used.

The battery capacity is decided from the consideration of maximum reserve energy which we want to store and maximum depth of discharge. Usually a battery capacity of twice the total solar energy of the day will be sufficient. However, where the weather conditions are uncertain a higher battery capacity should be used.

## 4.5 Problem Formulation

The objective is to maximize the load matching factor and consequently  $E_B$ , since  $E_{Bmax}$  is fixed for a given array and insolation and temperature profile. This can be stated mathematically as follows:

Maximize:

$$E_B = f(N_s, N_p, R_e) \quad (4.11)$$

Subject to:

$$N_s.N_p \leq N_a \quad (4.12)$$

where  $N_a$  is the maximum number of cells in the array.

The solution of the above optimization problem yields the optimum storable battery energy, from which the optimum load matching factor,  $M_{opt}$  and the corresponding series cells, parallel strings and internal resistance can be calculated.

## 4.6 Solution Procedure

The optimization problem is solved by the sequential quadratic programming method [Pike, 1986]. The EO4 UCF routine of NAG library is used for this purpose. In this routine the design variables  $N_s$ ,  $N_p$  and  $R_e$  are treated as real numbers. After the final solution is obtained, the nearest integer value of  $N_s$  and  $N_p$  is chosen.

In equation (4.3) I and in equation (4.8)  $I_{mp}$  is found using interval reducing methods [Pike, 1986]. The interval reducing methods guarantees the convergence of the solution. The overall computation time for the problem is 1-2 seconds of user time on HP-computers.

## 4.7 Results and Discussion

The PV generator data are obtained from literature [Appelbaum, 1986]. The two array sizes were selected - one array consisting of 400 cells is suitable for 100 W refrigerator, the other array consisting of 7040 cells is suitable for airconditioning of room. The results obtained from the simulation runs are discussed in the following subsections.

### 4.7.1 Optimized Combination of Cells and Internal Resistance

Table 4.1 shows the optimized parameters for the array and battery. It is observed that in all the cases internal resistance has to be kept zero. Physically zero internal resistance is not possible, but attempt should be to keep it at minimum. The optimum energy stored in the battery was 0.98 times maximum storable energy  $E_{Bmax}$  for bigger array and 0.97 times maximum storable energy  $E_{Bmax}$  for smaller array.

Here the optimization was done for maximizing the stored energy. If the optimization is done to maximize available energy the different solutions are obtained. For example, for 24-V battery the smaller array will give maximum available power for  $N_p = 6$ ,  $N_s = 66$  and  $R_e = 0.5 \Omega$ ; however, then a fraction of the energy will be wasted as the heat loss and useful energy will be only 0.92 times  $E_{Bmax}$ . Since our concern is to maximize stored energy, the optimization has to be done for maximizing the stored energy and not the available power.

Figure (4.1) shows the effect of proper array layout on the load matching factor. The curve has been drawn for 12-V battery and 400 cell array combination. On the horizontal axis, number of parallel strings are shown. The number of cells in series may be found by taking the nearest integer value of  $400/N_p$ . The Figure clearly shows the proper cell arrangement is the crucial thing to decide. The load matching factor is maximum at  $N_p = 12$ , and more the deviation from this value, we have, the lesser load matching factor will be obtained.

### 4.7.2 Effect of Internal Resistance

To study the effect of internal resistance on the load matching factor, first a system consisting of 12-volt battery and 400 cell array is considered. In Figure (4.2), the lower curve is for the load matching factor based on stored power, while the upper curve is

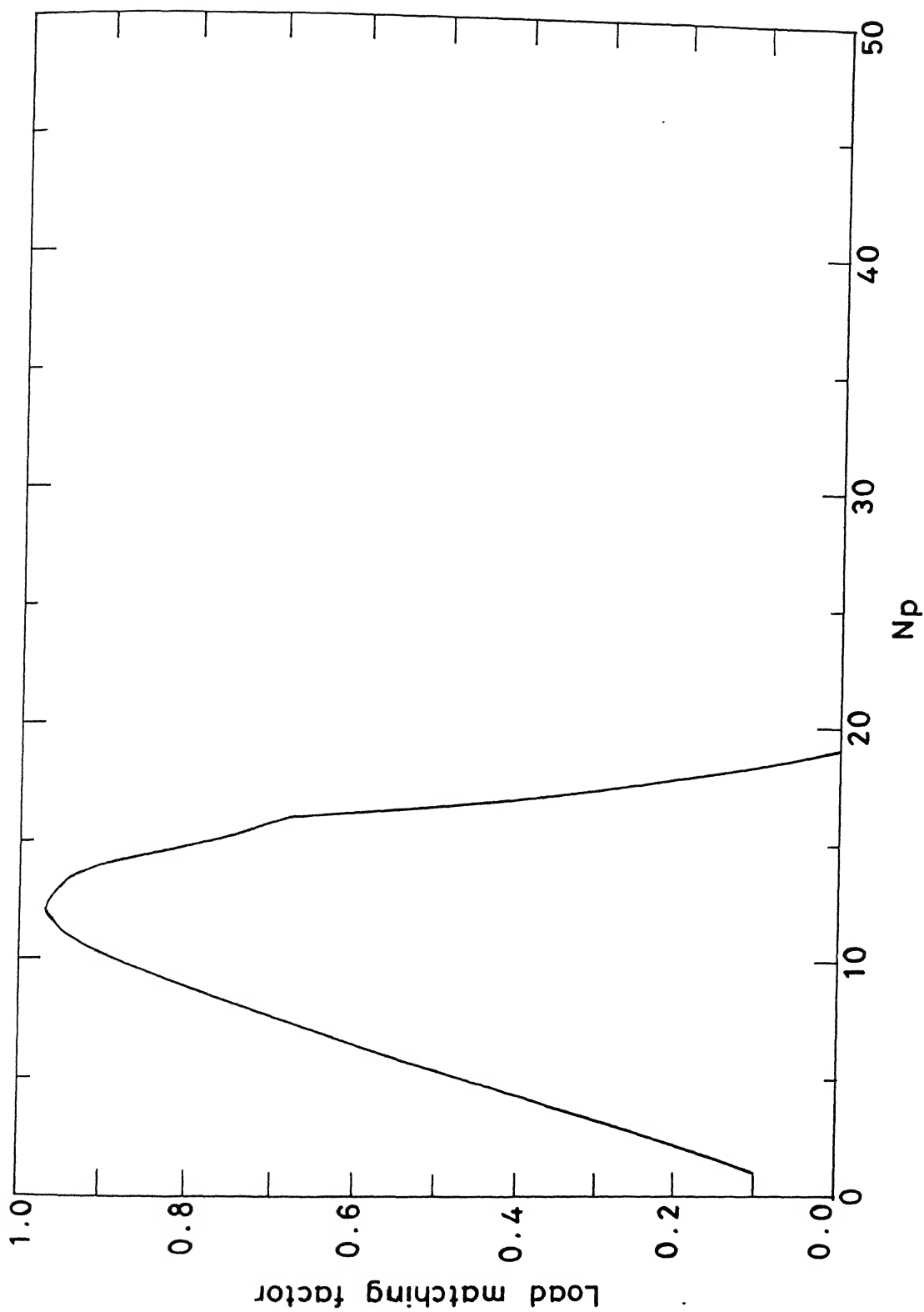


Fig. 4.1 Effect of array configuration ( $n \times n$ s) on the load matching factor (for 12 V battery and 400 cell array)

Table 4.1: Optimized Parameters for the Array

	Smaller array (400 cells)			Bigger array (7040 cells)		
	$N_p$	$N_s$	$r_e$	$N_p$	$N_s$	$r_e$
For 12-V Battery	12	33	0	227	31	0
For 24-V Battery	6	66	0	117	60	0

for available power. The figure shows clearly that internal resistance has the adverse effect on the load matching factor based on the stored power. However, observing the load matching factor based on the available array output, it is seen that it attains maxima at some value of internal resistance. Figure (4.3) is for bigger array (7040 cell array). Here, also the same trend is observed, with different pattern.

In practice, there is always some resistance in the battery. The question arises whether the array designed for the battery with zero internal resistance will be optimum for the battery with the resistance. From Table 4.2, we see that answer is 'No'. For example, for  $1.2\Omega$  internal resistance battery, the optimum array arrangement is  $N_p = 9$ ,  $N_s = 44$  and available array energy is  $0.98 E_{Bmax}$  which shows if we design the array suitable, the maximum power point tracker (MPPT) is not needed. However, because of  $i^2R$  losses, the stored energy is less. On the other hand, if we take  $N_p = 12$ ,  $N_s = 33$ , (which is optimum for 0 internal resistance battery) for  $1.2\Omega$  internal resistance battery we obtain lesser available and stored energy. This shows that with the change of internal resistance optimum combination also gets changed.

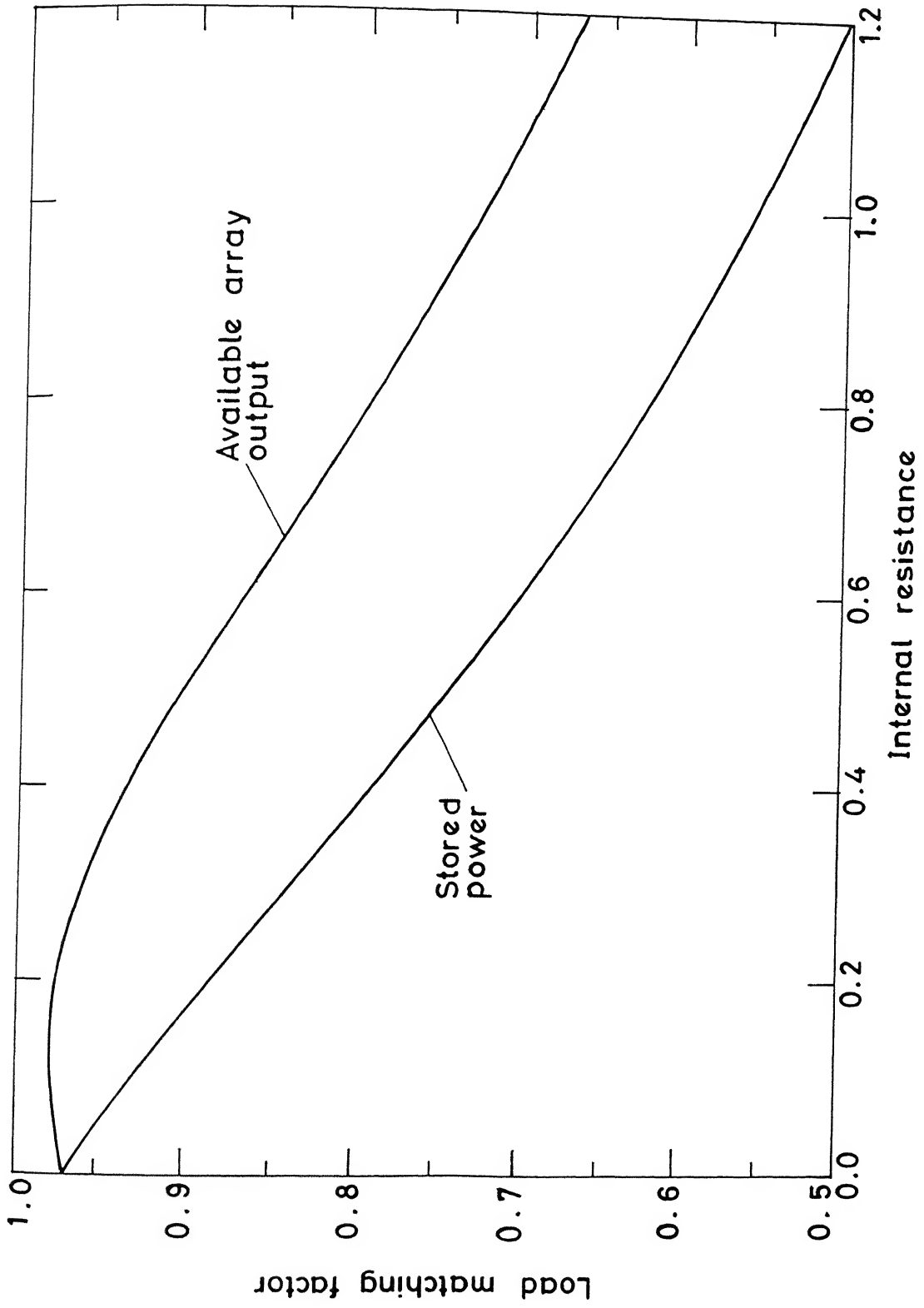


Fig. 4.2 Effect of internal resistance on load matching factor (for 12V battery and 400 Cell array)

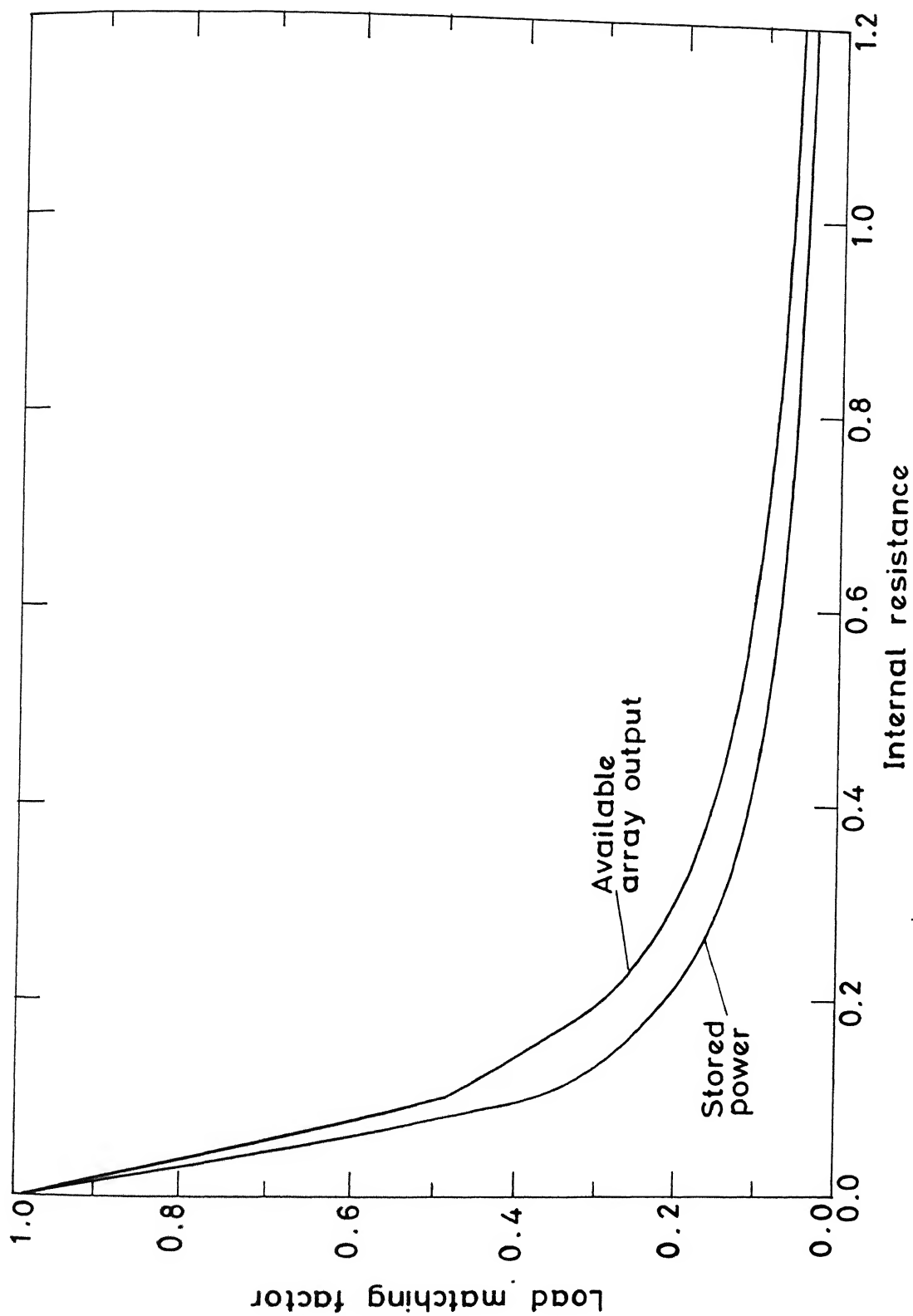


Fig. 4.3 Effect of internal resistance on load matching factor for (12V battery and 7040 Cell array)



Table 4.2: Arrangement of smaller array(400 cells) for  $1.2\Omega$  internal resistance battery

$R_e$	$N_p$	$N_s$	Stored energy	Available energy	Maximum energy
$1.2\ \Omega$	9	44	636.16 kWh	922.71 kWh	928.6 kWh
$1.2\ \Omega$	12	33	474.38 kWh	633.61 kWh	928.6 kWh

### 4.7.3 Sensitivity Analysis with Changing Battery Voltage

Figures (4.4-5) show the influence of battery voltage on the load matching factors for the arrays designed for 12 volt and zero internal resistance battery. It is seen that load matching factor drops first gradually, then at the high rate as the battery voltage deviates from 12 volt. The attempt should be to keep the variation of the battery voltage to the minimum possible value.

### 4.7.4 Load Matching Factor for Different Months

The load matching factors for different months for the smaller and bigger arrays were found. It was seen that the load matching factor is almost same for all months. This shows that the array which has been matched in one month will continue to operate at almost maximum load matching factor in other months as well.

### 4.7.5 Summary

In this chapter, an optimization code has been developed and simulation study is done. Based on the study, the following conclusions may be drawn.

1. There is no need of a maximum power point tracker (MPPT) if the array is properly matched with the battery. Because the value of load matching factor in the range of applications turn out to be around 0.97.
2. The internal resistance of the battery has to be kept at minimum.

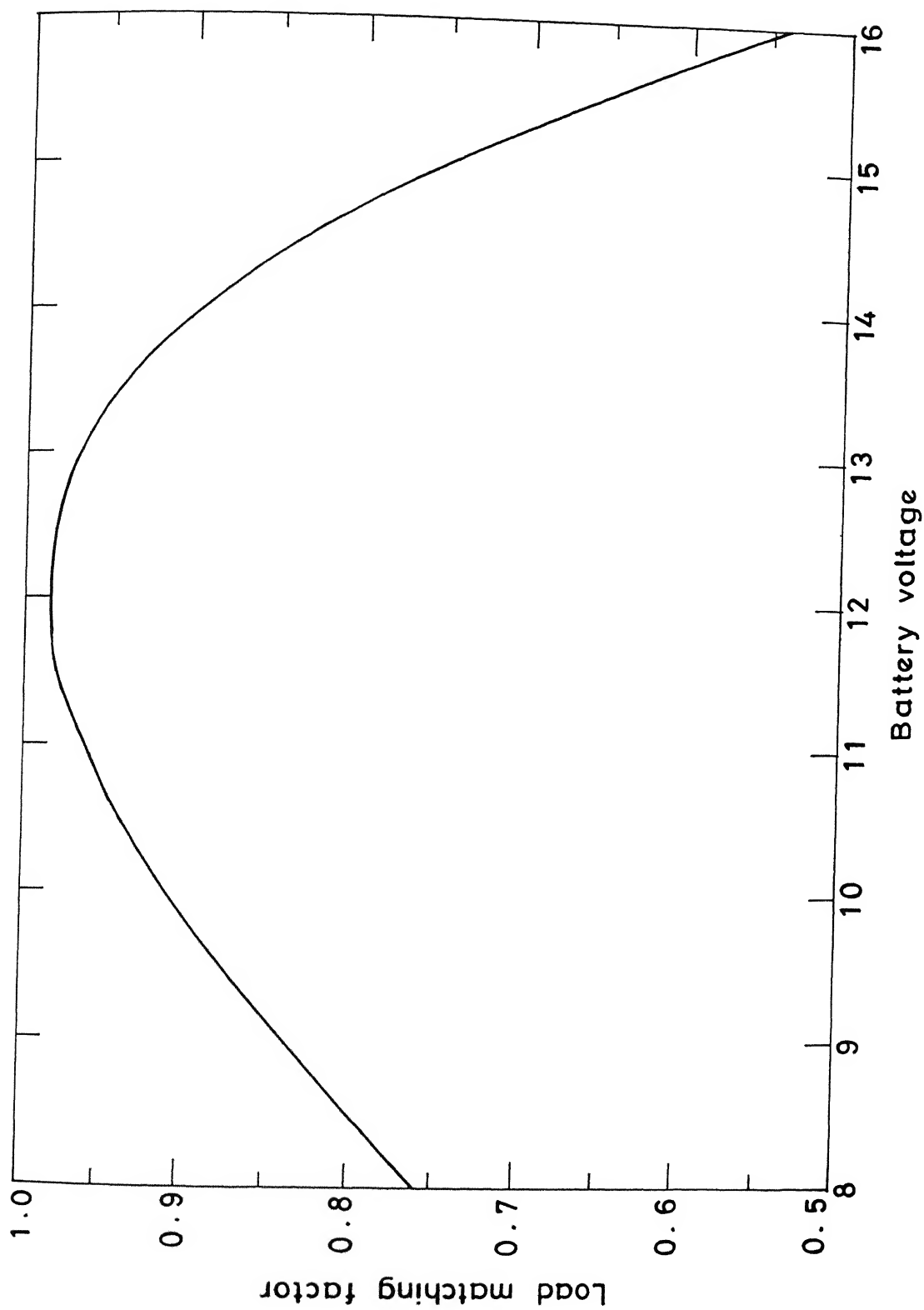


Fig.4.4.4 Variation of load matching factor with battery voltage.  
( $n_p=12$ ,  $n_s=33$ ,  $I_R=0$ ).

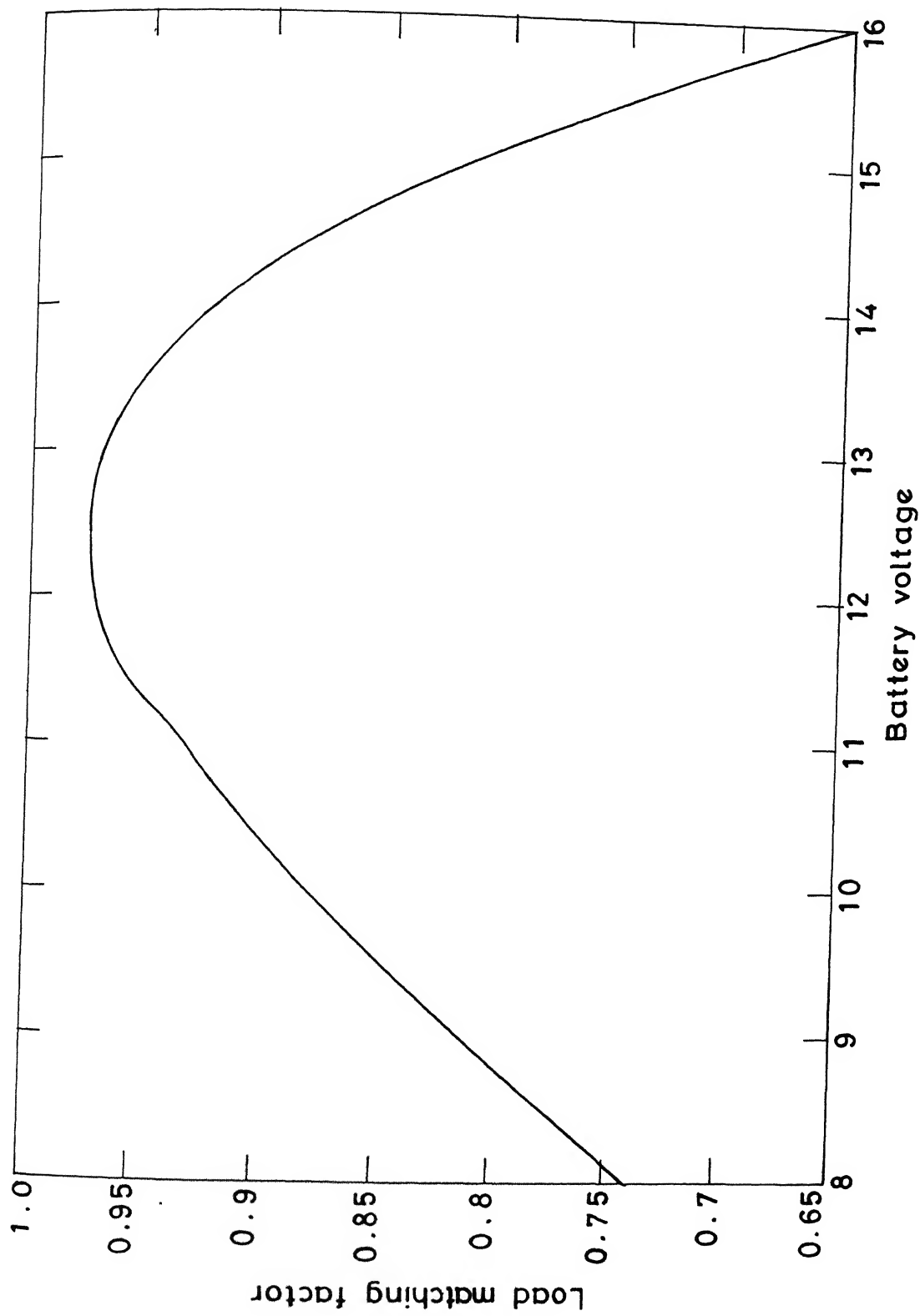


Fig.4.5 Variation of load matching factor with battery voltage .  
 ( $n_p=227$  ,  $n_s=31$  ,  $I_R=0$ )

3. In practice the internal resistance cannot be kept zero. Therefore, the array should be matched for  $N_p$  and  $N_s$  keeping the specified internal resistance value constant.
4. If an array is matched in one month, it will give good results in other months too.

## Chapter 5

# ARRANGEMENT OF PV ARRAY AND ENVIRONMENTAL BENEFITS

### 5.1 Introduction

The design of a photovoltaic array to meet the cooling load requirement of a room is very vital from the view point of economy. Once an array is selected, it has to be physically arranged in order to get maximum output from it. Usually, an array is put on the top of a roof. Then, the radiation falling on the roof is fruitfully converted into electrical energy. In this chapter, a complex search algorithm is used to reduce the array size by its optimum arrangement and tilt angle to get maximum power for known photovoltaic characteristics and cooling load. This is done to reduce the array size to as low value as possible. The adoption of photovoltaic array eliminates the radiation energy due to covered roof, rendering reduced cooling load and hence reduced power for airconditioning. Computations were carried out for replacing electrical energy from

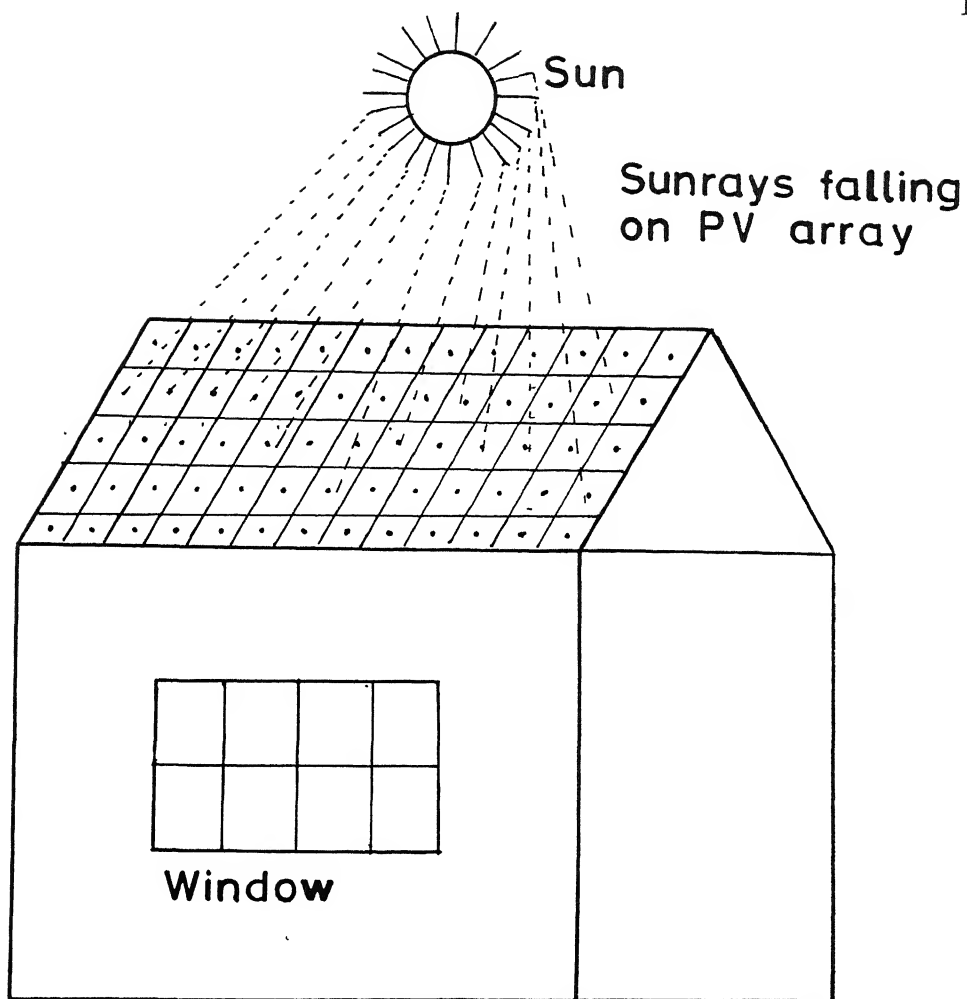
the conventional fuels by photovoltaic cells and subsequent reduction in global warming gases like  $\text{CO}_2$ . Results are presented in the graphical form. Thus photovoltaic array plays following roles:

- The reduced cooling load and hence reduced power for airconditioning.
- Elimination of production of global warming gases and thus reduced global warming effect.
- Conservation of depleting fossil fuels.

## 5.2 Reduction in the Cooling Load due to Coverage of Roof

Heat transfer through walls and roofs is a major component of cooling load. The solar radiation may render the roof temperature as high as 355 K in an environment at 315 K. Hence, installing the photovoltaic cells over roof provides a cover to the roof. The array size is found to be much more than the size of the roof. By mounting the array on the terrace, therefore, cooling load requirement is reduced because of the coverage. Figure (5.1) shows the array mounted on the terrace. A code has been developed which computes cooling load on hourly basis as given in Section 2.4.

The hourly cooling load helps determine a suitable size of the airconditioning system, and components can be designed accordingly. Integrating cooling load with respect to time using Simpson's formula, the energy requirement for 24 hour period is estimated, which is used for the estimation of PV array size. Using this code, one can find the cooling load requirement of an uncovered room and an array-covered room. It will be seen that a large portion of cooling load requirement is met just by covering the roof.



Roof covered with PV array

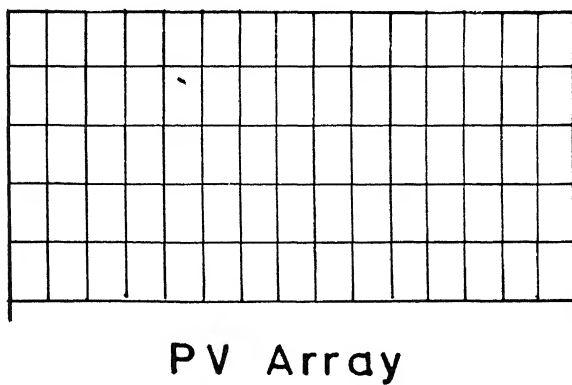


Fig. 5.1 PV array covered roof.

### 5.3 Optimum Arrangement of Array

From Section 2.2 and Section 2.3, it is clear that power output from the array is dependent on the slope  $\beta$  of the array, which is the angle made by the plane surface with the horizontal and the surface azimuth angle  $\gamma$  which is the angle made in the horizontal plane between the line due south and the projection of the normal to the surface on the horizontal plane. Two optimization routines (successive quadratic programming and complex search method) [Deb, 1995] were used for finding the optimum  $\beta$  and  $\gamma$ . The successive quadratic programming takes much time, because it has to calculate gradients by finite difference technique, while in complex search method gradient information is not needed. The algorithm of complex search method is given in Appendix L.

The optimization problem is:

$$\text{Maximize} \quad E_B(\beta, \gamma) \quad (5.1)$$

$$0 \leq \beta \leq 90, \quad -90 \leq \gamma \leq 90 \quad (5.2)$$

where  $E_B(\beta, \gamma)$  is the energy stored in the battery as given in the equation (4.7) which is dependent on the variables  $\beta$  and  $\gamma$ , besides other constant parameters. Sometimes the slope of the array may have to be fixed from the consideration that in rainy season, water falling on it should flow smoothly. In that case only  $\gamma$  is optimized, the value of  $\beta$  being a fixed value.

### 5.4 Results and Discussion

For parametric study a 7040 cell array is used which is suitable for airconditioning of a room details of which are given in Appendix-G. The PV generator data are given in Appendix-H.



### 5.4.1 Energy Saving due to Roof Coverage

As described in Section 2.4, a code for computing cooling load on hourly basis has been developed. This code was run for the room data given in Appendix-G. Figure (5.2) shows the cooling load variation with time for the month of May for a 3-side shaded room, in which the south side is exposed to the sun. Results for the covered and uncovered roof are shown in the same figure. It is seen that most of the time, the cooling load is different for the covered and uncovered roof rooms. Actually, the radiation falls only at day time, but due to time lag, its effect is experienced upto late night. The total cooling load for the uncovered roof is 72.22 kWh and for the covered roof it is 60.48 kWh. This shows that we obtain 16% saving in the cooling load by covering the roof. Figure (5.3) shows the variation of cooling load with time for the month of August. Figures (5.4-5) show electrical power needed for airconditioning respectively in the month of May and August. Figures (5.6-7) show the power given by the PV array as well as saving in electrical energy due to roof coverage. The effective power is the sum of two energies and is also shown in Figures (5.6-7).

Variation of cooling load with time for the same room conditions except that all the walls are exposed to the sun is exhibited in Figure(5.8). In this case also, the saving in the cooling load due to roof coverage is observed clearly. The total cooling load in a day is 83.74 kWh for uncovered roof and 72.01 kWh for covered roof. This renders about 14% saving in the cooling load with the covered roof. Figure (5.9) shows the cooling load variation for the month of August. Figures (5.10-11) show electrical power needed for May and August. Figures (5.12-13) depict the power obtained due to photovoltaic array.

Thus, a significant amount of radiation energy is saved by the array with its coverage. It can, therefore, be concluded that the large space required by the array is

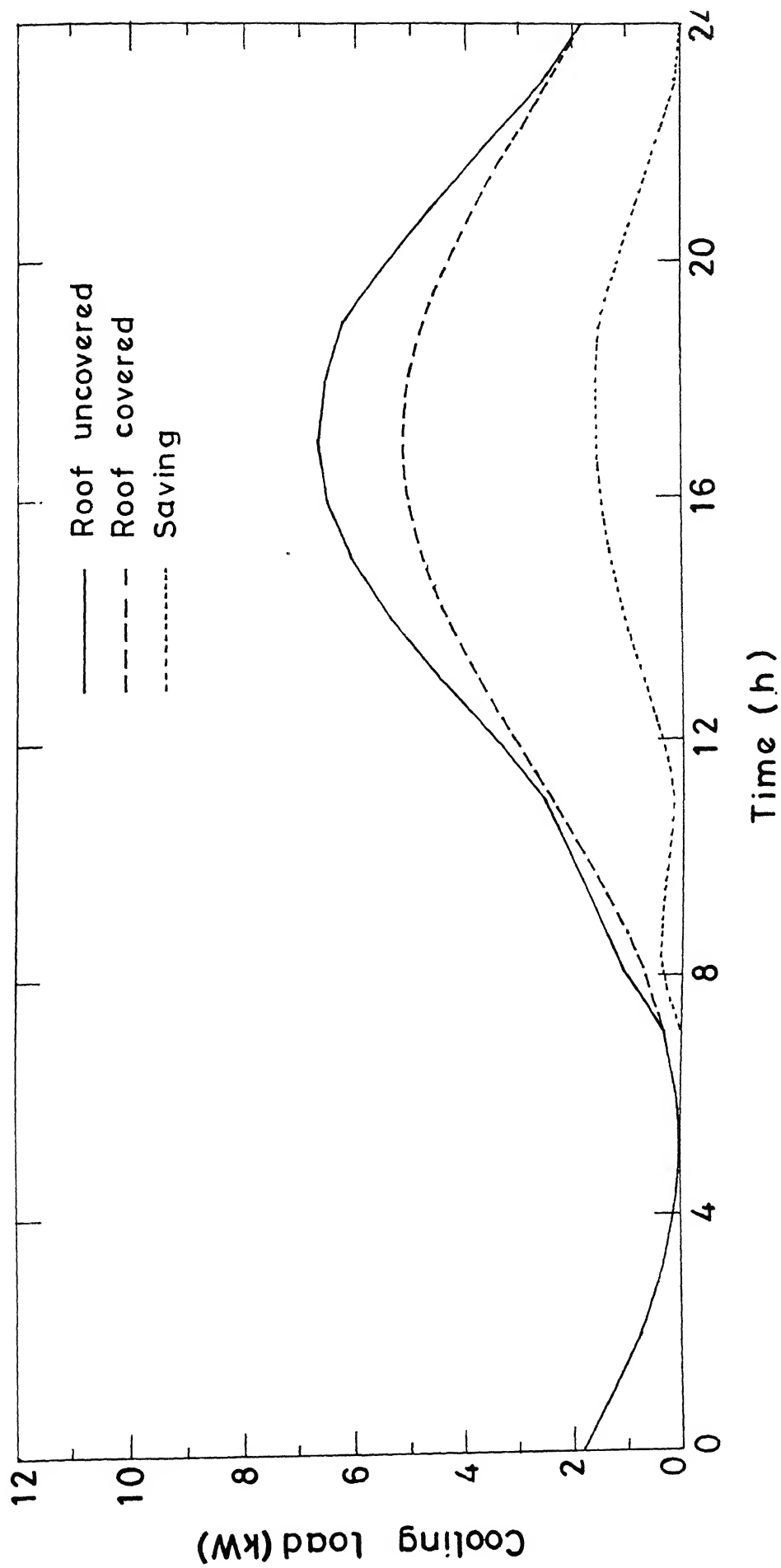


Fig.5.2 Variation of cooling load with time for May .

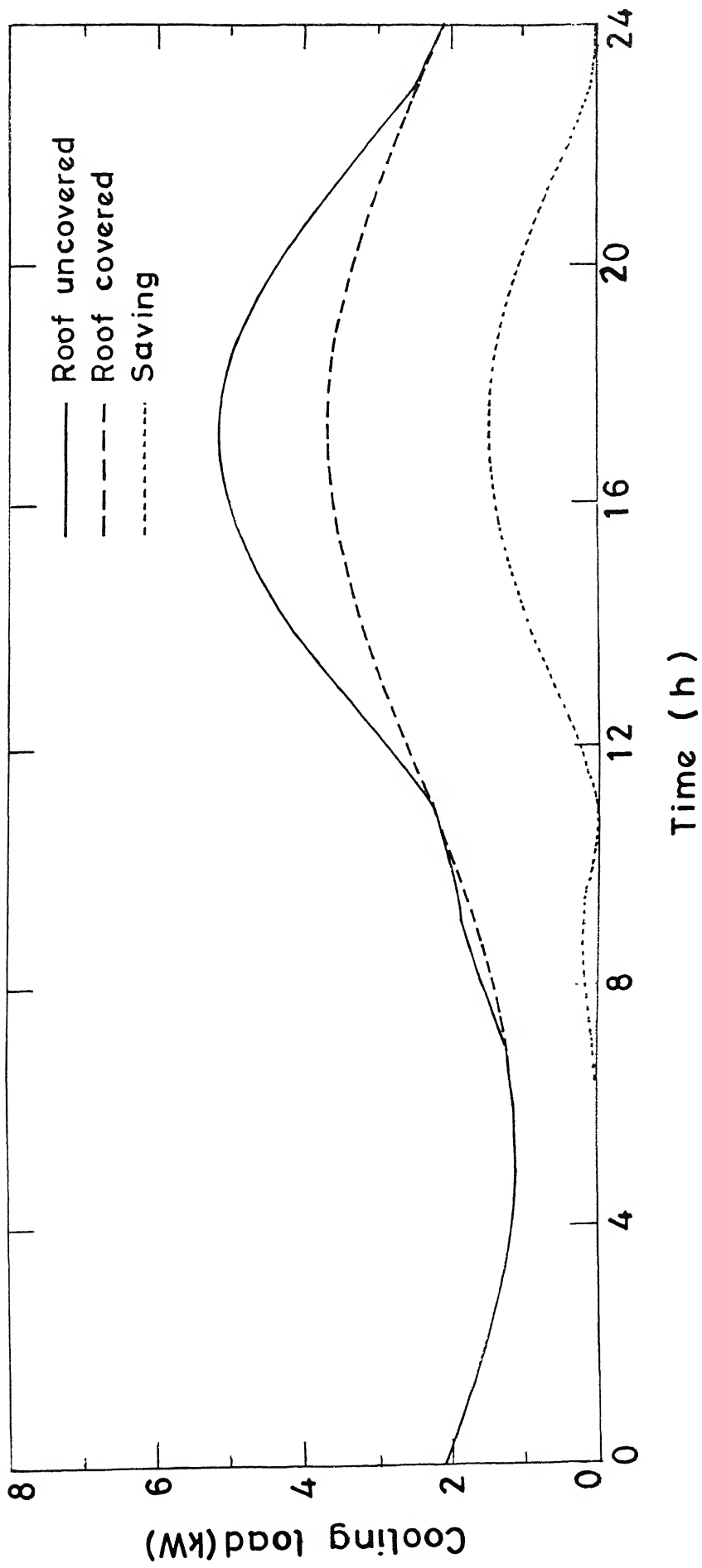


Fig.5.3 Variation of cooling load with time for August.

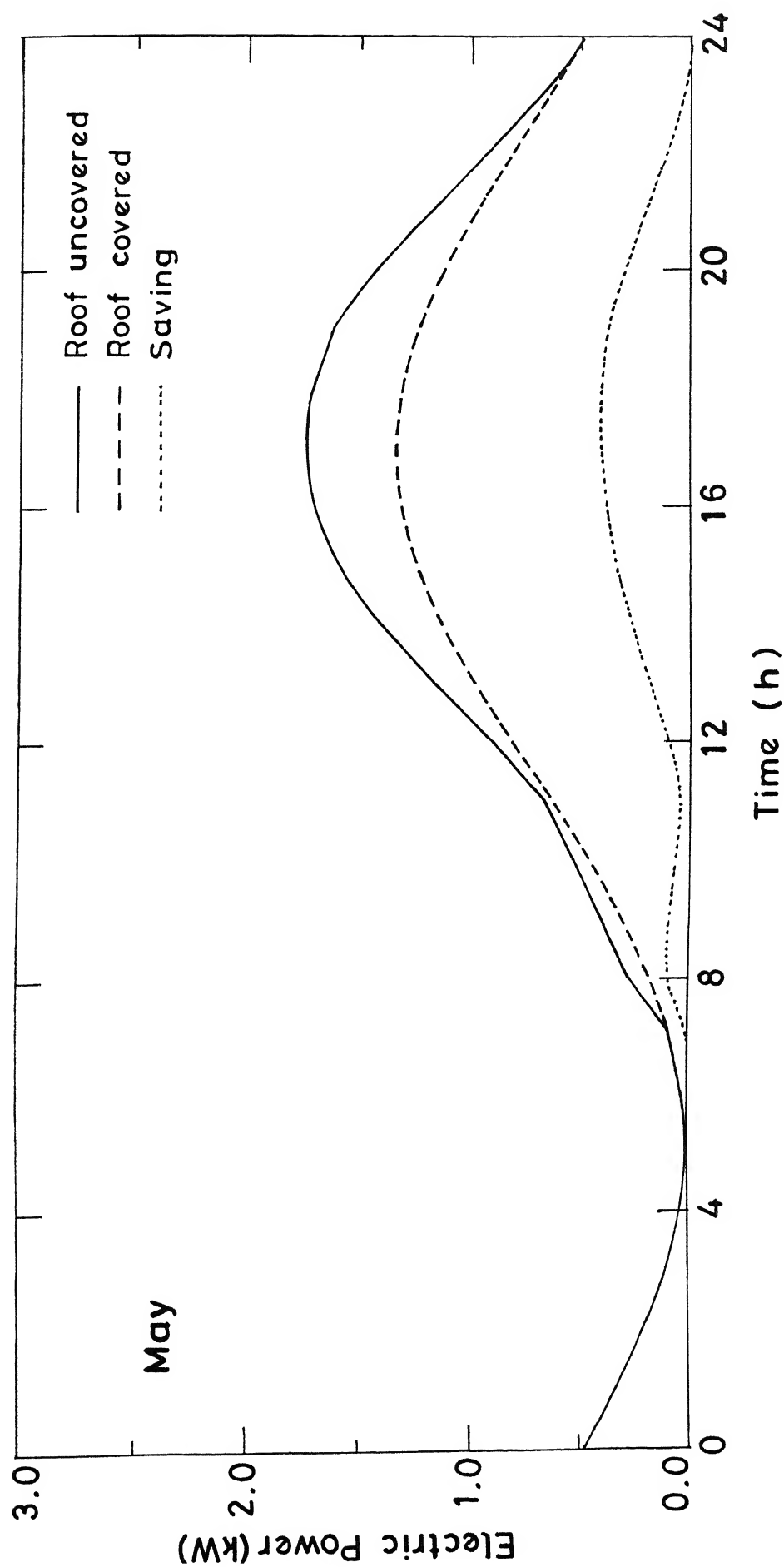


Fig.5.4 Electric power needed for airconditioning v/s Time.

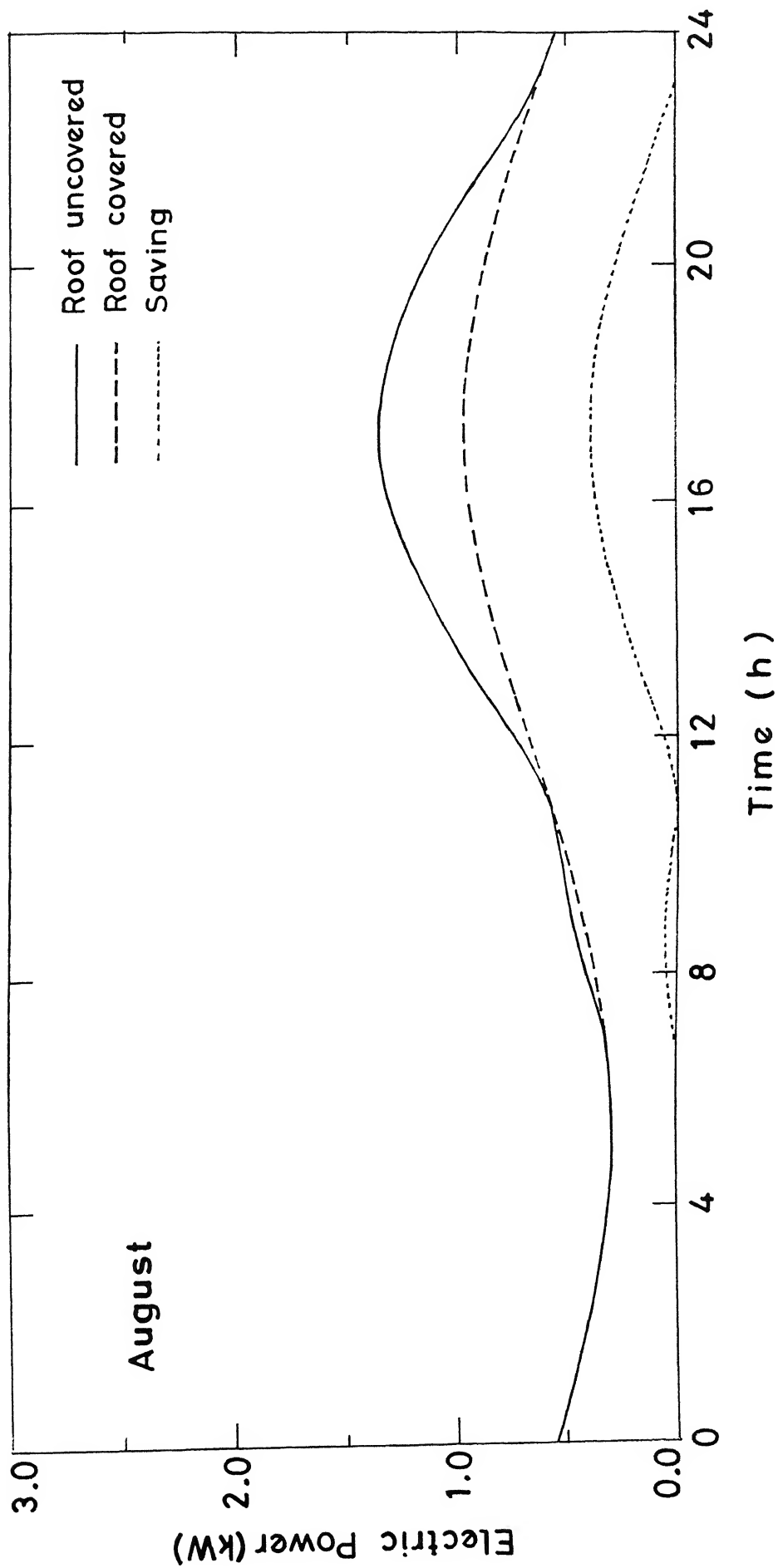


Fig.5.5 Electric power needed for air conditioning v/s Time .

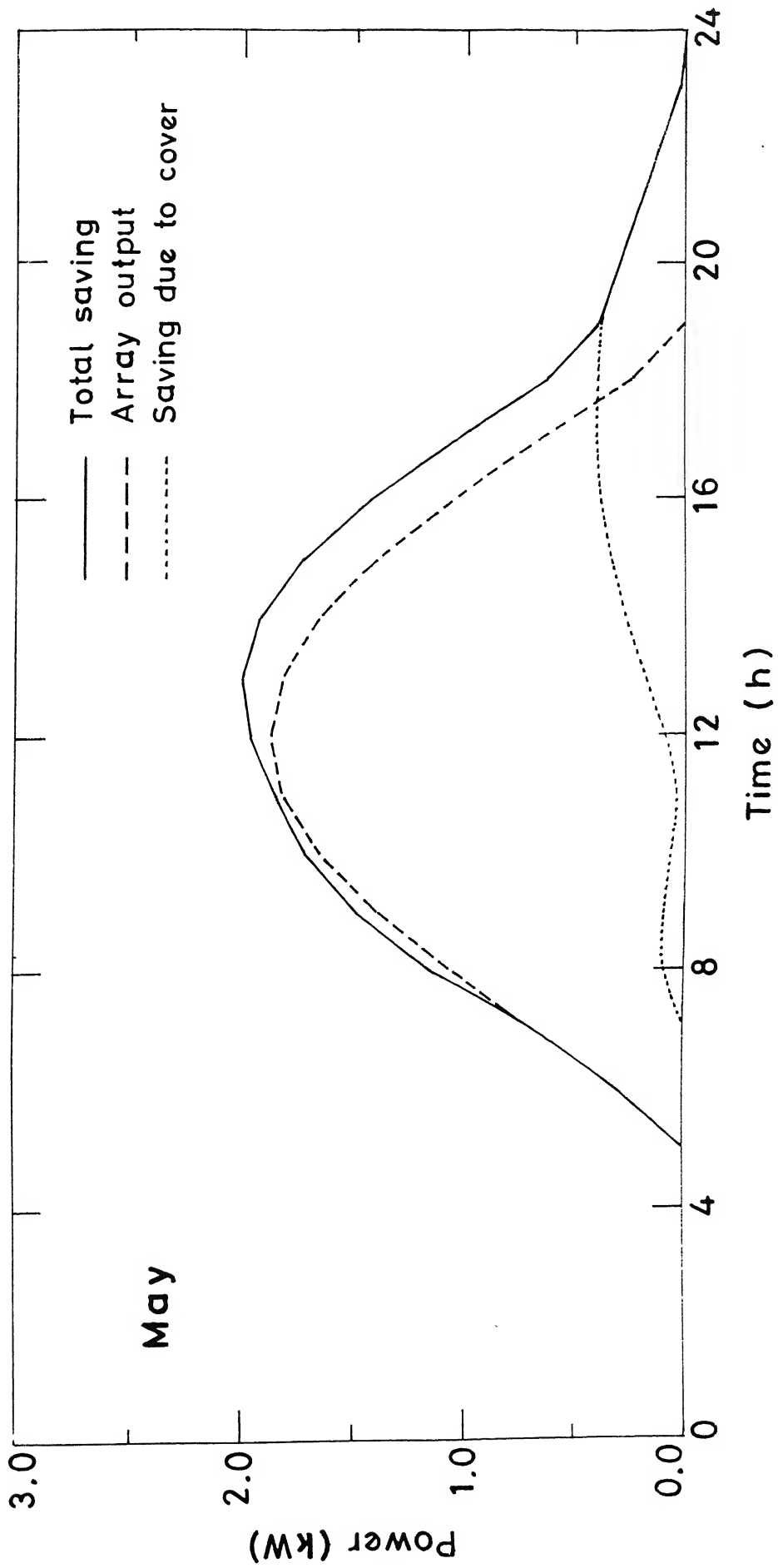


Fig.5.6 Effective power output from PV array v/s Time .

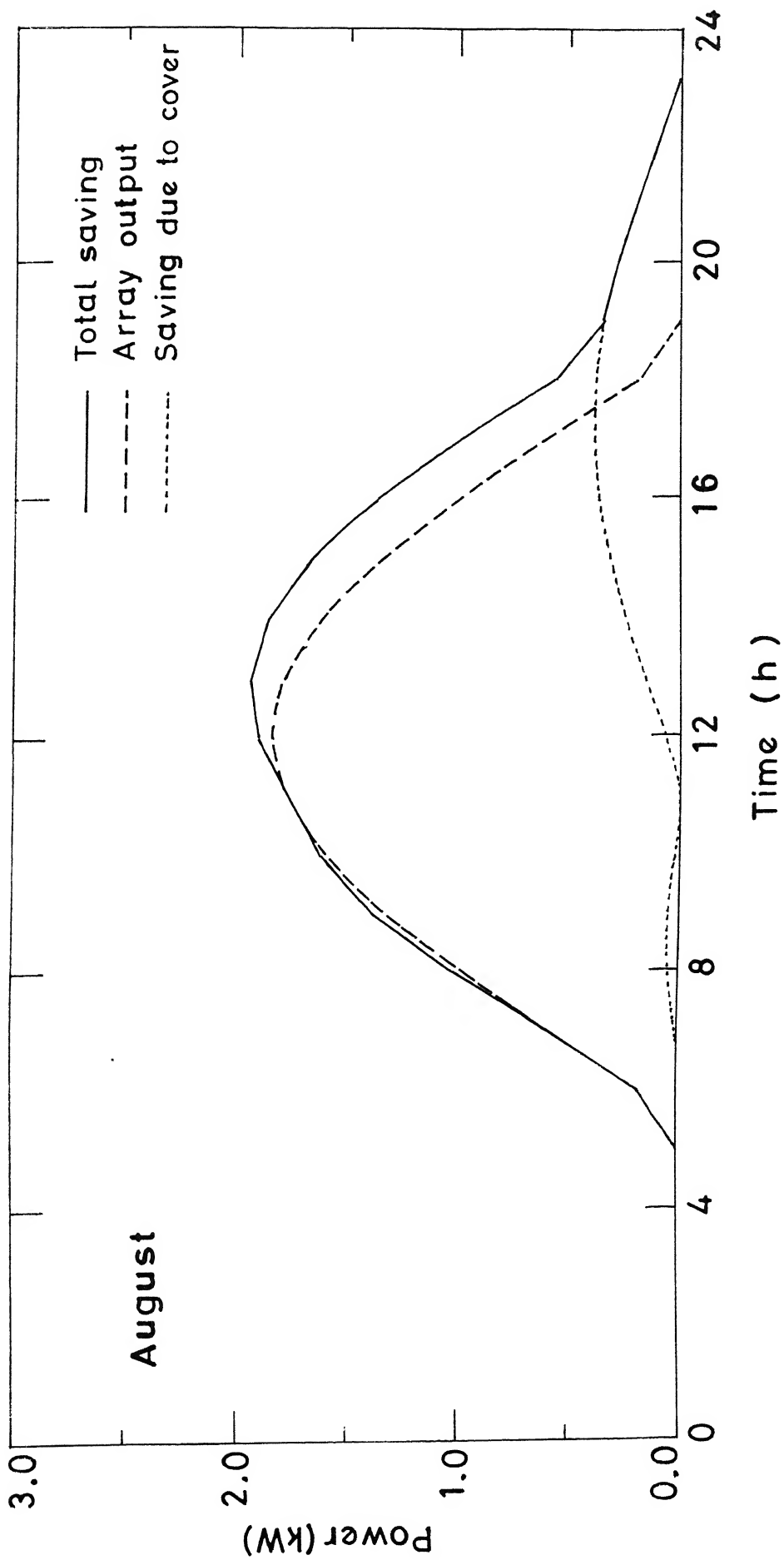


Fig.5.7 Effective power output from PV array v/s Time .

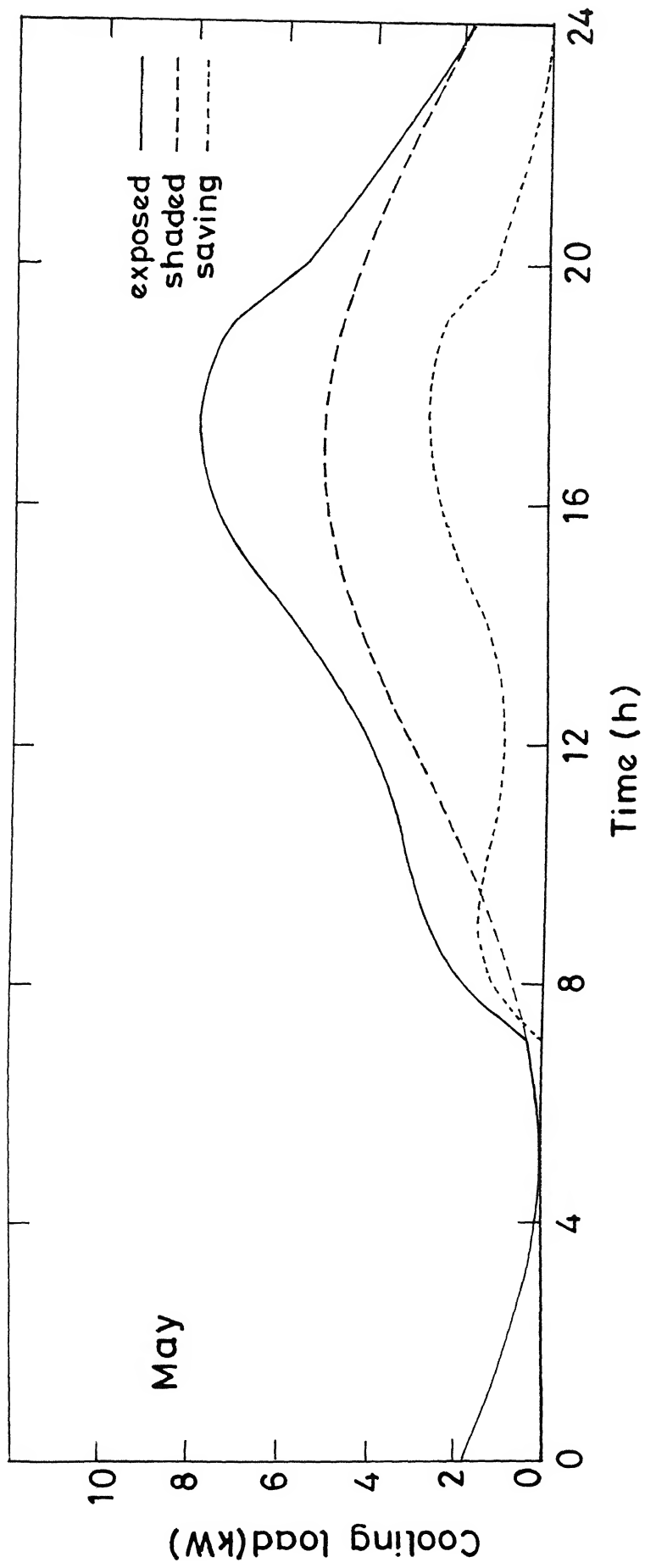


Fig.5.8 Variation of Cooling load with Time .



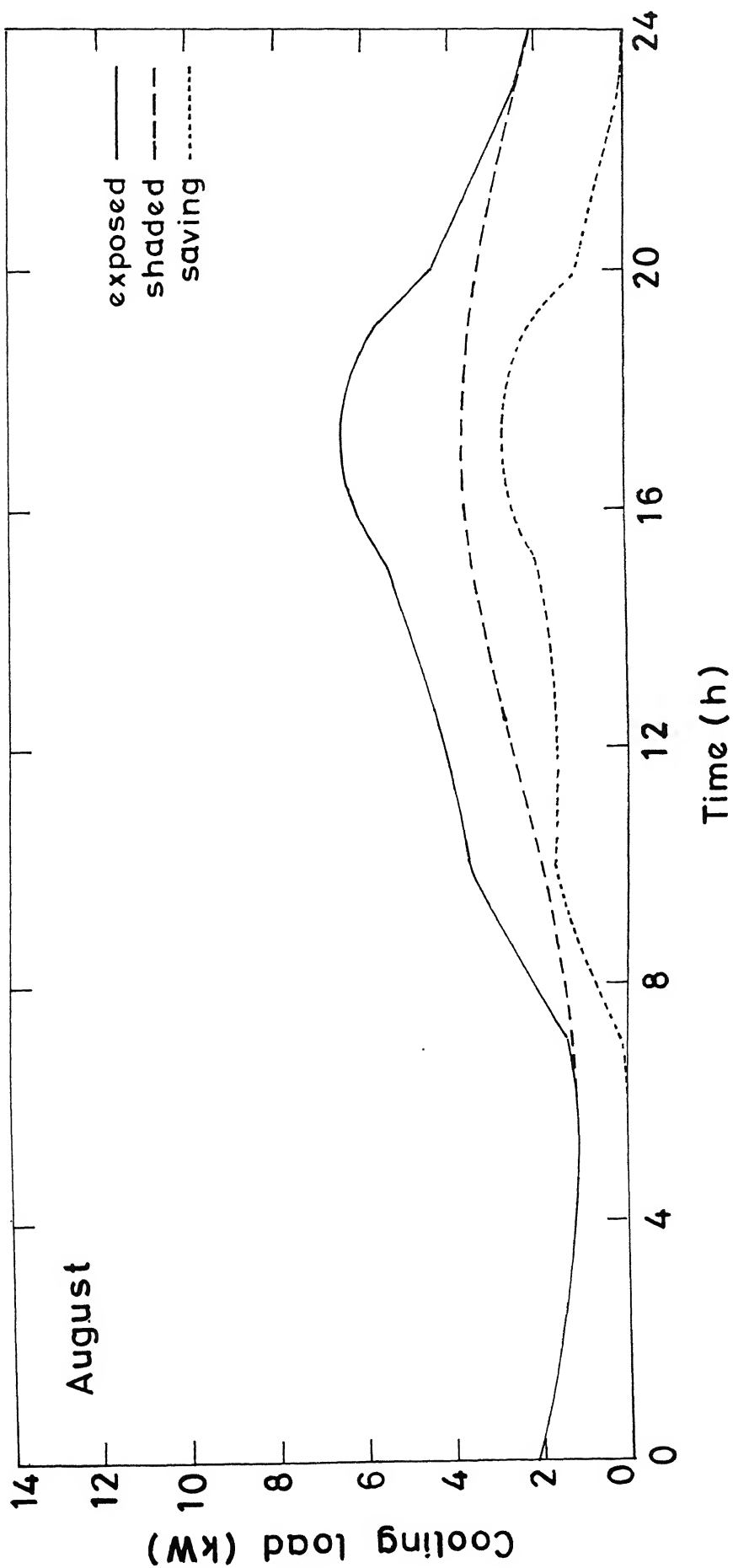


Fig.5.9 Variation of Cooling load with Time

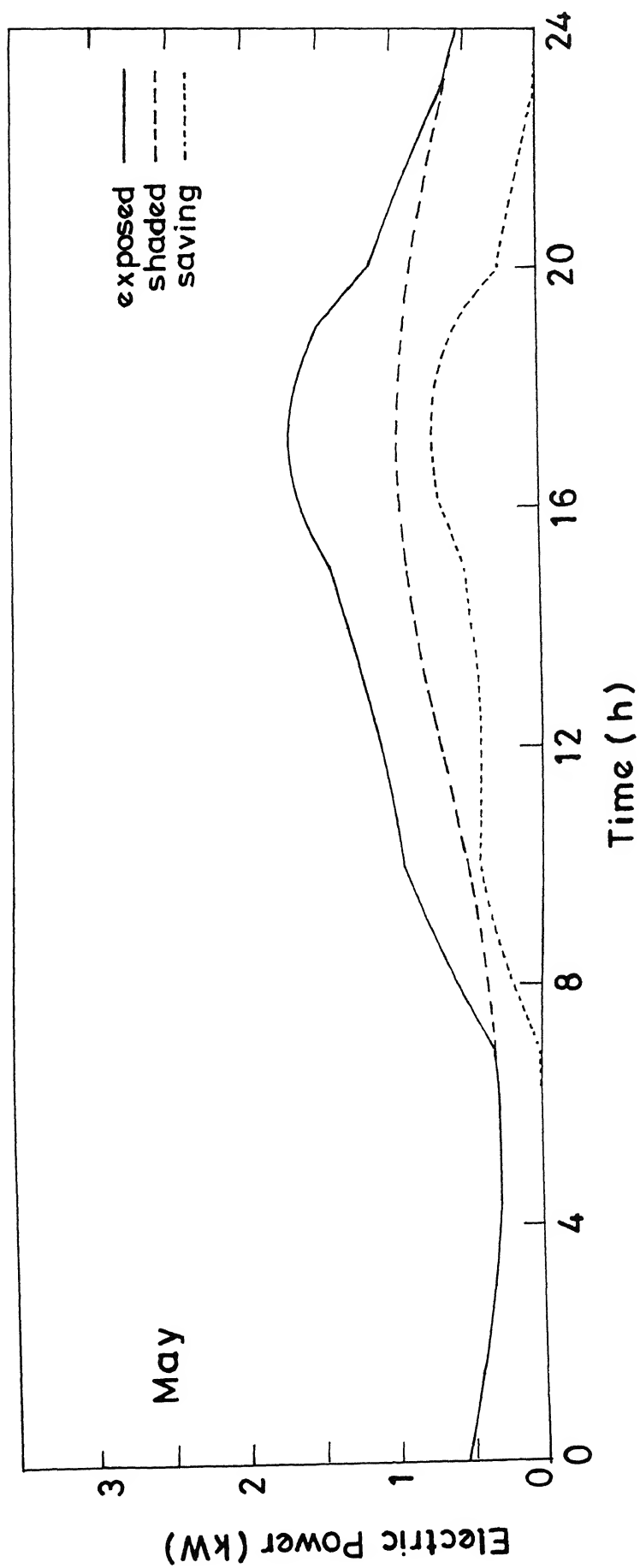


Fig.5.10 Electric power needed for Airconditioning v/s Time.

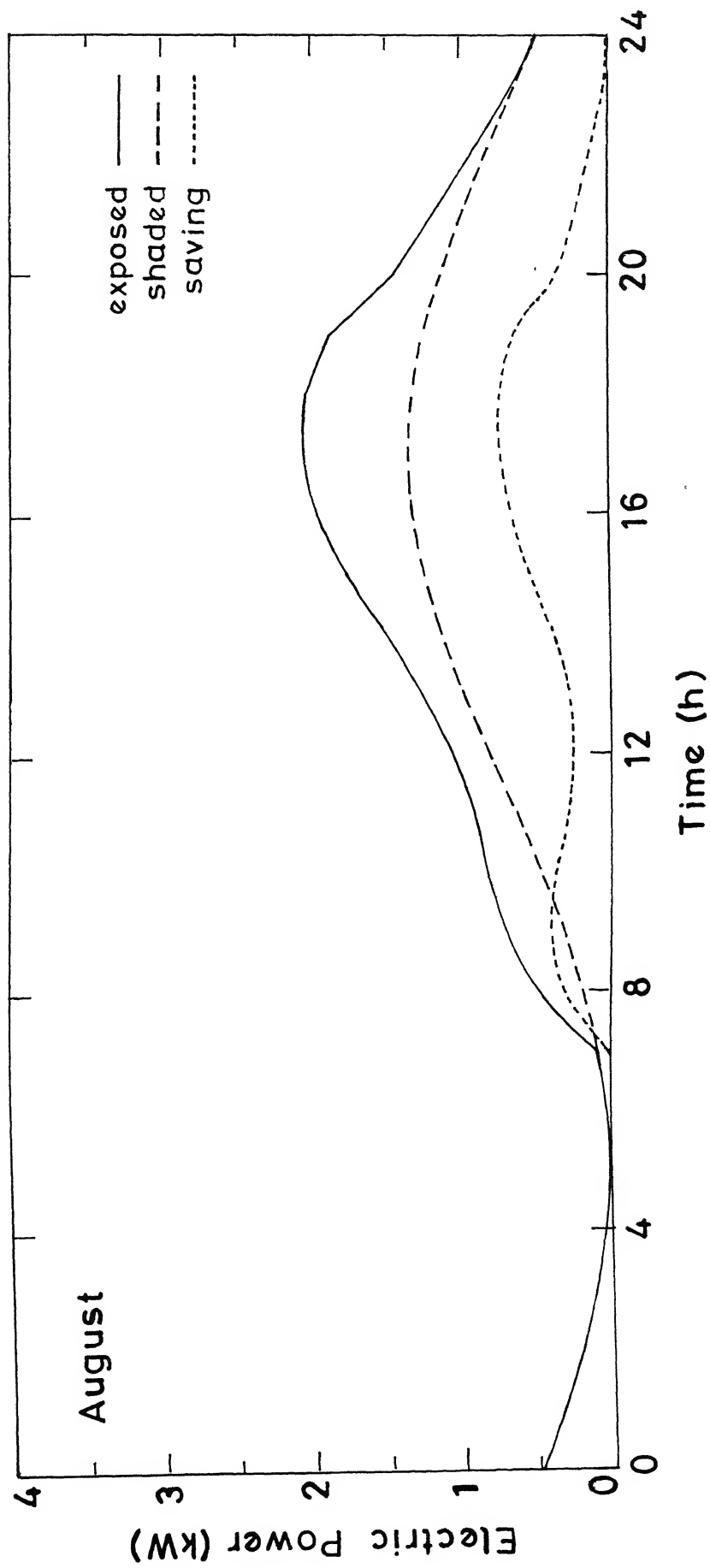


Fig.5.11 Electric Power needed for Airconditioning v/s Time

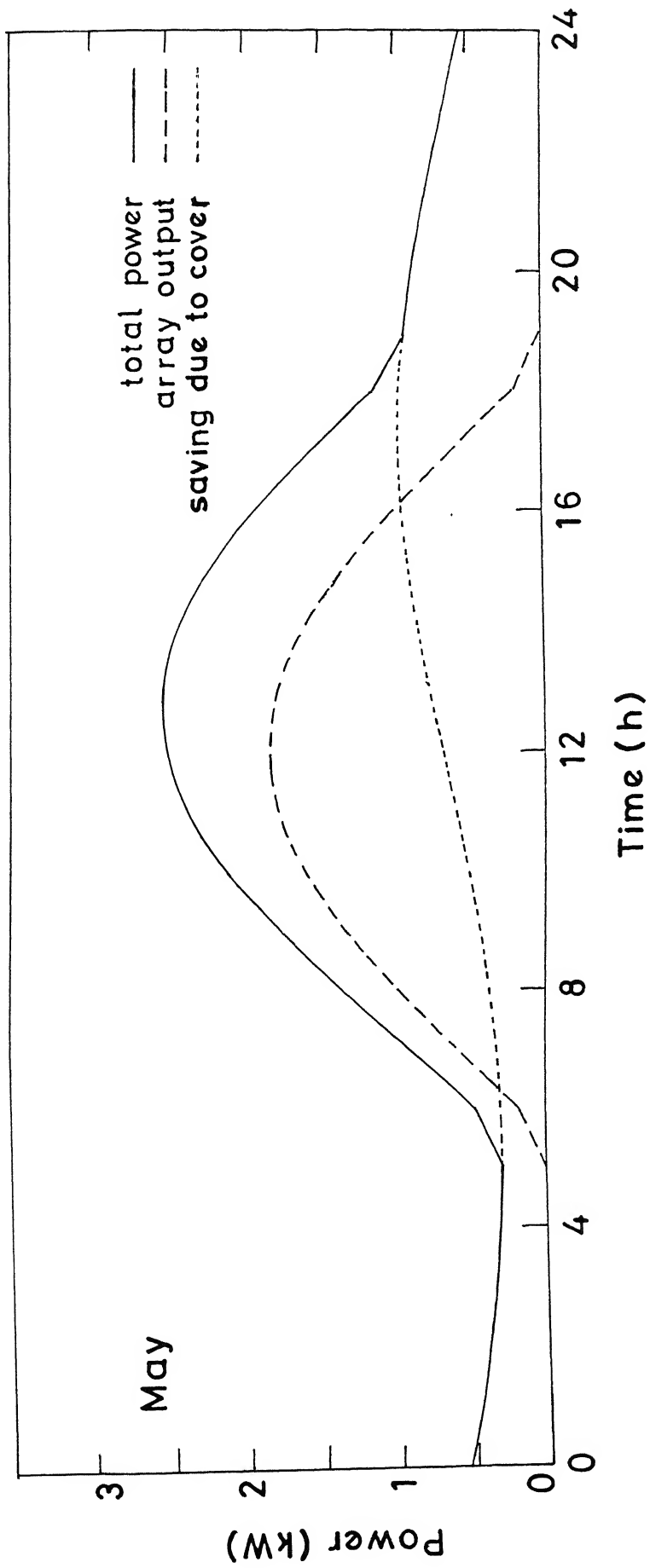


Fig.5.12 Effective Power output from PV array v/s Time

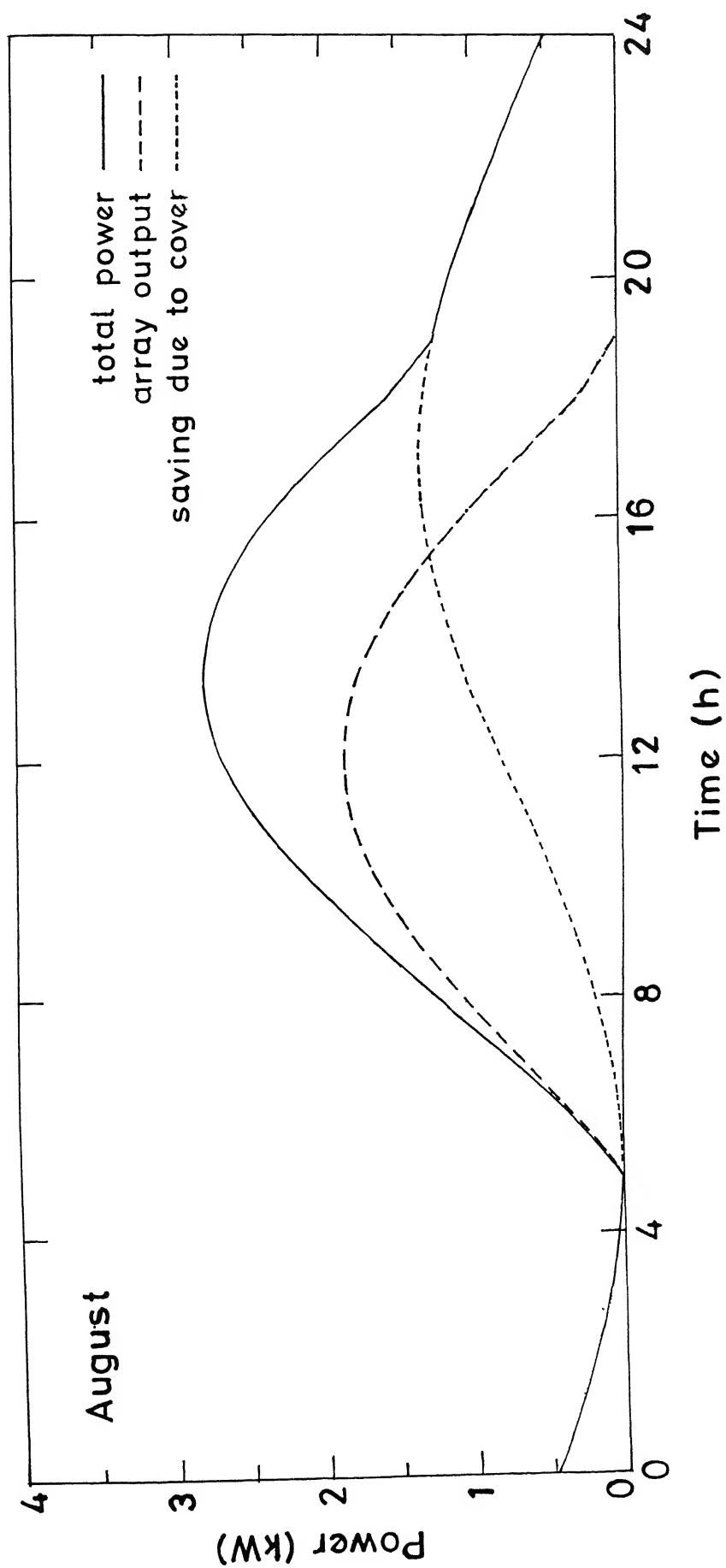


Fig. 5.13 Effective Power output from PV array v/s Time

not merely a drawback of PV array. It has its positive effect too. In fact in an unsurrounded room (roof and walls exposed to the sun), the roofs as well as walls can be covered by the large size of PV array required for airconditioning that room. In the case of example room, the cooling load for a bare room is 83.74 kWh for a day, whilst it is 60.19 kWh in a day, for a fully covered room. Thus about 28.12% cooling load is reduced in this case.

### 5.4.2 Optimum Arrangement of the Array

For Kanpur city, the optimum slope  $\beta$  comes out to be zero. The surface azimuth angle  $\gamma$  can be any value. However, array is usually kept at some angle in order to avoid free rain-fall. It is found that if array is kept at  $5^\circ$  angle, the total energy obtained is only 0.42% less than that obtained from horizontal array, whilst if it is kept at  $15^\circ$  angle, energy is 3.4% less. It is found that if the array is kept at some slope,  $\gamma$  should be  $90^\circ$ .

If the latitude of the place is  $50^\circ$ , then  $\beta = 18.7^\circ$  and  $\gamma = 0^\circ$  combination gives maximum power, whilst if the latitude is  $80^\circ$ , then  $\beta = 46^\circ$  and  $\gamma = 0^\circ$  combination gives maximum power. Thus it is seen that latitude of a place has much influence on the optimum arrangement of the array.

### 5.4.3 Reduction in the Atmospheric Pollution

When the electricity is generated by conventional fuels, like coal, oil or natural gas,  $\text{CO}_2$  is produced. Figures (5.14- 15) show how much  $\text{CO}_2$  will be reduced if photovoltaic array replaces these sources. The data about  $\text{CO}_2$  production is taken from [IIR Bulletin, 1994]. These values are 1.12, 0.94 and 0.57 kgs of  $\text{CO}_2/\text{kWh}$  for coal, oil and natural gas, respectively.

In addition to this, there are transmission and distribution losses which are taken

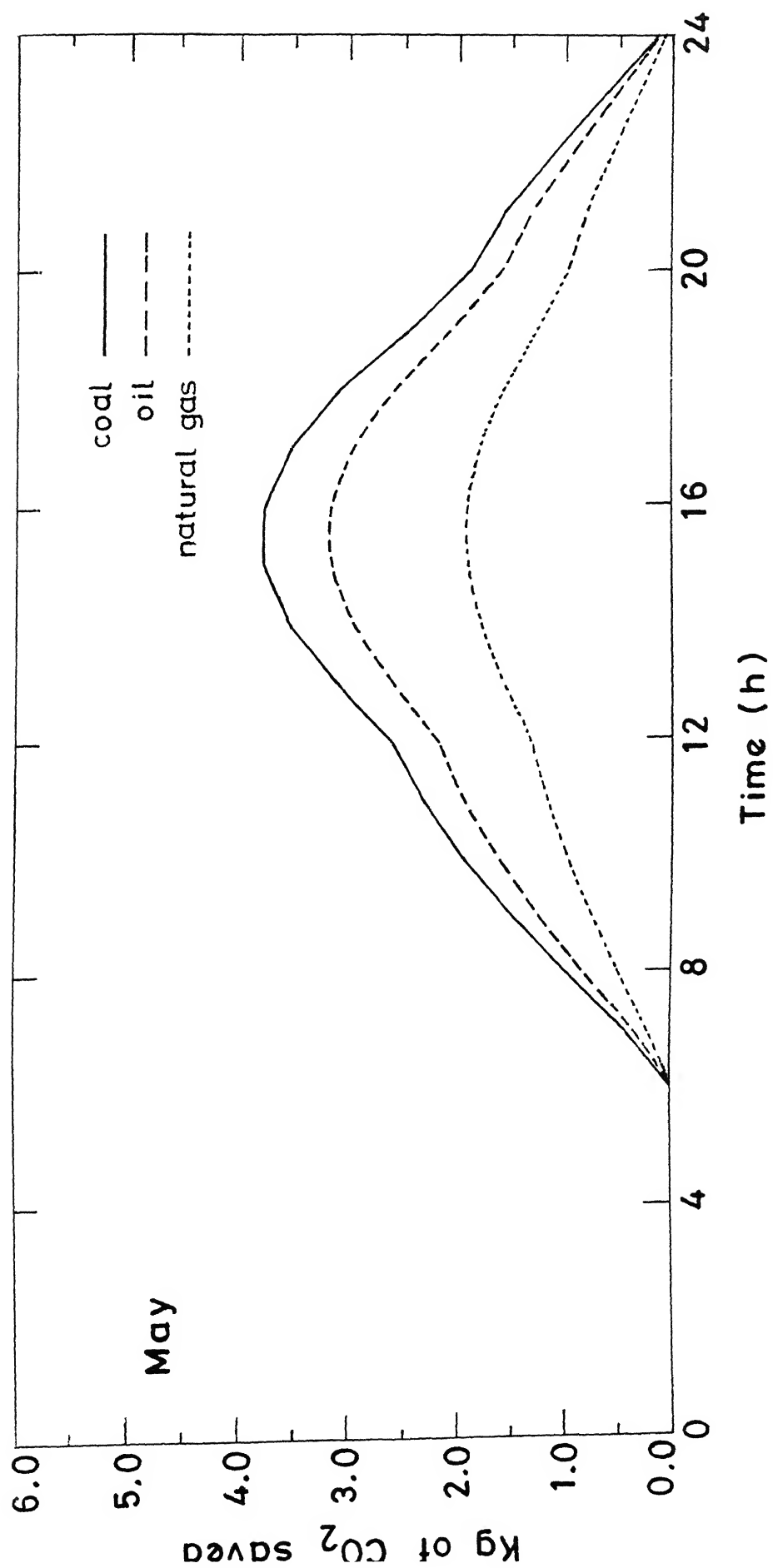


Fig.5.14 Kg of CO<sub>2</sub> v/s Time.

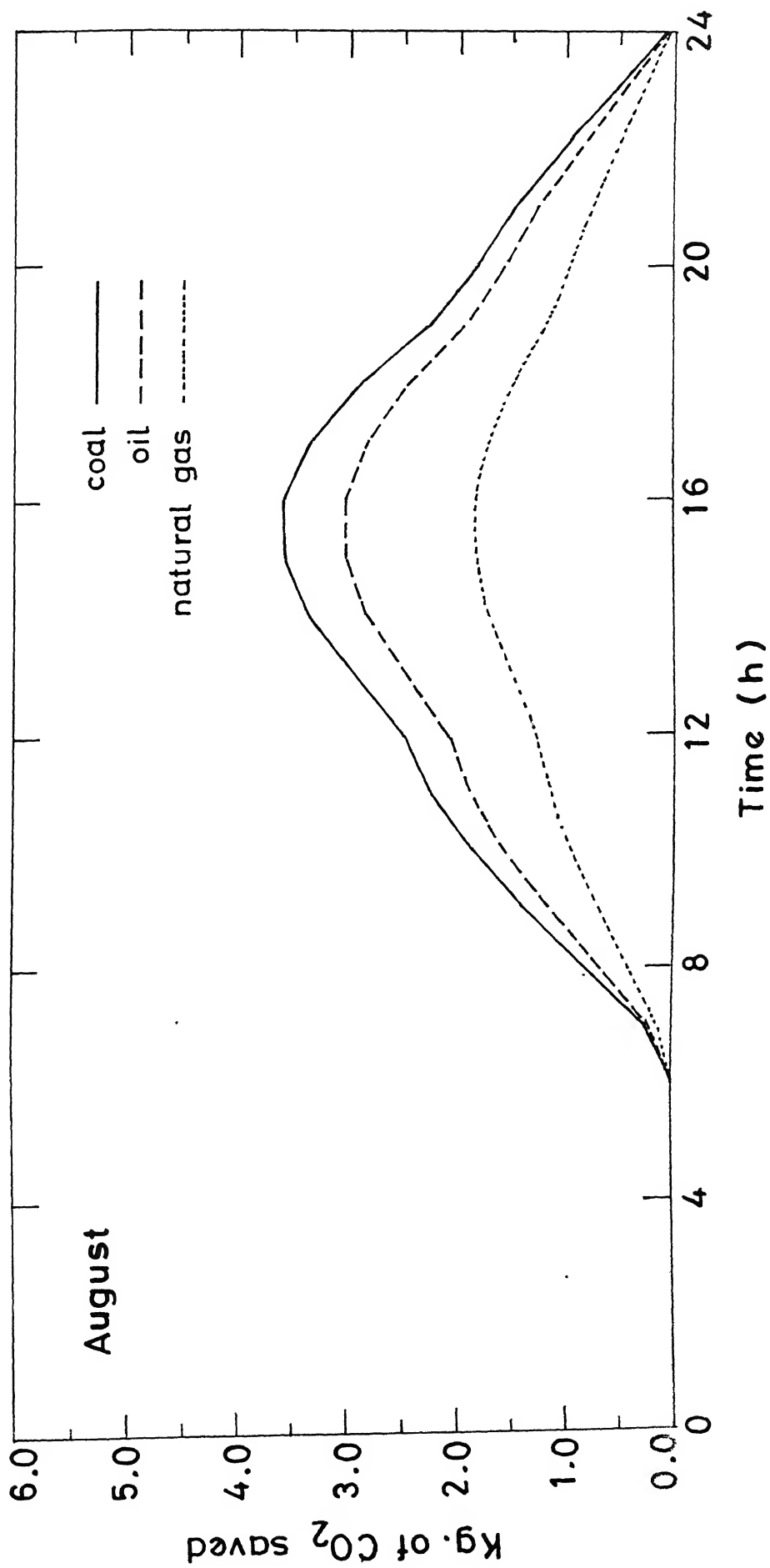


Fig.5.15 Kg of CO<sub>2</sub> v/s Time.



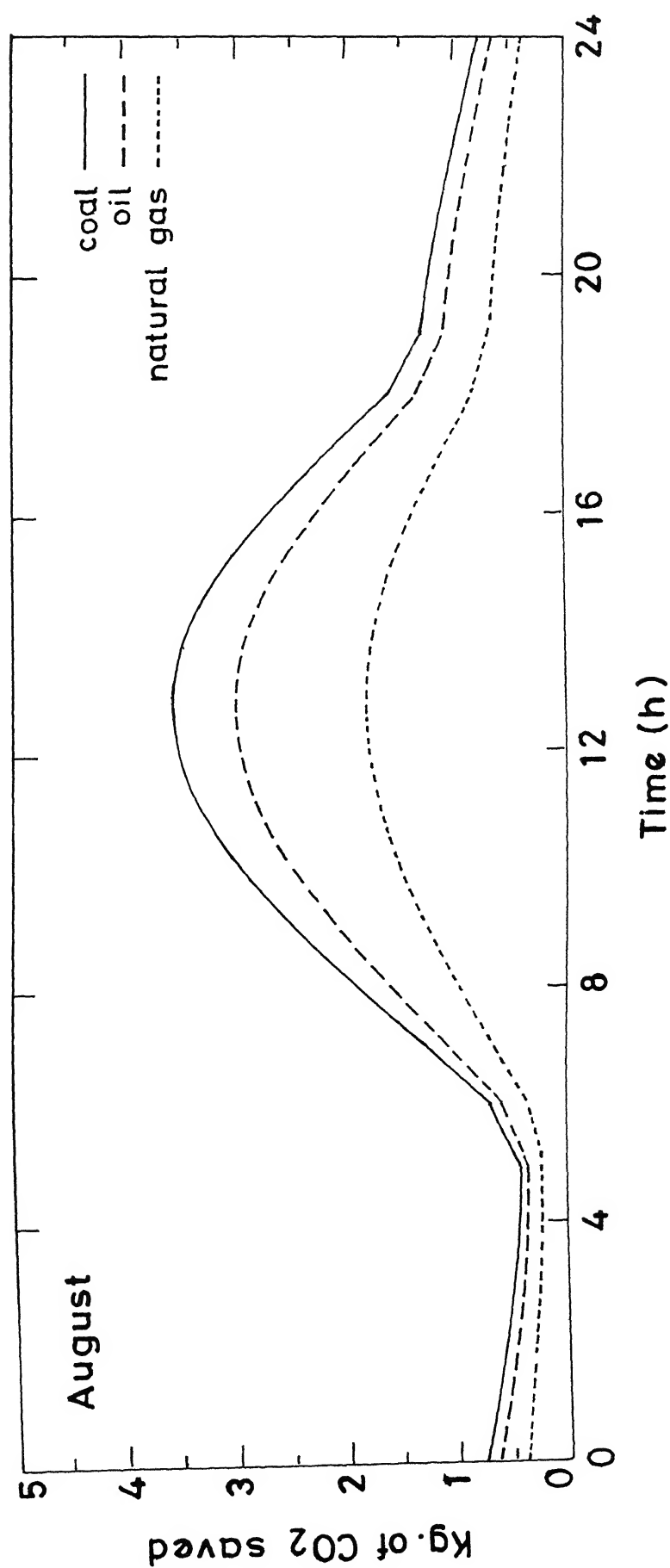


Fig.5.17 Kgs of CO<sub>2</sub> v/s Time for exposed room.

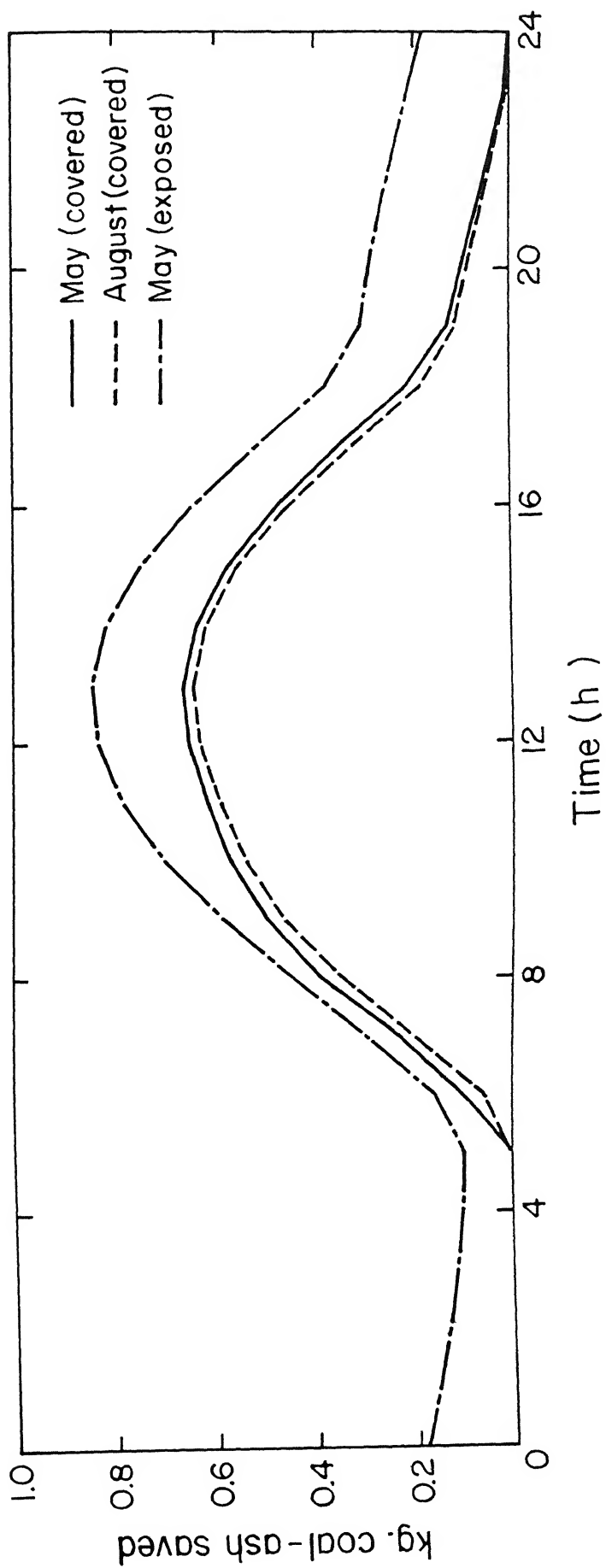


Fig.5.18 Kg of Coal-ash saved Vs time.

to be 25% on all India basis as given in [UPSEB, 90-91]. Therefore emission of  $\text{CO}_2$  is further increased by 25% due to these losses.

It is seen that for airconditioning of a room size as given in Appendix G,  $\text{CO}_2$  at the rate of as much as 3.75 kg/s at a peak time can be saved as shown in Figures (5.16-17). If photovoltaic energy is used in place of electricity, then ash which is produced when coal is burnt to generate electricity is eliminated. This solves the ash disposal problem in addition to rendering cleaner environment. The amount of ash saved is shown in Figure (5.18).

## 5.5 Summary

In this chapter energy saved due to roof coverage is discussed. The same is concluded as under:

- A complex search method code is used to find out the optimum arrangement of the array.
- It is seen that this arrangement is dependent on the place.
- It is shown that the array not only supplies the energy, but also reduces energy needed by providing shading.
- Finally, the reduction in the  $\text{CO}_2$  in the atmosphere is highlighted.

# Chapter 6

## CONCLUSIONS AND SUGGESTIONS

### 6.1 Conclusions

#### 6.1.1 Estimation of Photovoltaic Array Size for Airconditioning, Heating, and Refrigeration

A deterministic method to estimate array size for airconditioning heating and refrigeration system is presented and computer code has been developed for this purpose. For each of these cases, examples have been taken for estimating array sizes. For airconditioning and heating both vapour-absorption and vapour-compression systems were considered. It is observed that array size requirement is much more in the case of vapour-absorption system than in the case of vapour-compression system for both airconditioning and heating. This is due to the low COP of the vapour-absorption system.

For the case of a refrigerator, 100 W, 45 L capacity refrigerator can be constructed

which can successfully operate at Kanpur and Bombay, the two representative cities of India where environmental conditions differ much from each other.

### **6.1.2 Application of Fuzzy Set Theory for Array Size Estimation**

Fuzzy set theory is employed with a view to get more realistic estimate of array size for airconditioning the space. A computer code has been developed for this purpose and an office room at IIT Kanpur has been selected for estimating array size for the same. The use of fuzzy set theory in the determination of array size and selecting an optimum size of array is highlighted .

### **6.1.3 Optimum Matching of the Array with Battery**

Direct matching of photovoltaic array with battery eliminating the need for maximum power tracker is suggested. An optimization code has been developed and simulation study is done. Based on the study, the following conclusions may be drawn:

- There is no need of a maximum power point tracker (MPPT) if the array is properly matched with the battery. Because the value of load matching factor in the range of applications turn out to be around 0.97.
- The internal resistance of the battery has to be kept at minimum.
- In practice the internal resistance cannot be kept zero. Therefore, the array should be matched for  $N_s$  and  $N_p$  keeping the specified internal resistance value constant.
- If an array is matched in one month, it will give good results in other months too.

#### 6.1.4 Saving of Pollution by using Photovoltaic Array

- Energy saved due to roof coverage is discussed.
- A complex search method code is used to find out the optimum arrangement of the array.
- It is seen that this arrangement is dependent on the place.
- It is shown that the array not only supplies the energy, but also reduced energy needed by providing shading.
- Finally, the reduction in CO<sub>2</sub> in the atmosphere is highlighted.

A complex search method code is used to find out the optimum arrangement of the array. It is seen that this arrangement is dependent on the place. It is shown that the array not only supplies the energy, but also reduced energy needed by providing shading.

## 6.2 Suggestions

The present investigation has given a lot of scope for further work. The same is presented below:

### 6.2.1 Development of Photovoltaic Airconditioner without Battery:

This is suitable for airconditioning an office area during the day time. For this a maximum airconditioning tracker (MAT) should be developed which operates the photovoltaic array at an operating point ( $V^*$ ,  $I^*$ ) corresponding to which maximum airconditioning will be achieved. MAT will operate the PV array at ( $V^*$ ,  $I^*$ ) which results in

maximum rpm of the compressor motor. Maximum rpm of compressor motor results in maximum airconditioning as H.P. of the compressor is proportional to its rpm. MPPT is provided in between the PV array and the airconditioner motor.

This will be ideal for airconditioning offices. Provision will also be made to run the airconditioner from the electric supply available in the office. Therefore, if the need be, airconditioner can also be operated at night.

### **6.2.2 Development of Photovoltaic Airconditioner with Battery:**

This airconditioner is ideal for a place where there is no power supply or where airconditioning is required for all the 24 hours without interruption caused by power failures.

In this version, a battery is provided after the PV array. Energy from photovoltaic array is stored in the battery and the airconditioner is run from the battery.

### **6.2.3 Development of Photovoltaic 100W Refrigerator:**

This refrigerator will be ideally suitable for storing medicines in dispensary in villages where there is no power supply.

### **6.2.4 Development of Electrically Controlled Compressor:**

An electrically controlled multi-cylinder compressor to eliminate the problem associated with its starting (High Starting Current) should be developed, which can be used in photovoltaic airconditioner/refrigerator of high tonnage capacity to enhance energy conservation by providing load matching between load (number of loaded cylinders can be varied electrically) and photovoltaic array.

A multi-cylinder compressor with a capability of operating with one, two or three cylinders unloaded electrically can be developed. In the presently available multi-cylinder compressors, the unloading is achieved by opening the suction valves of the unloaded cylinders by some mechanical mechanisms driven by the suction pressure. In the electrically controlled multi-cylinder compressor, unloading should be achieved by using electrically actuated devices which will permit the compressor stage unloading operation to be carried out in response to electrical control signals. This method will not require any suction pressure. A simple controller will be developed to vary the number of stages as the solar insolation varies automatically unloading more stages as the insolation decreases. This will enhance energy conservation by improving matching between load and PV array.

With this development, it will be possible to start any airconditioner/refrigerator with all cylinders unloaded thereby having low starting current for the compressor motor. This will eliminate the electrical dip associated with starting of any airconditioner/refrigerator.



# REFERENCES

1. Alford J.S., Rajon J.E., Urban F.O.,1939, "Effect of heat storage and variation in outdoor temperature and solar intensity of heat transfer through walls", ASHVE Transactions, Vol. 45, p. 393-407.
2. Alghuwainem S.M., 1992, "Steady-State Performance of D.C. Motors supplied from Photovoltaic Generators with step-up Converter", IEEE Trans. Energy Conv. Vol. 7, No. 2, June.
3. Anis W.R., Mertes R.P., and Van Overstaeter R.J.,1985 "Coupling of a volumetric pump to a photovoltaic array", Solar Cells, Vol. 14, p. 27-42.
4. Appelbaum J., 1986, "Performance Characteristics of a permanent Magnet DC motor powered by solar cells" Solar Cells Vol. 17, p. 343-362.
5. Appelbaum J., 1987, "The quality of load matching in a direct- coupling photovoltaic system", IEEE Transactions on Energy Conversion, EC-2, No. 4, p. 534-541.
6. Arora C.P, 1981, Refrigeration and Airconditioning, Tata McGraw- Hill Publishing Co. Ltd., New Delhi, p. 726.
7. ASHRAE, 1982, Handbook of Fundamentals, Published by American Society of Heating, Refrigerating and Airconditioning Engineers, Inc., New York.

8. Bhat S.R., Pittet Andre, and Sonde B.S.,1987, "Performance optimization of Induction Motor Pump System using Photovoltaic Energy Source", IEEE Trans. Industry Applications Vol. IA-23, No. 6. Nov./Dec.
9. Bose Bimal K., Szczesny Paul M. and Steigerwald Robert L., 1985, "Microcomputer Control of a Residential Photovoltaic Power Conditioning system", IEEE Trans. Industry Applications Vol. IA-21, No. 5. Sept./Oct.
10. Braunstein A. and Zinger Z., 1981, "On the Dynamic Optimal Coupling of a solar cell array to a load and storage batteries", IEEE Trans. PAS Vol. PAS-100, No. 3, March.
11. IIR Bulletin, 1994, 6, Tome LXXIV - No. 6, p.12.
12. Cooper P.I., 1969, "The absorbtion of Solar Radiation in Solar Stills", Solar Energy, 12, 3.
13. Deb K., 1995, Optimization for Engg. Design; Algorithms and examples, Prentice-Hall India Pvt. Ltd., New Delhi.
14. Enslim J.H.R and Snyman D.B.,1991, "Combined Low-Cost, High- efficient inverter, Peak Power Tracker and Regulator for PV Applications", IEEE Trans. on Power Electronics, Vol. 6, No. 1, Jan.
15. Faldella Eugenio, Cardinali Gian Carlo and Calzolari Pier Ugo.,1991, "Architectural and Design Issues on Optimal Management of Photovoltaic Pumping Systems", IEEE Trans. Ind. Elec. Vol. 38, No. 5, Oct.
16. Jaboori Mongi G., Saied M.M. and Hanafy Adel A.R.,1991, "A Contribution to the Simulation and Design optimization of Photovoltaic Systems", IEEE Trans. Energy Conversion, Vol. 6, No. 3, September.

17. Kadambi V. and Hutchinson F.W.,1968, Refrigeration, Air-Conditioning and Environmental Control in India, Prentice-Hall of India Pvt. Ltd., New Delhi, pp. 14-69.
18. Kaufmann A. and Gupta M.M.,1985, Introduction to Fuzzy Arithmetic : Theory and applications, Von Nostran Reinhold Company Inc., New York.
19. Khouzam Kamal. Y., 1990, "Optimum load matching in direct-coupled photovoltaic power systems - application to resistive loads" IEEE transactions on Energy conversion, Vol. 5, No. 2, June, p.. 265-271.
20. Klier G.J. and Folger T.A., 1993, Fuzzy Sets, Uncertainty and Information, Prentice-Hall of India Private Limited, New Delhi.
21. Malhotra M.S.,1967, "The effects of Thermal Environment of Physical Performance of Indian People", All India Symposium on Refrigeration, Air Conditioning and Environmental Control, IIT Kanpur, pp. 25-30.
22. Ojo Olorunfemi,1991, "Analysis of current source Induction Motor Drive Fed from Photovoltaic Energy Source", IEEE Trans. on Energy Conv. Vol. 6, No. 1, March.
23. Pike R.W.,1986, Optimization for Engineering Systems, Van Nostrand Reinhold Company, New York.
24. Prasad M., 1993, Refrigeration and Airconditioning, Wiley Eastern Ltd, New Delhi, p. 544.
25. Ranade Satish J., Nadipuram R. P., Steve Omick and Kazda Loub F.,1989, "A study of Islanding in utility - connected Residential Photovoltaic Systems", IEEE Trans. Energy Conversion, Vol. 4, No. 3, September .(Part I and II).

26. Saied Mohamed M.,1988, "Matching of D.C. Motors to Photovoltaic Generators for Maximum Daily Gross Mechanical Energy", IEEE Trans. Energy Conv. Vol. 3, No. 3, Sept.
27. Saied M. M.,1991, "Optimal Design Parameters for A PV Array coupled to A D.C. Motor VIA A D.C.-D.C. Transformer", IEEE Trans. Energy Conv. Vol. 6, No. 4, Dec.
28. Salameh Ziyad M. and Dagher Fouad,1990, "The effect of Electrical Array Re-configuration On The performance of a PV-Powered Volumetric Water Pump", IEEE Trans. Energy Conversion, Vol. 5, No. 4, Dec.
29. Sekar K.,1986, "Optimisation of Hybrid Evaporative Cooling and AirConditioning Systems - An Economic Approach", M.Tech Thesis , Department of Mechanical Engineering, May.
30. Sukhatme S.P., 1994, Solar Energy, Tata McGraw-Hill Publishing Company Ltd, New Delhi, p.270.
31. Tata BP Solar India Ltd., Bangalore Product Catalogue.
32. Uttar Pradesh State Electricity Board statistics at a glance (1990-91), p. 107.
33. Vallippan S., Pham T.D,1995, "Elasto-Plastic Finite Element Analysis with Fuzzy Parameters", Int. J. Num. Methods Eng., Vol. 38,p.531.
34. Zadeh.L.A,1965, "Fuzzy Sets", Inform. and Control, vol. 8, pp. 338-353.

35. Zinger Z. and Braunstein A., 1981, "Dynamic Matching of a Solar- Electrical (Photovoltaic) System An Estimation of the Minimum Requirements On The Matching System", IEEE Trans. Power App. Systems Vol. PAS-100, No. 3, March.

# Appendix A

## Values of the Constants A, B and C used for Predicting Hourly Solar Radiation on Clear Days

[ Sukhatme, 1984 ]

	A(W/m)	B	C
January 21	1228	0.142	0.058
February 21	1213	0.144	0.060
March 21	1185	0.156	0.071
April 21	1134	0.180	0.097
May 21	1103	0.196	0.121
June 21	1087	0.205	0.134
July 21	1084	0.207	0.136
August 21	1106	0.201	0.122
September 21	1150	0.177	0.092
October 21	1191	0.160	0.073
November 21	1219	0.149	0.063
December 21	1232	0.142	0.057

## Appendix B

# Transmissivity and Absorptivity of Ordinary Glass

[Arora, 1993]

Angle of Incidence (in degrees)	Transmissivity	Absorptivity
0	0.87	0.05
20	0.87	0.05
40	0.86	0.06
50	0.84	0.06
60	0.79	0.06
70	0.67	0.06
80	0.42	0.06
90	0.00	0.00

# Appendix C

## Infiltration load

[Prasad, 1993]



Room volume ( $m^3$ )	Number of air changes per 24 h Average load	Number of air changes per 24 h heavy load	Number of air changes per 24 h long usage	Room volume $m^3$ long usage
5	22.6	35.45	12.65	55
10	20.5	32.26	11.26	60
15	19.25	30.44	10.69	70
20	18.25	28.76	9.92	80
25	17.37	27.27	8.92	90
30	16.60	26.04	8.26	100
35	15.91	25.10	7.22	120
40	15.29	24.45	6.44	140
45	14.74	24.08	6.13	150
50	14.25	23.99	5.85	160
55	13.80		5.37	180
60	13.40		4.99	200
65	13.03		4.42	240
70	12.70		4.30	250
75	12.40		4.01	280
80	12.12		3.86	300
85	11.87		3.55	350
90	11.67		3.38	400
95	11.43		3.19	450
			3.08	500
			2.94	600
			2.86	700
			2.82	800
			2.80	1000
			2.80	1500
			2.80	2000
			2.75	2500
			2.73	3000
			2.73	

# Appendix D

## Ventilation air requirement

[Prasad, 1993]

Application	Smoking	Ventilation ( $m^3/s$ per person)x $10^{-3}$		Ventilation $m^3/s/m^2$ of floor area Minimum x 1000+
		Recommended	Minimum	
Apartment, average...	Some...	9.5	4.7	1.0
Apartment, Deluxe...	Some...	14.2	12.0	1.676
Baking space...	Occasional	4.7	3.5	
Barber shops...	Considerable	7.1	4.7	
Beauty parlours...	Occasional	4.7	3.5	
Brokers'board rooms.	Very heavy	24.0	9.5	
Cocktail bars...	Heavy	19.0		12.0
Corridors (Supply or exhaust)	—	—	—	1.27
Department stores	None	3.5	2.4	0.254
Directors' room	Extreme	24		14.2
Drug stores+	Considerable	4.7	3.5	
Factories**	None	4.7	3.5	0.508
Five and ten cent stores	None	3.5	2.4	
Funeral parlours	None	4.7	3.5	
Garages++	—	—	—	5.08
Hospitals operating rooms	None	—	—	10.16
„ private rooms	None	14.2	12.0	1.676
„ wards	None	9.5	4.7	
Hotel rooms	Heavy	14.2	12.0	1.676
Kitchens, Restaurant	—	—	—	20.32
„ , Residence	—	—	—	10.16
Laboratories+	Some	9.5	7.1	
Meeting rooms	Very heavy	24	14.2	6.35
Offices, General	Some	7.1	4.7	
Private	None	12.0	7.1	1.27
Private	Considerable	14.2	12	1.27
Restaurant cafeteria+	,	, 5.7	4.7	
Dining Room+	„	7.1	0.7	
School Rooms	None	—	—	
Shop, Retail	None	4.7	3.6	
Theatre**	None	3.6	2.4	
Theatre	Some	7.1	4.7	
Toilets** (exhaust)	—	—	—	10.16

\* When minimum is used take the larger of two.

♣\* See local codes which may govern.

+ May be governed by exhaust.

++ May be governed by special sources of contamination of local codes.

All outside air recommended to overcome explosion hazard of anesthetics.

# Appendix E

## Heat Liberated due to Occupancy

[Arora, 1993]

Metabolic		Heat Liberated, W							
		Room Dry Bulb °C							
Activity	Rate W	20		22		24		26	
		S	L	S	L	S	L	S	L
Seated at rest	115	90	25	80	35	75	40	65	50
Office work	140	100	40	90	50	80	40	70	70
Standing	150	105	45	95	55	82	68	72	78
Eating in restaurant	160	110	50	100	60	85	75	75	85
Light work in factory	235	130	105	115	120	100	135	80	155
Dancing	265	140	125	125	140	105	160	90	175

S= Sensible Heat

L= Latent Heat

## Appendix F

### Heat of Respiration of Products in J/kg per 24 hours

[Arora, 1993]

Product	Storage Temperature		
	0°C	4.4°C	15.6°C
Apples	312-1560	625-2810	2390-8215
Bananas	—	—	—
Cabbage	1248	1770	4265
Carrots	2183	3640	8420
Cauliflower	—	4680	10500
Cherries	1352-1871	—	11400-13725
Cucumbers	—	—	2290-6860
Grape fruit	416-1040	730-1350	2290-4160
Grapes, American	624	1250	3640
Grapes, European	312-416	—	2290-2705
Lemons	520-936	625-1975	2390-5200
Melons	1350	2080	8840
Mushrooms	6446	—	—
Onions	728-1144	830	2495
Oranges	416-1040	1350-166	3850-5405
Peaches	936-1456	1455-2080	7590-9670
Pears	728-936	—	9150-13725
Peas	8526-8733	13520-16635	40860-46265
Plums	416-728	935-1560	2495-2910
Potatoes, immature	—	2705	3015-7070
Potatoes, mature	—	1350-1870	1560-2705
Strawberries	2807-3950	3745-7070	16220-21105
Tomatoes, green	625	1145	6445
Tomatoes, ripe	1040	1350	5820
Turnips	1975	2290	5510

# Appendix G

## Specifications of the room selected for study

Room size =  $4.85 \times 4.30 \times 4.20 \text{ m}^3$

Thickness of the wall = 0.24m

Thickness of the roof = 0.12m

Number of windows = 3 (South side)

Area of the window =  $7.2 \text{ m}^2$

Only south side exposed to the sun.

Number of occupants = 4

Number of fans = 1

Number of lights = 2

Ratings:

Fan = 60 Watts

Light = 40 W

The walls of the room have layers of plaster of 15 mm on both sides. The conductivity of plaster is  $0.72 \text{ W/m}^\circ\text{C}$  and that for brick structure  $1.30 \text{ W/m}^\circ\text{C}$ . The roof is made



of concrete with 15 mm mortar layers on both sides. The conductivities of mortar and concrete are  $0.72 \text{ W/m}^\circ\text{C}$  and  $1.73 \text{ W/m}^\circ\text{C}$  respectively. The absorptivity of whole structure is taken to be 0.3. Time lag and decrement factor for the room is taken from reference [Arora, 1993].

# Appendix H

## Specifications of Photovoltaic Array

[ Appelbaum, 1986] The PV array data per cell at 100 % sun and 25°C used for the

simulation are as follows:

$$I_G = 0.8 \text{ Amp.}$$

$$I_r = 0.0005 \text{ Amp.}$$

$$V_T = 0.731 \text{ Volt}$$

$$R_s = 0.05 \text{ Ohm}$$

$$a = 5.70 \times 10^{-4}$$

$$b = 4400$$

# Appendix I

## Particulars of the Refrigerator

Volume of refrigerator = 45 liter ( $42 \times 42 \times 26.5 \text{ cm}^3$ )

Thickness of the glass wool insulation = 8 cm.

Food item to be kept in refrigerator = 4 kg/h

Food item always present in refrigerator = 15 kg

Heat of respiration = 16 kJ/kg-day

Specific heat of food items = 4.2 kJ/kg-deg.C

Ice production = 12 kg/day

Temperature of refrigerator = 2 deg. C

Temperature of freezer = -10 deg. C

# Appendix J

## Calculations of COP for Refrigerant R-12

The p-h chart is shown in Figure (J.1). From the property values of R-12, we have,

$$\text{enthalpy at point 1} = h_1 = 184.22 \text{ kJ/kg} \quad (\text{J.1})$$

$$\text{entropy at point 1} = s_1 = 0.7060 \text{ kJ/kg-K} \quad (\text{J.2})$$

$$\text{specific heat of R-12 vapour } c_{pg} = 0.6 \text{ kJ/kg}$$

Considering a superheat of  $10^\circ\text{C}$  from 1 to  $1'$ , we have,

$$h'_1 = h_1 + 10c_{pg} = 190.22 \text{ kJ/kg and} \quad (\text{J.3})$$

$$s'_1 = s_1 + c_{pg} \ln T'_1/T_1 = 0.7060 + 0.6 \ln 273.15/263.15 = 0.7284. \quad (\text{J.4})$$

We assume that the efficiency of compressor is 0.8.

The ideal point after compression is  $2'$ , while the actual point is 2.

$$\text{Now, } s'_2 = s'_1 = 0.7284 = s_3 + c_{pg} \ln T'_2/T'_3 = 0.6863 + 0.6 \ln T'_2/318.15 \quad (\text{J.5})$$

which gives  $T'_2 = 341.28 \text{ K}$  and

$$h'_2 = h_3 + c_{pg}(T'_2 - T_3) = 220.338 \text{ kJ/kg} \quad (\text{J.6})$$

$$\text{Ideal compressor work} = h'_2 - h'_1 = 30.118 \text{ kJ/kg} \quad (\text{J.7})$$

$$\text{Actual work} = 30.118 / .9 = 33.46 \text{ kJ/kg} \quad (\text{J.8})$$

$$\text{Therefore, } h_2 = 190.22 + 33.46 = 223.68 \text{ kJ/kg} \quad (\text{J.9})$$

Assuming  $5^\circ\text{C}$  subcooling,

$$h_5 = h_4 - 5c_{pl} = 79.90 - 5 \times 1.0 = 74.94 \text{ kJ/kg} \quad (\text{J.10})$$

$$\text{Cooling effect} = h'_1 - h_5 = 115.32 \text{ kJ/kg} \quad (\text{J.11})$$

$$\text{COP} = \text{cooling effect} / \text{work done} = 115.32 / 33.46 = 3.405 \quad (\text{J.12})$$

Therefore we take  $\text{COP} = 3.5$

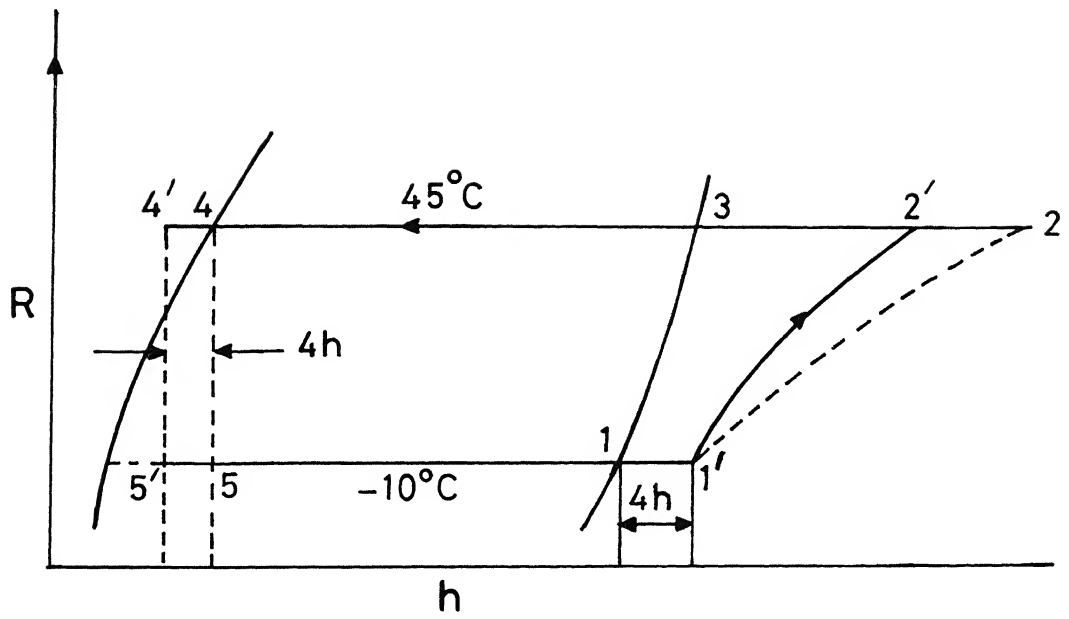


Fig. J.1  $p$ - $h$  chart of R12

# Appendix K

## Characteristic Function

The process by which individuals from the universal set  $X$  are determined to be either members or non members of a set can be defined by a characteristic or discrimination function. For a given set  $A$  this function assigns a value  $\mu_A(x)$  to every  $x \in X$  such that

$$\mu_A(x) = \begin{cases} 1 & \text{if and only if } x \in A \\ 0 & \text{if and only if } x \notin A \end{cases} \quad (K.1)$$

Thus the function maps elements of the universal set to the set containing 0 and 1. This can be indicated by

$$\mu_A : X \Rightarrow \{0, 1\} \quad (K.2)$$

## Fuzzy set

The characteristic function of a crisp set assigns a value of either 1 or 0 to each individual in the universal set. This function can be generalized such that the values assigned to the elements of the universal set fall within a specified range and indicate the membership grade of these elements in the set in question. Larger values denote

higher degrees of set membership. Such a function is called a membership function and the set defined by it is a fuzzy set.

If  $x_1$  is an element of the universal set and  $\mu_1$  is its grade of membership in A, then A is written as

$$A = \mu_1/x_1 + \mu_2/x_2 + \dots + \mu_n/x_n \quad (K.3)$$

where the slash is employed to link the elements of the support with their grades of membership in A and the “+” sign indicates that the listed pairs of elements and membership grades collectively form the definition of the set A. For the case in which a fuzzy set A is defined on a universal set that is finite and countable, we may write

$$A = \sum_{i=1}^n \mu_i/x_i \quad (K.4)$$

Similarly, when  $X$  is an interval of real numbers, a fuzzy set A is often written in the form

$$A = \int_x \mu_A(x)/x \quad (K.5)$$

## Fuzzy union

The union of fuzzy sets A and B is denoted by AUB which results in the maximum membership grades:

$$A \cup B = \int_x [\mu_A(x) \vee \mu_B(x)]/x \quad (K.6)$$

where  $\vee$  is interpreted as “maximum”.



## Fuzzy intersection

The intersection of fuzzy sets A and B is denoted by  $A \cap B$  (A and B) which results in the minimum membership grades:

$$A \cap B = \int_x [\mu_A(x) \wedge \mu_B(x)]/x \quad (K.7)$$

where  $\wedge$  is interpreted as “minimum”.

## Fuzzy product

The product of A and B is denoted by  $AB$  which results in the ordinary product of two membership grades:

$$AB = \int_x \mu_A(x) \mu_B(x) / x \quad (K.8)$$

## Convexity

An  $\alpha$ -cut of a fuzzy set A is a crisp set  $A_\alpha$  that contains all the elements of the universal set X that have a membership grade in A greater than or equal to the specified value of  $\alpha$ . This definition can be written as

$$A_\alpha = [x \in X | \mu_A(x) \geq \alpha] \quad (K.9)$$

A fuzzy set is convex if and only if each of its  $\alpha$ -cuts is a convex set. Equivalently, we may say that a fuzzy set A is convex if and only if

$$\mu_A(\lambda r + (1 - \lambda)s) \geq \min [\mu_A(r), \mu_A(s)] \text{ for all } r, s \in X \text{ and all } \lambda \in [0, 1] \quad (K.10)$$

## Normality

The fuzzy set  $A$  is called normal if the upper bound of its membership grades over  $X$  is unity, i.e.

$$\sup_x \mu_A(x) = 1 \quad (K.11)$$

## Fuzzy numbers

Fuzzy arithmetic is used for computations in which imprecise data exists in a simple or complex system. A convex and normalized fuzzy set defined on  $\mathbb{R}$  (set of real numbers) whose membership function is piecewise continuous is called a fuzzy number. Thus, a fuzzy number can be thought of as an interval containing the real numbers to varying degrees. Figure K.1 shows some examples of fuzzy numbers.

## Operations on fuzzy numbers

(a) Fuzzy addition-addition of two fuzzy intervals at an  $\alpha$ -cut in  $\mathbb{R}$  is defined by

$$A_\alpha(+)B_\alpha = [a_1^\alpha, a_2^\alpha](+)[b_1^\alpha, b_2^\alpha] = [a_1^\alpha + b_1^\alpha, a_2^\alpha + b_2^\alpha] \quad (K.12)$$

(b) Fuzzy subtraction-subtraction of two fuzzy intervals at an  $\alpha$ -cut in  $\mathbb{R}$  is defined by

$$A_\alpha(-)B_\alpha = [a_1^\alpha, a_2^\alpha](-)[b_1^\alpha, b_2^\alpha] = [a_1^\alpha - b_2^\alpha, a_2^\alpha - b_1^\alpha] \quad (K.13)$$

(c) Fuzzy multiplication-multiplication of two fuzzy intervals at an  $\alpha$ -cut in  $\mathbb{R}^{(+)}$  is defined by

$$A_\alpha(\times)B_\alpha = [a_1^\alpha, a_2^\alpha](\times)[b_1^\alpha, b_2^\alpha] = [a_1^\alpha \times b_1^\alpha, a_2^\alpha \times b_2^\alpha] \quad (K.14)$$

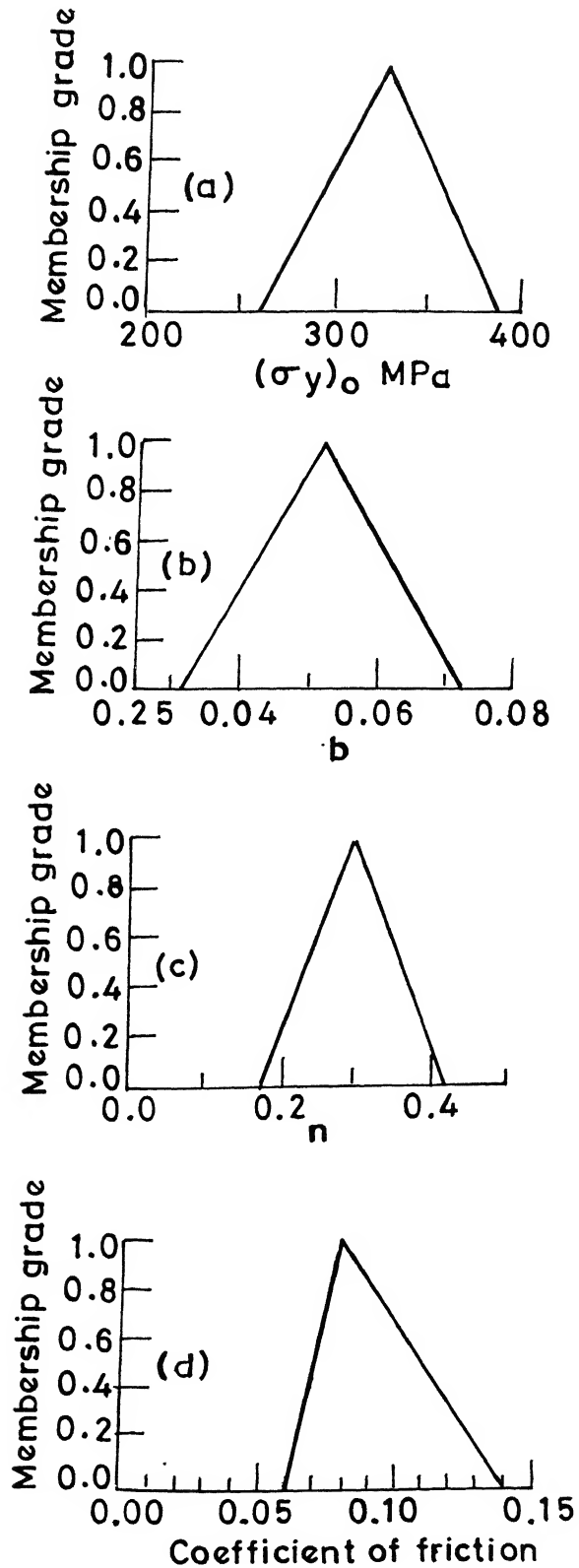


Fig.K-1 Membership functions of (a)  $(\sigma_y)_0$  ;  
(b)  $b$  ; (c)  $n$  ; (d) coefficient of friction

(d) Fuzzy division-division of two fuzzy intervals at an  $\alpha$ -cut in  $\mathbb{R}^{(+)}$  is defined by

$$A_\alpha(\div)B_\alpha = [a_1^\alpha, a_2^\alpha](\div)[b_1^\alpha, b_2^\alpha] = [a_1^\alpha \div b_2^\alpha, a_2^\alpha \div b_1^\alpha] \quad (K.15)$$

# Appendix L

## Complex Search Method

This method was developed by M.J. Box in 1965. The algorithm begins with a number of feasible points created at random. If a point is found to be infeasible, a new point is created using the previously-generated feasible points. Usually, the infeasible point is pushed towards the centroid of the previously-found feasible points. Once a set of feasible points is found, the worst point is reflected about the centroid of rest of the points to find a new point. Depending on the feasibility and function value of the new point, the point is further modified or accepted. If the new point falls outside the variable boundaries, the point is modified to fall on the violated boundary. If the new point is infeasible, the point is retracted towards the feasible points. The worst point is replaced by this new feasible point and the algorithm continues for the next iteration.

### Algorithm

Step 1 : Assume a bound in  $x(x^{(L)}, x^{(U)})$ , a reflection parameter  $\alpha$  and termination parameters  $\epsilon, \delta$ .

Step 2 : Generate an initial set of P (usually 2N) feasible points. For each point

- (a) Sample N times to determine the point  $x_i^{(p)}$  in the given bound.
- (b) If  $x^{(p)}$  is infeasible, calculate  $\bar{x}$  (centroid) of current set of points and reset

$$x^{(p)} = x^{(p)} + \frac{1}{2}(\bar{x} - x^{(p)})$$

until  $x^{(p)}$  is feasible;

Else if  $x^{(p)}$  is feasible, continue with (a) until P points are created.

- (c) Evaluate  $f(x^{(p)})$  for  $p = 0, 1, 2, \dots, (P-1)$ .

Step 3 : Carry out the reflection step:

- (a) Select  $x^R$  such that

$$f(x^R) = \max f(x^{(p)}) = F_{max}.$$

- (b) Calculate the centroid  $\bar{x}$  (of points except  $x^R$ ) and the new point

$$x^m = \bar{x} + \alpha(\bar{x} - x^R).$$

- (c) If  $x^m$  is feasible and  $f(x^m) \geq F_{max}$ , retract half the distance to the centroid  $\bar{x}$ .

Continue until  $f(x^m) < F_{max}$

Else if  $x^m$  is feasible and  $f(x^m) < F_{max}$ , go to Step 5.

Else if  $x^m$  is infeasible, go to Step 4.

Step 4 : Check for feasibility of the solution

- (a) For all  $i$ , reset violated variable bounds:

If  $x_i^m < x_i^{(L)}$  set  $x_i^m = x_i^{(L)}$ .

If  $x_i^m > x_i^{(U)}$  set  $x_i^m = x_i^{(U)}$ .

- (b) If the resulting  $x^m$  is infeasible, retract half the distance to the centroid until  $x^m$  is feasible. Go to Step 3(c).

Step 5 : Replace  $x^R$  by  $x^m$ . Check for termination.

- (a) Calculate  $\bar{f} = \frac{1}{P} \sum_p f(x^{(p)})$  and  $\bar{x} = \frac{1}{P} \sum_p x^{(p)}$ .

- (b) If  $\sqrt{\sum_p \left( f(x^{(p)}) - \bar{f} \right)^2} \leq \epsilon$  and  $\sqrt{\sum_p \|x^{(p)} - \bar{x}\|^2} \leq \delta$

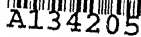
## **Terminate**

Else set  $k = k + 1$  and go to Step 3(a).

A

## Date Slip

This book is to be returned on  
the date last stamped.

[illegible]



TH  
EE/1999/P  
D5354  
A134205